

Fundamental Limits on Delivery Time in Cloud- and Cache-Aided Heterogeneous Networks

Jaber Kakar, *Member, IEEE*, Soheil Gherekhloo, *Member, IEEE*,
and Aydin Sezgin, *Senior Member, IEEE*

Abstract

A Fog radio access network (F-RAN) is considered as a network architecture candidate to meet the soaring demand in terms of reliability, spectral efficiency, and latency in next generation wireless networks. This architecture combines the benefits associated with centralized cloud processing and wireless edge caching enabling primarily low-latency transmission under moderate fronthaul capacity requirements. The F-RAN we consider in this paper is composed of a centralized cloud server which is connected through fronthaul links to two edge nodes (ENs) serving two mobile users through a Z-shaped partially connected wireless network. We define an information-theoretic metric, the delivery time per bit (DTB), that captures the worst-case per-bit delivery latency for conveying any requested content to the users. For the cases when cloud and wireless transmission occur either sequentially or in parallel, we establish coinciding lower and upper bounds on the DTB as a function of cache size, backhaul capacity and wireless channel parameters. Through optimized rate allocation, our achievability scheme determines the best combination of private, common signalling and interference neutralization that matches the converse. Our converse bounds use subsets of wireless, fronthaul and caching resources of the F-RAN as side information that enable a single receiver to decode either one or both users' requested files. We show the optimality on the DTB for all channel regimes. In case of serial transmission, the functional DTB-behavior changes at fronthaul capacity thresholds. In this context, we combine multiple channel regimes to *classes of channel regimes* which share the same fronthaul capacity thresholds and as such the same DTB-functional. In total, our analysis identifies four classes; in only three of those edge caching and cloud processing can provide nontrivial synergistic and non-synergistic performance gains. Interestingly, in these three classes, we show that *only* under parallel fronthaul-edge transmission strategies edge caching becomes obsolete as long as a certain fronthaul capacity is exceeded.

This paper was presented in part at the IEEE International Conference on Communications 2017 [1].

Index Terms

Caching, Cloud Radio Access Network (C-RAN), Fog Radio Access Network (F-RAN), degrees-of-freedom, latency, delivery time.

I. INTRODUCTION

In recent years, mobile usage characteristics in wireless networks have changed profoundly from conventional connection-centric (e.g., phone calls) to content-centric (e.g, HD video) behaviors. This shift is mainly driven by the rapid growth in multimedia content, particularly by video [2], [3]. Over the last decade, however, while the demand for rich multimedia content has increased tremendously, the capacity of the mobile radio and backhaul network, could not cope at the same pace with the exponentially growing mobile traffic (despite PHY and MAC layer improvement) due to the *centralized* nature of mobile network architectures [4]. As part of standardizing next generation (5G) mobile networks, two major solutions that have great potential to facilitate this shift are content *in-network* caching [5] and multi-tier networks [6] in the form of *heterogenous* networks. These solutions go hand in hand with the design of more *decentralized* network (HetNet) architectures.

In-network caching prefetches popular content during off-peak traffic hours in intermediate servers potentially belonging to various hierarchical network layers of the mobile network. Two main places where caches can be deployed are at the core network and/or at the radio access network (RAN) [5]. In this regard, placing caches to the very edge of the network is a RAN-based caching approach which is generally known as *edge caching* and in the small-cell scenario as *femto caching* [7]. It has the advantage that it brings popular content very close to destinations; thus, reducing the usage of expensive backhaul connections from edge nodes (EN) to remote cloud servers and thereby lessening the latency to address the increasing demand in content retrieval. Recent trends in the immensely growing number of base stations [8], suggest that future networks will be highly heterogeneous in which both small and macro ENs coexist in a HetNet¹. Thus, recently research interests have shifted towards the investigation of edge caching of HetNets [3]. However, deploying solely cache-based HetNets prevents the eNBs from joint centralized baseband processing; thus, avoiding to some extent advantages of *cooperative* communication strategies [9], [10]. Typically, joint processing enables, amongst others, enhanced interference

¹Henceforth, we call small and macro ENs as eNB and HeNB (Home eNB).

management, flexibility, scalability and power efficiency [11]; all of which are key factors in the design of HetNets [6].

Cache and cloud-aided architectures (e.g., Fog radio access networks (F-RAN)) are new hybrid solutions that bring together the advantages of both centralized cloud processing and edge caching [12]. F-RAN is particularly relevant for HetNets. A simplistic HetNet involving both cloud and edge processing is shown in Fig. 1, which has been first introduced in [13]. We aim at understanding the synergistic benefits of cloud and edge processing for HetNets from a delivery time perspective [14]. To this end, we focus in this work on characterizing the fundamental trade-off on delivery time in cloud and cache-aided HetNets of the model as shown in Fig. 1.

Recently, the impact of caching on the delivery time for cache-aided networks has been investigated [15], [16], [17], [18]. In this regard, receiver (Rx) [15], [19], [20], [21] and transmitter (Tx) caching [16], [17], [22] as well as simultaneous Tx/Rx caching [18], [23] offer great potential for reducing the induced delivery time for file retrieval. Rx caching, on the one hand, was first studied in [15] for a shared link with one server and multiple cache-enabled receivers. The authors show that caching can exploit multicast opportunities and as such significantly reduces the delivery latency over the shared link. On the other hand, the impact of Tx caching on the delivery time has mainly been investigated by analyzing the inverse degrees-of-freedom (DoF) metric for Gaussian networks. To this end, the authors of [16] developed a novel interference alignment achievability scheme characterizing the metric as a function of the cache storage capability for a 3-user Gaussian interference network. The cache placement was designed to facilitate transmitter cooperation such that interference coordination techniques can be applied. A converse on this metric was developed in [17] for a network with arbitrary number of edge nodes and users showing the optimality of schemes presented in [16] for certain regimes of cache sizes. Extensions of this work include the characterization of the latency-memory tradeoff to cloud and cache-assisted F-RAN [24], [13]. Tx-caching through cache-enabled helpers can also significantly reduce the delivery time than a system without caching as was shown in [25] for a MIMO broadcast channel. As opposed to [16], [17], [24], authors of [13] modeled the wireless channel by a binary fading channel [26]. Through this simplification, their results gave first insight on the delivery time as a function of the cache size and *probabilistic* parameters on the wireless channel. Related papers that study the influence of cloud and edge processing on achievable rates, backhaul costs and power consumption for non-uniform file requests are, amongst others, [27], [28], [29], [30].

In this paper, we study the fundamental limits on the delivery time for the cloud and cache-aided HetNet introduced in [13] and shown in Fig. 1 which consists of two eNBs and two users. For this network, two distinct cloud-edge transmission policies are feasible. In the first policy, the so-called *serial* policy, the cloud transmission terminates before the wireless transmission initiates, whereas in the second policy, the so-called *parallel* policy, cloud and wireless transmissions are executed simultaneously. For both policies, we measure the performance through the latency-centric metric *delivery time per bit* (DTB) [17]. As opposed to the results established in [13], where a binary fading channel is used to determine the DTB for serial transmission only, we instead use the linear deterministic model (LDM) [31], [32] as a model that comes closest to the Gaussian system model of the proposed network. Under this particular channel which takes into account distinct channel strengths, we characterize the DTB of the network through means of lower bounds (converse) and upper bounds (achievability) on the DTB. For serial and parallel transmissions, we establish five lower bounds that utilize five distinct combinations of cached information, fronthaul and wireless signals that enable reliable decoding of either one or two requested files of the users at any arbitrary decoder, respectively. All bounds are tight and required for the characterization of the DTB. As far as the achievability is concerned, we propose a generalized scheme that is based on rate splitting of private, common and interference-neutralizing information. We formulate a linear *max-min* optimization problem to maximize the least number of desired bits conveyable to the users per block of channel uses. Hereby, the least number of desired bits conveyable corresponds to the *per-user rate* of the *weaker* user. Thus, *maximizing* this quantity optimizes the weaker users' rate. This optimization problem intrinsically captures the importance of treating each user equally from a rate perspective. Since the per-user rate of the weaker user is inverse proportional to the DTB, we are able to minimize the achievable DTB and determine the optimal rate splitting which achieves the lower bound. To the best of the author's knowledge, existing work [16], [17], [19], [24] treat all channel links as equally strong and use the inverse DoF as their delivery time metric. However, these results do not capture the inherent dependency of the time for file delivery on the wireless channel strength. Instead, apart from cloud and cache parameters, our DTB metric also captures the influence of channel strength on the latency. Through the additional perspective on channel strength, we are able to broadly identify channel regimes for which edge caching and cloud processing can provide nontrivial synergistic and non-synergistic performance gains.

The rest of the paper is organized as follows. In Section II, we introduce the system model.

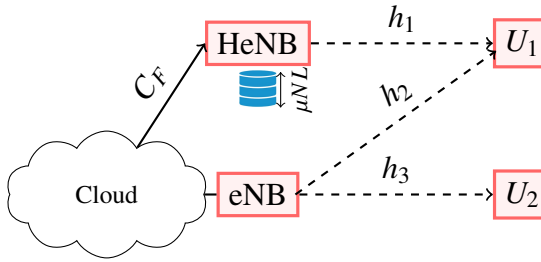


Fig. 1: System Model of Cache- and Cloud-aided HetNet

The main results on the DTB, including achievability and converse, for serial and parallel cloud-edge transmissions are presented in sections III through V and VI through VIII, respectively. Finally, Section IX concludes the paper. The appendix of this paper is devoted to give further details on lower and upper bounds.

Notation: Throughout the paper, we use \mathbb{F}_2 to denote the binary field and \oplus to denote the modulo 2 addition. We use normal lower-case, normal upper-case, boldface lower-case, and boldface upper-case letters to denote scalars, scalar random variables, vectors, and matrices, respectively. $\text{Bern}(a)$ is a Bernoulli distribution with probability a . The vector $\mathbf{0}_q$ denotes the zero-vector of length q and the matrix I_q is the $q \times q$ identity matrix. We use the superscript $(\cdot)^T$ to represent the transpose of a matrix. Furthermore, for any two integers a and b with $a \leq b$, we define $[a : b] \triangleq \{a, a + 1, \dots, b\}$. When $a = 1$, we simply write $[b]$ for $\{1, \dots, b\}$. Furthermore, we define the function $(x)^+ \triangleq \max\{0, x\}$.

II. SYSTEM MODEL AND LATENCY METRIC

In this section, we first outline the system model for the cloud and cache-aided F-RAN in Fig. 1. Then, we introduce the delivery time per bit (DTB) metric, along with its operational meaning to provide additional context on the adopted model and performance metric. In sub-section II-C, we introduce the linear-deterministic model (LDM) as an approximation method of the Gaussian system model of sub-section II-A and further alter the DTB metric of sub-section II-C to make it applicable for the LDM.

A. System Model

We study the downlink of a cache and cloud-aided HetNet as shown in Fig. 1. The HetNet consists of a HeNB and a macro eNB which serves two users – a small-cell user (U_1) and a

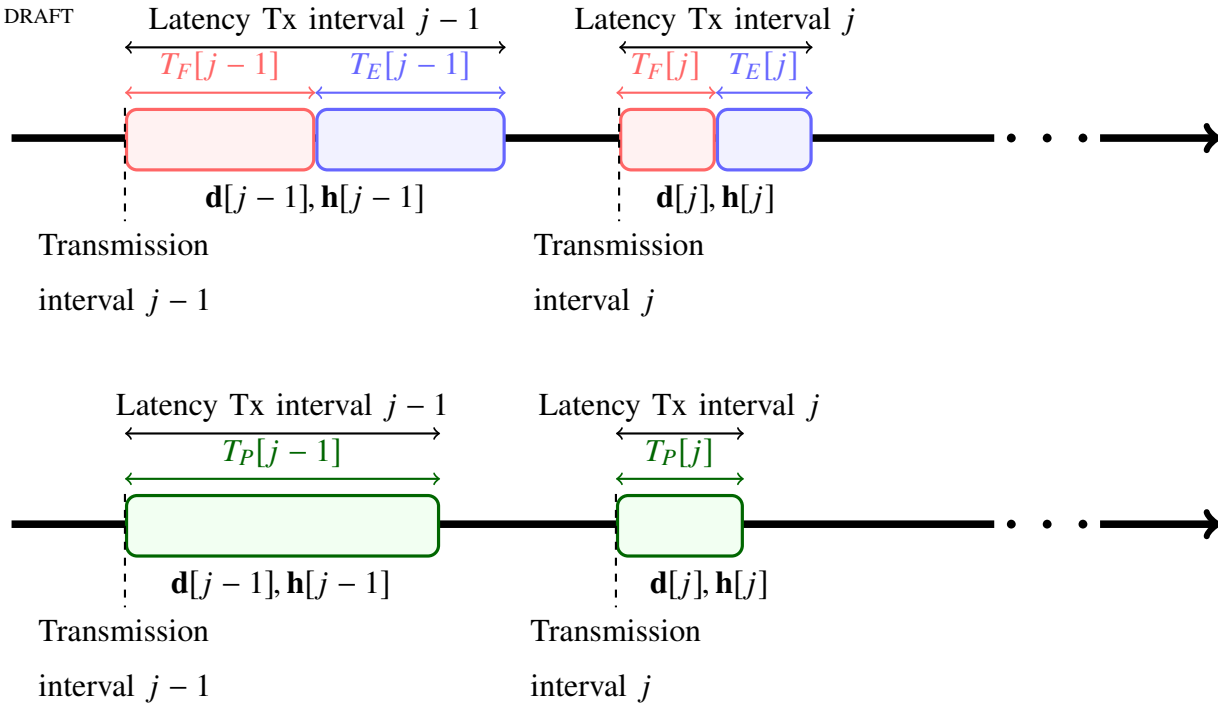


Fig. 2: Illustration of the delivery latency within each transmission interval for the F-RAN of Fig. 1 with (a) serial and (b) parallel fronthaul-edge transmission.

macro cell user (U_2) – over a wireless channel. As the HeNB transmits at much lower power than the eNB, we model the wireless channel by a partially connected network in the spirit of a Z-channel. At every transmission interval j , both users request any file W_i , all of which are of L bits in size, from a library of N popular files. The request pattern of both users is revealed to the cloud and the edge nodes (eNB and HeNB) prior to the transmission which seek to satisfy the users' demands at the lowest possible latency. Hereby, cloud and edge transmission can, amongst others, be carried out in two ways: (a) *serial/sequential* transmission, where the cloud transmission over the fronthaul link terminates before the edge transmission over the wireless channel initiates; (b) *parallel/pipelined* transmission, where cloud and edge transmission are executed simultaneously in which the HeNB operates as a causal full-duplex cache-aided relay (cf. Fig. 2). The transmission scheme of interval j terminates when the requested files have been delivered. This induces a total delivery time consisting of the sum of fronthaul and edge latencies ($T_F[j] + T_E[j]$) for (a) serial and $T_P[j]$ for (b) parallel transmissions. The system model, notation and main assumptions are summarized as follows:

- Let $\mathcal{W} = \{W_1, \dots, W_N\}$ denote the library of popular files, where each file W_i is of size L bits. Each file W_i is chosen uniformly at random from $[2^L] \triangleq \{1, 2, \dots, 2^L\}$. We define the demand vector $\mathbf{d}[j] = (d_1[j], d_2[j])^T \in [N]^2$ to denote the request pattern of both users. Thus, at every transmission interval j , U_1 and U_2 request files $W_{d_1[j]}$ and $W_{d_2[j]}$ from the library \mathcal{W} , respectively.
- The HeNB is endowed with a cache capable of storing μNL bits, where $\mu \in [0, 1]$ corresponds to the *fractional cache size*. It denotes how much content can be stored at the HeNB relatively to the entire library \mathcal{W} .
- The cloud server has access to all N files. The cloud server and the eNB are co-located whereas the HeNB is connected to the cloud via a fronthaul link of fixed capacity C_F . For $C_F = 0$, we explicitly assume that the link from HeNB-to-cloud is absent only in the file delivery phase; and, the user can still prefetch some content in its local cache in the off-peak hours. In doing so, the HeNB may still have some useful contents even though the link between HeNB and cloud may not be present while the files ought to be delivered.
- Global channel state information (CSI) at transmission interval j is summarized by the channel vector $\mathbf{h}[j] = (h_1[j], h_2[j], h_3[j])^T \in \mathbb{C}^3$, where $h_1[j]$, $h_2[j]$ and $h_3[j]$ represent the complex channel coefficients from HeNB and eNB to U_1 and U_2 , respectively. Hereby, the channel coefficients in $\mathbf{h}[j]$ are constant over a single transmission interval j . The channel coefficients are assumed to be drawn i.i.d. from a continuous distribution.

Communication over the wireless channel occurs in two consecutive phases, *placement phase* followed by the *delivery phase*. In the following, we will describe the modeling of placement and delivery phase for both serial and parallel fronthaul-edge transmission.

- 1) *Placement phase*: During this phase, the HeNB is given full access to the database of N files. *Irrespective* of serial and parallel fronthaul-edge transmission, the cached content at the HeNB is generated through its caching function.

Definition 1 (Caching function). The HeNB maps each file $W_i \in \mathcal{W}$ to its local *file cache content*

$$S_i = \phi_i(W_i), \quad \forall i = 1, \dots, N.$$

All S_i are concatenated to form the total cache content

$$S = (S_1, S_2, \dots, S_N)$$

at the HeNB. Hereby, due to the assumption of symmetry in caching, the entropy $H(S_i)$ of each component S_i , $i = 1, \dots, N$, is upper bounded by $\mu^{NL}/N = \mu L$. The definition of the caching function presumes that every file W_i is subjected to *individual* caching functions. Thus, permissible caching policies allow for intra-file coding but avoid inter-file coding. Moreover, the caching policy is kept fixed over multiple transmission intervals. Thus, it is indifferent to the user's request pattern and of channel realizations.

2) *Delivery phase*: In this phase, a fronthaul and edge transmission policy at the cloud as well as at HeNB and eNB is applied in each transmission interval j to satisfy the given user's requests $\mathbf{d}[j]$ under the current channel realizations $\mathbf{h}[j]$. In the sequel, we will focus on a *single* transmission interval and therefore omit indexing the transmission interval explicitly. Hereafter, the main differences between serial and parallel fronthaul-edge transmission are outlined.

Definition 2 (Encoding functions). For $C_F \geq 0$, the cloud encoding function

$$\psi_C : \begin{cases} [2^{NL}] \times [N]^2 \times \mathbb{C}^3 \rightarrow \mathbb{C}^{T_F} \text{ for serial transmission} \\ [2^{NL}] \times [N]^2 \times \mathbb{C}^3 \rightarrow \mathbb{C}^{T_P} \text{ for parallel transmission} \end{cases} \quad (1)$$

determines the fronthaul messages \mathbf{x}_F^T as a function of \mathcal{W}, \mathbf{d} and \mathbf{h} . Depending on the edge-fronthaul transmission, these messages are transmitted in $T \in \{T_F, T_P\}$ channel uses. Note that in T channel uses, the fronthaul message cannot exceed TC_F bits. The encoding function of the HeNB for *serial* fronthaul-edge transmission on the one hand is defined by

$$\psi_1 : [2^{\mu NL}] \times \mathbb{C}^{T_F} \times [N]^2 \times \mathbb{C}^3 \rightarrow \mathbb{C}^{T_E}. \quad (2)$$

This encoding function ψ_1 maps the cached content S , the demand vector \mathbf{d} , the fronthaul messages $\mathbf{x}_F^{T_F}$ and global CSI given by \mathbf{h} to the codeword $\mathbf{x}_1^{T_E}$ of T_E channel uses in duration while satisfying the average power constraint given by the parameter P . On the other hand, to account for parallel fronthaul-edge transmission, we modify (2) as follows:

$$\psi_1^{[t]} : [2^{\mu NL}] \times \mathbb{C}^{t-1} \times [N]^2 \times \mathbb{C}^3 \rightarrow \mathbb{C}, \quad t \in [T_P] \quad (3)$$

For any time instant t , (3) accounts for the simultaneous reception and transmission through fronthaul and wireless links at the HeNB. More precisely, the transmitted signal at the t -th

channel use is generated by $\mathbf{x}_1[t] = \psi_1^{[t]}(S, \mathbf{x}_F^{[t-1]}, \mathbf{d}, \mathbf{h})$. Similarly to (2) and (3), the macro eNB uses the encoding function

$$\psi_2 : \begin{cases} [2^{NL}] \times [N]^2 \times \mathbb{C}^3 \rightarrow \mathbb{C}^{T_E} & \text{for serial transmission} \\ [2^{NL}] \times [N]^2 \times \mathbb{C}^3 \rightarrow \mathbb{C}^{T_P} & \text{for parallel transmission} \end{cases} \quad (4)$$

to construct the codeword $\mathbf{x}_2^T = \psi_2(\mathcal{W}, \mathbf{d}, \mathbf{h})$ for $T \in \{T_E, T_P\}$ subjected to an average power constraint of P .

Definition 3 (Decoding function). The decoding operation at U_k , $k \in \{1, 2\}$, follows the mapping

$$\eta_k : \begin{cases} \mathbb{C}^{T_E} \times [N]^2 \times \mathbb{C}^3 \rightarrow [2^L] & \text{for serial transmission} \\ \mathbb{C}^{T_P} \times [N]^2 \times \mathbb{C}^3 \rightarrow [2^L] & \text{for parallel transmission} \end{cases}. \quad (5)$$

The decoding function η_k takes as its arguments \mathbf{h} , the available demand pattern \mathbf{d} and the channel outputs \mathbf{y}_k^T for $T \in \{T_E, T_P\}$ given by

$$\mathbf{y}_k^T = \begin{cases} h_1 \mathbf{x}_1^T + h_2 \mathbf{x}_2^T + \mathbf{z}_1^T & \text{for } k = 1 \\ h_3 \mathbf{x}_2^T + \mathbf{z}_2^T & \text{for } k = 2 \end{cases} \quad (6)$$

to provide an estimate $\hat{W}_{d_k} = \eta_k(\mathbf{y}_k^T, \mathbf{d}, \mathbf{h})$ of the requested file W_{d_k} . \mathbf{z}_k^T denotes complex Gaussian noise of zero mean and unit power which is i.i.d. across time and users.

A proper choice of a caching, encoding and decoding function that satisfies the reliability condition; that is the worst-case error probability

$$P_e = \max_{\mathbf{d} \in [N]^2} \max_{k \in \{1, 2\}} \mathbb{P}(\hat{W}_{d_k} \neq W_{d_k}) \quad (7)$$

approaches 0 as $L \rightarrow \infty$, is called a *feasible policy*.

B. Latency Metric: Delivery Time per Bit

We next define the proposed performance metric of delivery time per bit (DTB) for a serial and pipelined fronthaul-edge transmission scheme.

Definition 4 (Delivery time per bit). The DTB for \mathbf{d} and \mathbf{h} is defined as

$$\Delta(\mu, C_F, \mathbf{h}, P) = \max_{\mathbf{d} \in [N]^2} \limsup_{L \rightarrow \infty} \begin{cases} \frac{T_F(\mathbf{d}, \mathbf{h}) + T_E(\mathbf{d}, \mathbf{h})}{L} & \text{for serial transmission} \\ \frac{T_P(\mathbf{d}, \mathbf{h})}{L} & \text{for parallel transmission} \end{cases}. \quad (8)$$

The minimum DTB Δ^* is the infimum of the DTB of all achievable schemes.

Remark 1. The DTB measures the overall per-bit latency within a transmission interval for the worst-case request pattern of U_1 and U_2 . In case of serial transmission, the latency consists of the fronthaul latency incurred from cloud to HeNB and the latency of the wireless channel from (H)eNB to the users. Note that parallel transmission naturally outperforms serial transmission. This is mainly because the HeNB operates as a cache-aided full-duplex relay such that schemes utilizing serial transmission are special cases of the more general parallel transmission.

Remark 2 (Cache-Only F-RAN and Cloud-Only F-RAN). When establishing converse and achievability for both serial and parallel transmission, we differentiate between *cache-only F-RAN* and *cloud-only F-RAN*. The former refers to the case when the fronthaul link is absent during the delivery phase ($C_F = 0$). The latter, on the other hand, encompasses a C-RAN system, i.e., a radio network without edge caching capabilities ($\mu = 0$). For the network under study, the special case when $\mu = 0$, $C_F = 0$ reduces to a (Gaussian) broadcast channel [33]. This is because there is neither local information stored in the HeNB's cache nor can useful information on requested files be made available through the cloud-to-HeNB link. In one of the following lemmas to come (Lemma 2), we will specify the optimal DTB for this broadcast setting.

C. Linear-Deterministic Model

To gain insight into the DTB for the Gaussian system model, we suggest to approximate (6) by the linear-deterministic model (LDM) [31]. In the LDM, an input symbol at the (H)eNB is given by the binary input vector $\mathbf{x}_k \in \mathbb{F}_2^q$ where $q = \max\{n_{d1}, n_{d2}, n_{d3}\}$. The integers $n_{dm} \in \mathbb{N}_0^+$, $m \in \{1, 2, 3\}$, given by

$$n_{dm} = \lceil \log(P|h_m|^2) \rceil \quad (9)$$

approximate the number of bits which can be communicated over each link reliably. Similarly to the parameters n_{dm} , we define $n_F = \lceil C_F \rceil$ in the LDM. The channel output symbols \mathbf{y}_k^T received in $T \in \{T_E, T_P\}$ channel uses (depending on whether the system operates under serial or parallel transmission) at U_k is given by a deterministic function of the inputs; that is

$$\mathbf{y}_k^T = \begin{cases} \mathbf{S}^{q-n_{d1}} \mathbf{x}_1^T \oplus \mathbf{S}^{q-n_{d2}} \mathbf{x}_2^T & \text{for } k = 1 \\ \mathbf{S}^{q-n_{d3}} \mathbf{x}_2^T & \text{for } k = 2 \end{cases}, \quad (10)$$

where $\mathbf{S} \in \mathbb{F}_2^{q \times q}$ is a down-shift matrix defined by

$$\mathbf{S} = \begin{pmatrix} \mathbf{0}_{q-1}^T & 0 \\ \mathbf{I}_{q-1} & \mathbf{0}_{q-1} \end{pmatrix}. \quad (11)$$

The input-output equation (10) approximates the input-output equation of the Gaussian channel given in (6) in the high SNR regime. A graphical representation of the transmitted and received binary vectors $\mathbf{x}_k[t]$ and $\mathbf{y}_k[t]$, $k \in \{1, 2\}$, in the t -th channel use is shown in Fig. 3(a). Each circle in the figure represents a signal level which holds a binary digit for transmission. For any link between HeNB/eNB to U_1 or U_2 , only the most $\mathbf{n} = (n_{d1}, n_{d2}, n_{d3})^T$ significant bits are received at the destinations while less significant bits are not. In analogy to (8), we denote the DTB for the LDM by $\Delta_{\text{det}}(\mu, n_F, \mathbf{n})$. The remainder of this paper focuses on characterizing the DTB on the basis of the LDM.

We show next that irrespective of the type of fronthaul-edge transmission the DTB is convex in the fractional cache size μ for any given value of fronthaul capacity n_F and wireless channel parameters \mathbf{n} . This is proven through a memory-sharing argument that is based on splitting a file into two distinct fractions and applying different fronthaul-edge policies to each of it. Due to the additivity in delivery time, the overall DTB becomes the sum of individual DTB's obtained on each file fraction.

Lemma 1 (Convexity of Minimum DTB). The minimum DTB Δ_{det}^* is a convex function of $\mu \in [0, 1]$ for any given value $n_F \geq 0$ and $\mathbf{n} \in (\mathbb{N}_0^+)^3$.

Proof: For any given $n_F \geq 0$ and $\mathbf{n} \in (\mathbb{N}_0^+)^3$, consider two *feasible* policies that require fractional cache sizes μ_1 and μ_2 that achieve a minimum (optimal) DTB of $\Delta_{\text{det}}^*(\mu_1, n_F, \mathbf{n})$ and $\Delta_{\text{det}}^*(\mu_2, n_F, \mathbf{n})$, respectively. At a fractional cache size $\mu = \alpha\mu_1 + (1 - \alpha)\mu_2$ for any $\alpha \in [0, 1]$, the system can apply *file splitting* into subfiles; the first subfile being of size αL and the second being of size $(1 - \alpha)L$. Note that this strategy is in agreement with the cache constraints. Using the first policy on the first subfile and the second policy on the second subfile consecutively through *time sharing* achieves a DTB equal to the convex combination $\alpha\Delta_{\text{det}}^*(\mu_1, n_F, \mathbf{n}) + (1 - \alpha)\Delta_{\text{det}}^*(\mu_2, n_F, \mathbf{n})$. This achievable DTB is at best as low as the minimal DTB $\Delta_{\text{det}}^*(\mu, n_F, \mathbf{n})$ at fractional cache size μ . Thus, the convex combination $\alpha\Delta_{\text{det}}^*(\mu_1, n_F, \mathbf{n}) + (1 - \alpha)\Delta_{\text{det}}^*(\mu_2, n_F, \mathbf{n})$ functions as an upper bound on $\Delta_{\text{det}}^*(\mu, n_F, \mathbf{n})$. ■

Lemma 2 (Optimal DTB of the Broadcast Channel). For the LDM-based cloud and cache-aided HetNet in Fig. 1 with $n_F = 0$ and $\mu = 0$, the optimal DTB is given by

$$\Delta_0(\mathbf{n}) \triangleq \Delta_{\text{det}}^*(\mu = 0, n_F = 0, \mathbf{n}) = \max \left\{ \frac{2}{\max\{n_{d2}, n_{d3}\}}, \frac{1}{n_{d2}}, \frac{1}{n_{d3}} \right\}. \quad (12)$$

Proof: For $\mu = 0$ and $n_F = 0$, the HeNB has no relevant information on the requested files W_{d1} and W_{d2} . Thus, the eNB is involved in broadcasting files W_{d1} and W_{d2} to U_1 and U_2 while the HeNB remains silent. In the LDM, this is equivalent to $n_{d1} = 0$. For a feasible scheme, either user can reliably decode W_{dk} (W_{d1} and W_{d2}) if it is aware of \mathbf{y}_k^T (\mathbf{y}_1^T and \mathbf{y}_2^T) for $T \in \{T_E, T_P\}$. These observations can be used to generate lower bounds on the DTB $\Delta_{\text{det}}^*(\mu = 0)$ that correspond to (12). Since the requested files are of the same size, an optimal scheme that minimizes the latency would try to split the transmission load equally to the two users. Depending on the channel conditions, the load balancing is done as follows. For instance, when $n_{d2} \geq n_{d3}$, $n_{d2}/2$ bits can be send in one channel use from the eNB to both U_1 and U_2 , if the weaker channel n_{d3} is stronger than $n_{d2}/2$ ($n_{d2}/2 \leq n_{d3}$). On the other hand, if $n_{d2} \geq n_{d3}$ and $n_{d2}/2 \geq n_{d3}$, the latency is governed by the weaker channel and n_{d3} bits are transmitted in one channel use to each user. In summary, for $n_{d2} \geq n_{d3}$ we can reliably convey $\min\{n_{d2}/2, n_{d3}\}$ bits per channel use to each user, or in other words, $\Delta_{\text{det}}^*(\mu = 0) = \max\{2/n_{d2}, 1/n_{d3}\}$ channel uses are needed to provide each user with one bit. Due to symmetry, a similar observation holds for $n_{d2} \leq n_{d3}$. This concludes the proof. ■

Remark 3 (Broadcast Conditions). One can verify from Eq. 12 of Lemma 2 that the optimal DTB corresponds to

$$\Delta_0(\mathbf{n}) = \begin{cases} \frac{2}{n_{d2}} & \text{if } \mathbf{n} \in \mathcal{I}_0 \triangleq \{2n_{d3} \geq n_{d2} \geq n_{d3}\} \\ \frac{1}{n_{d3}} & \text{if } \mathbf{n} \in \mathcal{I}_0^C \triangleq \{n_{d2} \geq 2n_{d3}\} \\ \frac{2}{n_{d3}} & \text{if } \mathbf{n} \in \mathcal{I}_1 \triangleq \{2n_{d2} \geq n_{d3} \geq n_{d2}\} \\ \frac{1}{n_{d2}} & \text{if } \mathbf{n} \in \mathcal{I}_1^C \triangleq \{n_{d3} \geq 2n_{d2}\} \end{cases}. \quad (13)$$

Hereby, \mathcal{I}_0 , \mathcal{I}_0^C , \mathcal{I}_1 and \mathcal{I}_1^C are mutually exclusive broadcast channel regimes, or broadcast conditions, for which the optimal DTB are distinct. Throughout this paper, we refer to $\Delta_0(\mathbf{n})$ as the *broadcast DTB*.

III. SERIAL TRANSMISSION – MAIN RESULT

In this section, we state our main result on the minimum DTB for the F-RAN in Fig. 1 for a serial fronthaul-edge transmission. Hereby, our result is a complete DTB characterization stated in the following theorem.

Theorem 1. The DTB of the LDM-based cloud and cache-aided HetNet in Fig. 1 for any $n_F \geq 0$ and $\mu \in [0, 1]$ is given by

$$\Delta_{\text{det}}^*(\mu, n_F, \mathbf{n}) = \begin{cases} \max \left\{ \frac{1-\mu}{n_{d2}}, \frac{2-\mu}{\max\{n_{d2}, n_{d3}\}}, \Delta'_{\text{LB}}(\mathbf{n}) \right\} & \text{for } n_F \leq n_{d2} \\ \max \left\{ \frac{1-\mu}{n_F} + \left(1 - \frac{n_{d2}}{n_F}\right) \Delta''_{\text{LB}}(\mathbf{n}), \frac{2-\mu}{\max\{n_{d2}, n_{d3}\}}, \Delta'_{\text{LB}}(\mathbf{n}) \right\} & \text{for } n_{d2} \leq n_F \leq \max\{n_{d2}, n_{d3}\} \\ \max \left\{ \begin{array}{l} \frac{2-\mu}{n_F} + \left(1 - \frac{\max\{n_{d2}, n_{d3}\}}{n_F}\right) \Delta'_{\text{LB}}(\mathbf{n}), \\ \frac{1-\mu}{n_F} + \left(1 - \frac{n_{d2}}{n_F}\right) \Delta'_{\text{LB}}(\mathbf{n}), \\ \Delta'_{\text{LB}}(\mathbf{n}) \end{array} \right\} & \text{for } n_F \geq \max\{n_{d2}, n_{d3}\} \end{cases}, \quad (14)$$

where

$$\Delta'_{\text{LB}}(\mathbf{n}) = \max \left\{ \frac{1}{n_{d3}}, \frac{1}{\max\{n_{d1}, n_{d2}\}}, \frac{2}{\max\{n_{d1} + n_{d3}, n_{d2}\}} \right\} \quad (15)$$

and

$$\Delta''_{\text{LB}}(\mathbf{n}) = \max \left\{ \frac{1}{n_{d3} - n_{d2}}, \Delta'_{\text{LB}}(\mathbf{n}) \right\}. \quad (16)$$

Proof: (Theorem 1) Lower (converse) and upper bounds (achievability) on the DTB are derived for the case of active and inactive ($n_F = 0$) fronthaul links. Specifically, for the case of inactive fronthauling, we provide lower and upper bounds on the DTB in sub-sections IV-A and V-A through V-E, respectively, whereas we relegate the reader to sub-sections IV-B and V-F, respectively, for lower and upper bounds in case of active fronthauling. ■

We extract from Theorem 1 that the behavior in DTB in terms of the fronthaul capacity n_F changes in the intervals $[0, n_{d2}]$, $[n_{d2}, \max\{n_{d2}, n_{d3}\}]$ and $[\max\{n_{d2}, n_{d3}\}, \infty)$. The change in behavior occurs at cut-off/threshold fronthaul capacities n_{d2} and $\max\{n_{d2}, n_{d3}\}$. As shown in Fig. 3, there are in total four mutually exclusive *classes of channel regimes* for which the number and/or the magnitude of the threshold fronthaul capacities differ. We term these classes as Class I, II, III and IV for which the optimal DTB of Theorem 1 simplifies to:

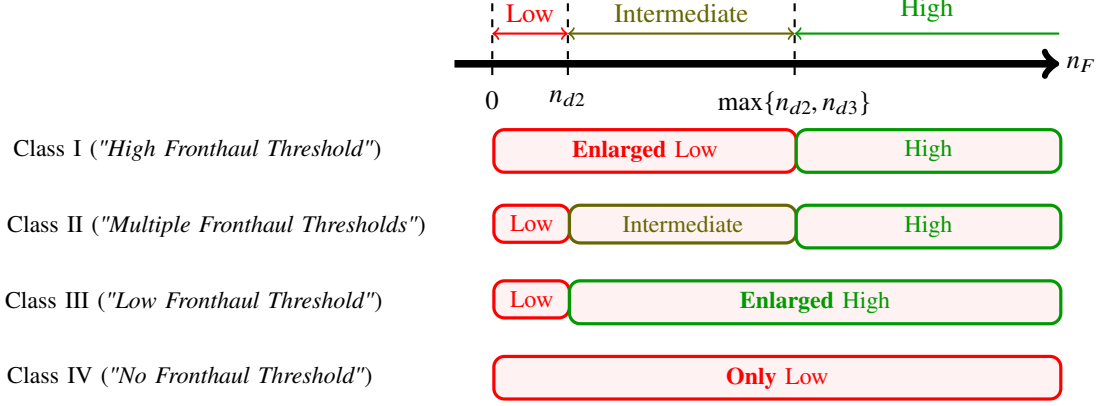


Fig. 3: The figure illustrates the differences between the four classes of channel regimes in terms of their number and magnitude of fronthaul capacity thresholds. In the fronthaul regimes for classes I, II, III and IV that are denoted as "Low", the DTB performance is as if the system operates with no fronthaul link in the delivery phase ($n_F = 0$).

- Class I (if $\mathbf{n} \in \{\mathcal{I}_0 \cap \{n_{d1} + n_{d3} \geq n_{d2}\}\} \cup \mathcal{I}_1$):

$$\Delta_{\text{det}}^*(\mu, n_F, \mathbf{n}) = \begin{cases} \max \left\{ \frac{2-\mu}{\max\{n_{d2}, n_{d3}\}}, \Delta'_{\text{LB}}(\mathbf{n}) \right\} & \text{for } n_F \leq \max\{n_{d2}, n_{d3}\} \\ \max \left\{ \frac{2-\mu}{n_F} + \left(1 - \frac{\max\{n_{d2}, n_{d3}\}}{n_F}\right) \Delta'_{\text{LB}}(\mathbf{n}), \Delta'_{\text{LB}}(\mathbf{n}) \right\} & \text{for } n_F \geq \max\{n_{d2}, n_{d3}\} \end{cases}, \quad (17)$$

- Class II (if $\mathbf{n} \in \{\mathcal{I}_1^C \cap \{\frac{1}{n_{d3}-n_{d2}} \geq \Delta'_{\text{LB}}(\mathbf{n})\} \cap \{\frac{1}{n_{d2}} \geq \Delta'_{\text{LB}}(\mathbf{n})\}\}$):

$$\Delta_{\text{det}}^*(\mu, n_F, \mathbf{n}) = \begin{cases} \max \left\{ \frac{1-\mu}{n_{d2}}, \frac{2-\mu}{n_{d3}}, \Delta'_{\text{LB}}(\mathbf{n}) \right\} & \text{for } n_F \leq n_{d2} \\ \max \left\{ \frac{1-\mu}{n_F} + \left(1 - \frac{n_{d2}}{n_F}\right) \Delta'_{\text{LB}}(\mathbf{n}), \frac{2-\mu}{n_{d3}}, \Delta'_{\text{LB}}(\mathbf{n}) \right\} & \text{for } n_{d2} \leq n_F \leq n_{d3} \\ \max \left\{ \frac{2-\mu}{n_F} + \left(1 - \frac{n_{d3}}{n_F}\right) \Delta'_{\text{LB}}(\mathbf{n}), \Delta'_{\text{LB}}(\mathbf{n}) \right\} & \text{for } n_F \geq n_{d3} \end{cases}, \quad (18)$$

- Class III (if $\mathbf{n} \in \{\mathcal{I}_1^C \cap \{\frac{1}{n_{d3}-n_{d2}} \leq \Delta'_{\text{LB}}(\mathbf{n})\} \cap \{\frac{1}{n_{d2}} \geq \Delta'_{\text{LB}}(\mathbf{n})\}\}$):

$$\Delta_{\text{det}}^*(\mu, n_F, \mathbf{n}) = \begin{cases} \max \left\{ \frac{1-\mu}{n_{d2}}, \Delta'_{\text{LB}}(\mathbf{n}) \right\} & \text{for } n_F \leq n_{d2} \\ \max \left\{ \frac{1-\mu}{n_F} + \left(1 - \frac{n_{d2}}{n_F}\right) \Delta'_{\text{LB}}(\mathbf{n}), \Delta'_{\text{LB}}(\mathbf{n}) \right\} & \text{for } n_F \geq n_{d2} \end{cases}, \quad (19)$$

- Class IV (if $\mathbf{n} \in \{\mathcal{I}_0^C \cup \{n_{d1} + n_{d3} \leq n_{d2}\}\} \cup \{\mathcal{I}_1^C \cap \{\frac{1}{n_{d2}} \leq \Delta'_{\text{LB}}(\mathbf{n})\}\}$):

$$\Delta_{\text{det}}^*(\mu, n_F, \mathbf{n}) = \Delta'_{\text{LB}}(\mathbf{n}) \quad \forall n_F. \quad (20)$$

The DTB for each of these classes including their characteristic corner points A_r , $r \in \{1, \dots, 4\}$, B_s , $s \in \{1, 2\}$ and C_1 are illustrated in Fig. 4. Note that $\Delta'_{\text{LB}}(\mathbf{n})$ is the *lowest* attainable DTB as

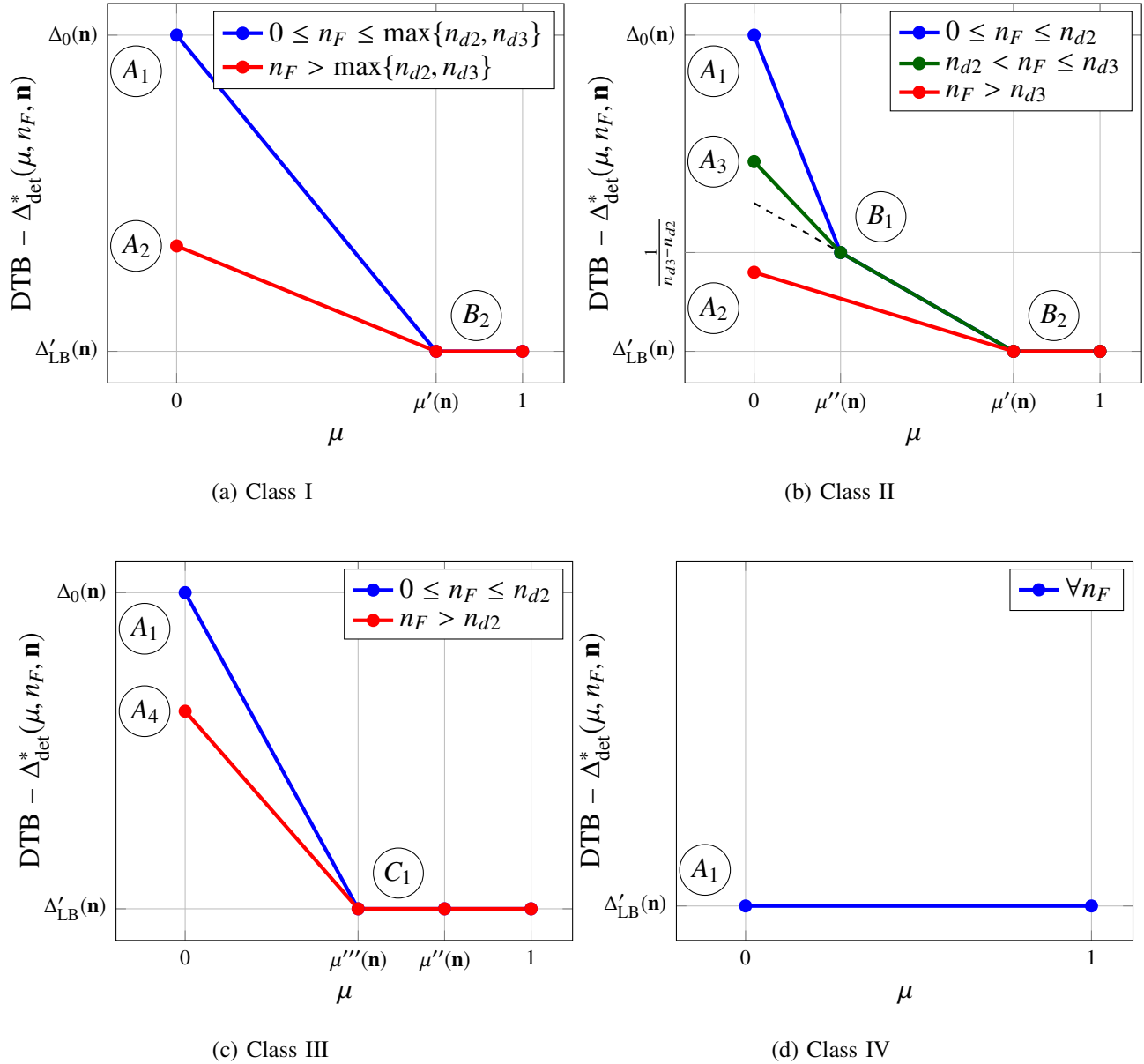


Fig. 4: DTB as a function of μ for four classes of channel regimes (Class I, II, III and IV) at distinct fronthaul capacities. In Fig. 4, depending on the operating channel regime, we use the notation A_r , $r \in \{1, \dots, 4\}$, B_s , $s \in \{1, 2\}$, and C_1 to denote corner points in the convex latency-memory curves.

shown in the figure. It is independent of μ and n_F such that neither an increase in the fractional cache size μ nor in the fronthaul capacity n_F can lead to any further decrease in the DTB. Instead it only depends on the given wireless channel parameters \mathbf{n} and as such characterizes the wireless bottleneck in the DTB. Thus, we term $\Delta'_{LB}(\mathbf{n})$ as the *wireless bottleneck DTB*. We now discuss our results through some remarks.

Remark 4 (Monotonously Decreasing DTB). In all classes of channel regimes specified in Eqs. (17), (18) and (19), edge caching and fronthauling decrease the DTB with increasing fractional cache size (cf. Fig. 4a–4c). At the threshold cache size $\mu_{\text{th}}(\mathbf{n})$ (e.g., in channel regimes of Class I and II: $\mu_{\text{th}}(\mathbf{n}) = \mu'(\mathbf{n})$), the lowest overall DTB corresponds to the wireless bottleneck DTB $\Delta'_{\text{LB}}(\mathbf{n})$. This incurred DTB is only governed by the wireless channel and thus cannot be further minimized by fronthaul-edge scheme adjustments². In other words, at this cache size prefetched information at the HeNB is just enough so that the requested files are transmitted directly over the wireless channel from eNB/HeNB to the users without requiring any fronthauling transmissions ($T_F = 0$). This observation is independent of the fronthaul capacity. When operating at any fractional cache size *below* $\mu_{\text{th}}(\mathbf{n})$, however, edge caching along with fronthauling reduces the latency further than a system without cloud processing ($n_F = 0$) either partially or entirely over the cache size range $[0, \mu_{\text{th}}(\mathbf{n})]$ as a function of the fronthaul capacity. For instance, in Class II channel regimes (cf. Fig 4b) where $n_{d3} \geq n_{d2}$, optimal cloud-and cache-based schemes with fronthaul links

(A) in the *medium-fronthaul capacity* range $(n_{d2}, \max\{n_{d2}, n_{d3}\}]$

(B) and in the *high-fronthaul capacity* range $(\max\{n_{d2}, n_{d3}\}, \infty)$

strictly outperform cache-only schemes

(A) partially in the sub-interval $[0, \mu''(\mathbf{n})]$ of $[0, \mu'(\mathbf{n})]$

(B) and entirely over the interval $[0, \mu'(\mathbf{n})]$.

As one would expect intuitively, we observe that for any fronthaul capacity the extent to which *serial* fronthauling (in addition to edge caching) reduces the latency to a system without cloud capabilities decays with increasing cache size.

Remark 5 (Constant DTB). In all channel regimes of Class IV (20), edge caching and/or fronthauling is not beneficial. This means that neither a large HeNB cache nor high-fronthaul capacities from cloud to the HeNB can lead to any latency improvement in comparison to the case for $\mu = 0, n_F = 0$. Consequently, only the eNB is involved in the transmission while the HeNB remains silent. As a result, the optimal latency corresponds to the optimal DTB given

²For instance, when $\mathbf{n} \in \{2n_{d3} \geq n_{d2} \geq n_{d1} \geq n_{d3}\}$, caching more than a fraction $\mu'(\mathbf{n}) = (2n_{d3} - n_{d2})/n_{d3}$ of any file will not lead to any improvement of the optimal DTB of $\Delta'_{\text{LB}}(\mathbf{n}) = 1/n_{d3}$. This is because in this case the wireless link from eNB to U_2 is able to carry at most n_{d3} bits per channel use; thus, representing the bottleneck.

in Lemma 2 for the broadcast channel, i.e., when $\Delta'_{\text{LB}}(\mathbf{n}) = \Delta_0(\mathbf{n})$. This includes all channel regimes for which broadcast and wireless bottleneck DTB are identical.

Remark 6 (Threshold Fronthaul Capacity $n_{F,\text{th}}$). We see from Theorem 1 that for low fronthaul capacities below a threshold $n_{F,\text{th}}$ (e.g. $n_{F,\text{th}} = n_{d2}$ for channel regimes of Class III), cache-only schemes remain optimal. This means that even though the fronthaul capacity is present/active, in DTB-sense the channel behaves as if the fronthaul link is absent in the delivery phase.

IV. SERIAL TRANSMISSION – LOWER BOUND

In this section, we develop lower bounds on the DTB for the cases of inactive (cf. IV-A) and active (cf. IV-B) fronthaul links. To this end, we specify two propositions applicable for either case. Details on the proofs can be found in the appendices A and B. First, we start with the case of inactive fronthaul links ($n_F = 0$).

A. Lower Bound (Converse) on the Minimum DTB for $n_F = 0$

Proposition 1 (Lower Bound on the Minimum DTB on Cache-Only F-RAN). For the LDM-based cloud and cache-aided HetNet in Fig. 1 with $n_F = 0$, the optimal DTB $\Delta_{\text{det}}^*(\mu, \mathbf{n})$ is lower bounded as

$$\Delta_{\text{det}}^*(\mu, \mathbf{n}) \geq \Delta_{\text{LB}}(\mu, \mathbf{n}), \quad (21)$$

where

$$\Delta_{\text{LB}}(\mu, \mathbf{n}) = \max \left\{ \frac{1}{n_{d3}}, \frac{1}{\max\{n_{d1}, n_{d2}\}}, \frac{2}{\max\{n_{d1} + n_{d3}, n_{d2}\}}, \frac{1 - \mu}{n_{d2}}, \frac{2 - \mu}{\max\{n_{d2}, n_{d3}\}} \right\}. \quad (22)$$

Proof: The proof of Proposition 1 is presented in Appendix A. Shortly, the first three bounds inside the outer max-expression leverage the fact that reliable decoding of the user's requested files is feasible through the user's received signal(s) spanning T_E channel uses. The remaining two bounds use two distinct combinations of cached and wireless information enabling reliable decoding of requested files to establish two lower bounds on the wireless delivery time T_E and ultimately on the DTB as a function of μ when $n_F = 0$. For instance, any receiver can decode the user's requested files as long as they are aware of the information subset $\{\mathbf{S}^{q - \max\{n_{d2}, n_{d3}\}} \mathbf{x}_2^{T_E}, S_{d1}, S_{d2}\}$. ■

B. Lower Bound (Converse) on the Minimum DTB for $n_F \geq 0$

We now state the DTB lower bound for the more general case of active fronthaul links ($n_F \geq 0$) through the following proposition.

Proposition 2 (Lower Bound on the Minimum DTB). For the LDM-based cloud and cache-aided HetNet in Fig. 1 with $n_F \geq 0$, the optimal DTB $\Delta_{\text{det}}^*(\mu, n_F, \mathbf{n})$ is lower bounded as

$$\Delta_{\text{det}}^*(\mu, n_F, \mathbf{n}) \geq \Delta_{\text{LB}}(\mu, n_F, \mathbf{n}), \quad (23)$$

where $\Delta_{\text{LB}}(\mu, n_F, \mathbf{n})$ is the solution of the linear optimization problem

$$\underset{\Delta_E, \Delta_F}{\text{minimize}} \quad \Delta_E + \Delta_F \quad (24a)$$

$$\text{subject to} \quad \Delta_E + \Delta_F \frac{n_F}{\max\{n_{d2}, n_{d3}\}} \geq \frac{2 - \mu}{\max\{n_{d2}, n_{d3}\}} \quad (24b)$$

$$\Delta_E + \Delta_F \frac{n_F}{n_{d2}} \geq \frac{1 - \mu}{n_{d2}} \quad (24c)$$

$$\Delta_E \geq \max \left\{ \frac{1}{n_{d3}}, \frac{1}{\max\{n_{d1}, n_{d2}\}}, \frac{2}{\max\{n_{d1} + n_{d3}, n_{d2}\}} \right\} \quad (24d)$$

$$\Delta_F \geq 0 \quad (24e)$$

and Δ_E and Δ_F denoting the individual DTBs of wireless and fronthaul transmissions, respectively.

Proof: The proof of Proposition 2 is presented in Appendix B. ■

We next present multiple corollaries that specialize the lower bound of Proposition 2 to different settings of fronthaul capacities n_F .

Corollary 1 (Lower Bound for Low-Fronthaul Capacity Regime). For the F-RAN under study in the low-fronthaul capacity regime with $n_F \leq n_{d2}$, the DTB is lower bounded as

$$\Delta_{\text{det}}^*(\mu, n_F, \mathbf{n}) \geq \max \left\{ \frac{1}{n_{d3}}, \frac{1}{\max\{n_{d1}, n_{d2}\}}, \frac{2}{\max\{n_{d1} + n_{d3}, n_{d2}\}}, \frac{1 - \mu}{n_{d2}}, \frac{2 - \mu}{\max\{n_{d2}, n_{d3}\}} \right\}. \quad (25)$$

Proof: We note that the lower bound on the wireless DTB Δ_E (see (24d)) is also a valid bound on the DTB $\Delta_E + \Delta_F$ due to the non-negativity of the fronthaul DTB Δ_F (cf. (24e)). Furthermore, for $n_F \leq n_{d2}$ the left-hand side (LHS) of (24b) and (24c) are upper bounded by the overall DTB $\Delta_E + \Delta_F$. Thus, (24b)–(24d) are all active lower bounds on the DTB. This concludes the proof. ■

Remark 7. We see that the lower bound on the DTB $\Delta_E + \Delta_F$ in (25) coincides with the lower bound on Δ_E for $n_F = 0$ in Proposition 1. This means in DTB sense that in the low-fronthaul capacity regime $n_F \leq n_{d2}$, the network behaves as if the fronthaul link is non-existent.

Corollary 2 (Lower Bound for High-Fronthaul Capacity Regime). For the F-RAN under study in the high-fronthaul capacity regime with $n_F \geq \max\{n_{d2}, n_{d3}\}$, the DTB is lower bounded as

$$\Delta_{\text{det}}^*(\mu, n_F, \mathbf{n}) \geq \max \left\{ \frac{2 - \mu}{n_F} + \left(1 - \frac{\max\{n_{d2}, n_{d3}\}}{n_F} \right) \Delta'_{\text{LB}}(\mathbf{n}), \right. \\ \left. \frac{1 - \mu}{n_F} + \left(1 - \frac{n_{d2}}{n_F} \right) \Delta'_{\text{LB}}(\mathbf{n}), \Delta'_{\text{LB}}(\mathbf{n}) \right\}, \quad (26)$$

where $\Delta'_{\text{LB}}(\mathbf{n})$ is defined in (15).

Proof: First, we note that $\Delta'_{\text{LB}}(\mathbf{n})$ is identical to the right-hand side (RHS) of (24d). This bound is a valid bound on the DTB $\Delta_E + \Delta_F$. For $n_F \geq \max\{n_{d2}, n_{d3}\}$, we combine (24b) and (24c) with (24d), which yields

$$\Delta_E + \Delta_F \geq \frac{2 - \mu}{n_F} + \left(1 - \frac{\max\{n_{d2}, n_{d3}\}}{n_F} \right) \Delta'_{\text{LB}}(\mathbf{n}) \quad (27a)$$

$$\Delta_E + \Delta_F \geq \frac{1 - \mu}{n_F} + \left(1 - \frac{n_{d2}}{n_F} \right) \Delta'_{\text{LB}}(\mathbf{n}). \quad (27b)$$

The RHSs of inequalities (27a), (27b) and (24d) result in (26) of Corollary 2. ■

Corollary 3 (Lower Bound for Medium-Fronthaul Capacity Regime in \mathcal{I}_1). For the F-RAN under study in the medium-fronthaul capacity regime $n_F \in [n_{d2}, \max\{n_{d2}, n_{d3}\}]$ and channel regime $\mathbf{n} \in \mathcal{I}_1$, the DTB is lower bounded as

$$\Delta_{\text{det}}^*(\mu, n_F, \mathbf{n}) \geq \max \left\{ \frac{2 - \mu}{n_{d3}}, \Delta'_{\text{LB}}(\mathbf{n}) \right\}, \quad (28)$$

where $\Delta'_{\text{LB}}(\mathbf{n})$ is defined in (15).

Proof: We observe that for $n_F \leq \max\{n_{d2}, n_{d3}\}$, $\Delta_E + \Delta_F$ is an upper bound on the LHS of (24b). For $\mathbf{n} \in \mathcal{I}_1$, it is easy to see that for any $\mu \in [0, 1]$

$$\Delta_E + \Delta_F \geq \frac{2 - \mu}{n_{d3}} \geq \frac{1 - \mu}{n_{d2}} \quad (29)$$

holds. Thus, only (24b) and (24d) are active lower bounds on the DTB. Combining these two bounds leads to (28). ■

Corollary 4 (Lower Bound for Medium-Fronthaul Capacity Regime in \mathcal{I}_1^C). For the F-RAN under study in the medium-fronthaul capacity regime $n_F \in [n_{d2}, \max\{n_{d2}, n_{d3}\}]$ and channel regime $\mathbf{n} \in \mathcal{I}_1^C$, the DTB is lower bounded as

$$\Delta_{\text{det}}^*(\mu, n_F, \mathbf{n}) \geq \begin{cases} \frac{1-\mu}{n_F} + \left(1 - \frac{n_{d2}}{n_F}\right) \Delta''_{\text{LB}}(\mathbf{n}) & \text{for } \mu \leq \mu''(\mathbf{n}) \\ \max\left\{\frac{2-\mu}{n_{d3}}, \Delta'_{\text{LB}}(\mathbf{n})\right\} & \text{for } \mu \geq \mu''(\mathbf{n}) \end{cases}, \quad (30)$$

where $\Delta'_{\text{LB}}(\mathbf{n})$ is defined in (15) and $\Delta''_{\text{LB}}(\mathbf{n})$ equals

$$\Delta''_{\text{LB}}(\mathbf{n}) = \max\left\{\frac{1}{n_{d3} - n_{d2}}, \Delta'_{\text{LB}}(\mathbf{n})\right\}. \quad (31)$$

Proof: We observe that for $n_F \leq n_{d3}$, $\Delta_E + \Delta_F$ is an upper bound on the LHS of (24b). For $\mathbf{n} \in \mathcal{I}_1^C$, one can show that for any $\mu \in [\mu''(\mathbf{n}), 1]$

$$\Delta_E + \Delta_F \geq \frac{2-\mu}{n_{d3}} \geq \frac{1-\mu}{n_{d2}} \quad (32)$$

holds. We infer that for this case only (24b) and (24d) are active lower bounds on the DTB. Combining these two bounds leads to the second case of (30). For $\mu \in [0, \mu''(\mathbf{n})]$, on the other hand, we bound (24b) as follows:

$$\Delta_E + \Delta_F \geq \Delta_E + \Delta_F \frac{n_F}{n_{d3}} \geq \Delta_E \geq \frac{2-\mu}{n_{d3}} \geq \frac{2-\mu}{n_{d3}} \Big|_{\mu=\mu''(\mathbf{n})} = \frac{1}{n_{d3} - n_{d2}} \quad (33)$$

Using (33) and (24d) together gives us a new lower bound (31) on Δ_E . We obtain a bound on the DTB by combining (31) and (24c). This concludes the proof. ■

V. SERIAL TRANSMISSION – UPPER BOUND

In this section, we present the upper bounds on the DTB for the cases of active and inactive fronthaul links. In the respective sub-sections, we introduce transmission schemes which achieve the optimal DTB provided in Theorem 1 (cf. Fig. 4). To this end, various schemes are proposed to cover different operating channel regimes of the network under study. Initially, we will focus on the cache-only ($n_F = 0$) case. This will turn to be useful when considering the achievability in the more general setting of non-negative fronthaul capacity links ($n_F \geq 0$) in sub-section V-F. Due to the convexity of the DTB (cf. Lemma 1), we establish the achievability of corner points in the latency-cache tradeoff curves. In Fig. 4, depending on the operating channel regime, these corner points are denoted by A_r , $r \in \{1, \dots, 4\}$, B_s , $s \in \{1, 2\}$, and C_1 . In this regard, we will show that corner points

- A_1, B_1, B_2 and C_1 involve only edge caching and do not require any fronthaul transmission ($n_F = 0$); thus, representing cache-only transmission policies, whereas
- $A_r, r \in \{2, 3, 4\}$, involve only fronthauling and do not require edge caching ($\mu = 0$); thus, representing cloud-only transmission policies.

Generally speaking, the DTB at fractional cache size μ which lies between two neighboring corner points (say D and E) cache sizes' is achieved through file splitting and time sharing between the policies at corner points D and E . This strategy is only operational at a channel regime under which the transmission policy at D , \mathcal{R}_D , and the transmission policy at E , \mathcal{R}_E are *both* feasible. This is given by the *non-empty* set $\mathcal{R}_D \cap \mathcal{R}_E$.

A. Establishing Upper Bound (Achievability) for $n_F = 0$ through Rate Maximization

We propose a transmission scheme which minimizes the delivery time per bit Δ_{det} for $n_F = 0$ and $\mu > 0$ under various channel regimes. To this end, we determine the best possible achievability scheme by solving a *per-user* rate maximization problem. In fact, minimizing the DTB is equivalent to *maximizing* the number of *desired* bits \bar{L} that are conveyed to U_1 and U_2 in *one* channel use. Essentially, our proposed transmission scheme seeks to determine the optimal vector of design variables³ \mathbf{r}^* that solves the following two *equivalent* optimization problems

$$\min_{\mathbf{r}} \Delta_{\text{det}}(\mathbf{r}) \qquad \max_{\mathbf{r}} \bar{L}(\mathbf{r})$$

for which the optimum becomes $\Delta_{\text{det}}^* = 1/\bar{L}^*$. The components of the design vector \mathbf{r} will be specified later after we present the general transmission scheme. The solution to above optimization problem reveals the DTB-achievability at corner points B_1, B_2 and C_1 . The achievability of corner point A_1 readily follows from Lemma 2. Remaining intermediate points in the tradeoff curves on the DTB follow from the argument of convexity (cf. Lemma 1). But before we describe the schemes for various channel regimes in detail, we suggest a general building block structure in the next section V-B that all schemes have in common. This block structure is applicable to cache-only schemes ($n_F = 0$) for $\mu > 0$.

³These design variables are in fact rate allocation parameters as we shall see later.

B. Building Blocks ($n_F = 0$)

Due to the partial wireless connectivity of the network under study, in which only the eNB is connected to both users while the HeNB is only connected to U_1 , we propose that the eNB sends

- private information
 - $\mathbf{w}_{1,p}[t]$, $w \in \{u, v\}$ intended for either U_1 if $w = u$ or for U_2 if $w = v$,
- common information
 - $\mathbf{u}_c[t]$ intended for U_1
 - $\mathbf{v}_c[t]$ intended for U_2 ,
- and interference neutralizing information
 - $\mathbf{v}_{\text{IN}}[t]$ intended for U_2 ,

while the HeNB transmits

- additional private information $\mathbf{u}_{2,p}[t]$ intended for U_2
- and XORed information $\mathbf{n}_{\text{IN}}[t] \triangleq \mathbf{v}_{\text{IN}}[t] \oplus \mathbf{u}_{\text{IN}}[t]$ for interference neutralization

(in the t -th channel use ($t = 1, \dots, T_E$)), where in all schemes $\mathbf{n}_{\text{IN}}[t] = \mathbf{v}_{\text{IN}}[t] \oplus \mathbf{u}_{\text{IN}}[t]$ is introduced such that the interference caused by the signal $\mathbf{v}_{\text{IN}}[t]$ is completely neutralized at U_1 . Depending on the particular channel regime, certain signal levels are zero-padded to either avoid collision of private and common information at U_1 or to reduce the transmission power level of the HeNB. More details will follow as we elaborate on the encoding (see section V-C) and the decoding (see section V-D) procedure. In the LDM, this is captured by null vectors $\mathbf{0}_l$ of length l . Since we are interested in maximizing \bar{L} , we focus on transmission schemes that utilize a single channel use $T_E = 1$. Thus, in the sequel, we drop the time dependency in our notation. We denote the length of signal vectors $\mathbf{w}_{1,p}$, $\mathbf{u}_{2,p}$, \mathbf{u}_c , \mathbf{v}_c , \mathbf{v}_{IN} and \mathbf{n}_{IN} by $R_{1,p}^w$, $R_{2,p}^u$, R_c^u , R_c^v , R_{IN}^v and R_{IN}^n , respectively. In the sequel, we will differentiate between DTB-optimal schemes for (a) strong cross-link (SCL) channel regimes and (b) weak cross-link regimes⁴ (WCL). We now move to the description of the encoding at the transmitters.

⁴SCL and WCL channel regimes include cases where either the cross-link is stronger or weaker than the eNB- U_2 link, i.e., $n_{d2} \geq n_{d3}$ or $n_{d2} \leq n_{d3}$, respectively.

C. Encoding at the Transmitters ($n_F = 0$)

The transmission signal of the HeNB and eNB use the signal vectors described in section V-B according to:

$$\mathbf{x}_1 = \begin{pmatrix} \mathbf{0}_{l_4} \\ \mathbf{u}_{2,p} \\ \mathbf{0}_{l_3} \\ \mathbf{n}_{\text{IN}} \\ \mathbf{0}_{l_2} \end{pmatrix}, \quad \mathbf{x}_2 = \begin{pmatrix} \mathbf{u}_c \\ \mathbf{v}_c \\ \mathbf{v}_{\text{IN}} \\ \mathbf{w}_{1,p} \\ \mathbf{0}_{l_1} \end{pmatrix} \text{ for } w \in \{u, v\}. \quad (34)$$

As shown in Figs. 5 and 6 private information $\mathbf{w}_{1,p}$ corresponds to $\mathbf{u}_{1,p}$ in the SCL case ($n_{d2} \geq n_{d3}$) and to $\mathbf{v}_{1,p}$ in the WCL case ($n_{d2} \leq n_{d3}$). For $q = \max\{n_{d1}, n_{d2}, n_{d3}\}$, it is obvious that the eNB, on the one hand, can generate its signal vector \mathbf{x}_2 as long as

$$l_1 + R_{1,p}^w + R_{\text{IN}}^v + R_c^v + R_c^u \leq q, \quad (35)$$

while the HeNB, on the other hand, can construct its signal vector \mathbf{x}_1 only if

$$l_2 + l_3 + l_4 + R_{2,p}^u + R_{\text{IN}}^n \leq q, \quad (36)$$

$$R_{2,p}^u + R_{\text{IN}}^n \leq \mu \bar{L}. \quad (37)$$

The condition (37) guarantees that the HeNB is endowed with a finite-size cache of fractional size μ . Next, we outline the decoding strategy for both users.

D. Decoding at the Receivers ($n_F = 0$)

The transmission according to the block structure of Eq. (34) requires that at the respective receivers interference-decoding and treating interference as noise (TIN) is applied successively. The received signal vectors at U_1 and U_2 are shown in Figs. 5 and 6 for the SCL ($n_{d2} \geq n_{d3}$) and WCL ($n_{d2} \leq n_{d3}$) case, respectively. In what follows, we will specify the conditions under which both U_1 and U_2 can decode their desired signal components *reliably*.

First, let us consider U_2 . This receiver is interested in retrieving \mathbf{v}_c , \mathbf{v}_{IN} and $\mathbf{w}_{1,p}$ if $w = v$ from its received signal $\mathbf{S}^{q-n_{d3}} \mathbf{x}_2$. Successive decoding, however, starting from the top-most significant bit levels necessitates that prior to decoding these signals, the undesired common signal vector

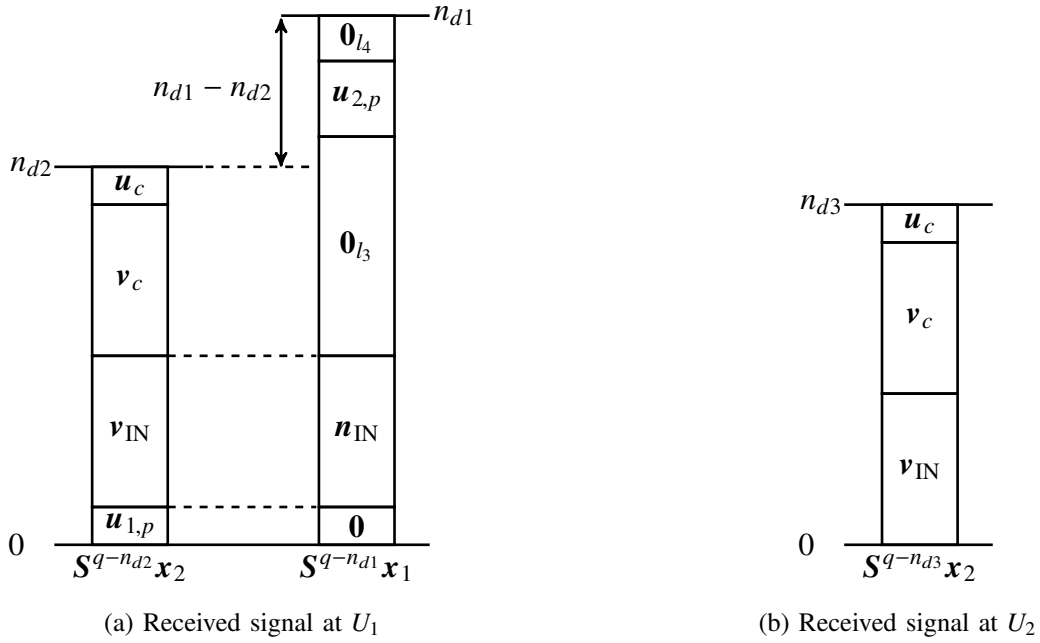


Fig. 5: The received signal vector of (a) U_1 and (b) U_2 are shown for the SCL case $n_{d2} \geq n_{d3}$. In the SCL case, we fix $\mathbf{w}_{1,p} = \mathbf{u}_{1,p}$. Note that U_1 receives the superposition $\mathbf{S}^{q-n_{d1}} \mathbf{x}_1 \oplus \mathbf{S}^{q-n_{d2}} \mathbf{x}_2$.

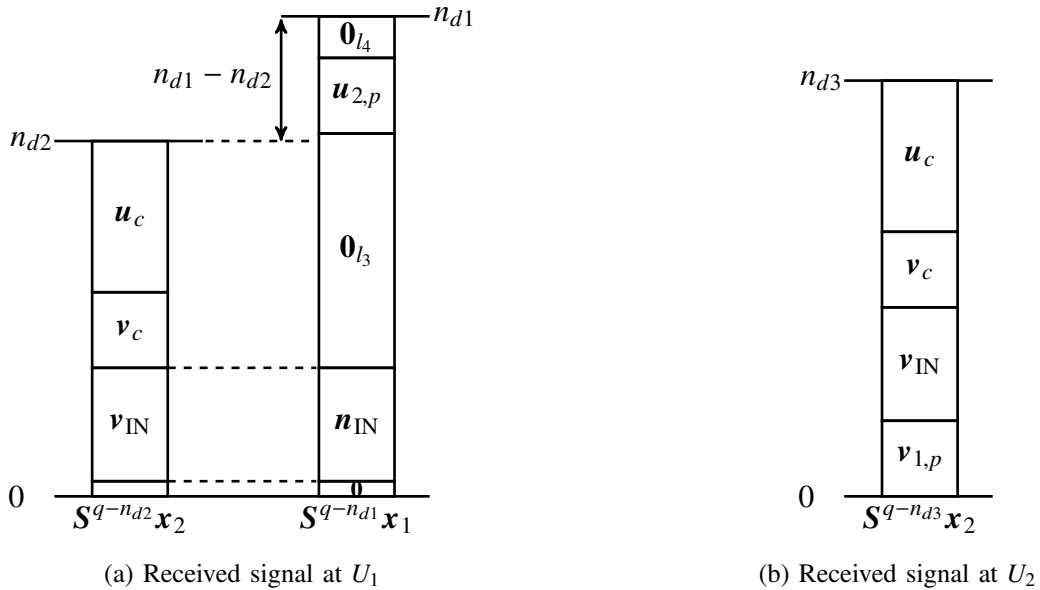


Fig. 6: The received signal vector of (a) U_1 and (b) U_2 are shown for the WCL case $n_{d2} \leq n_{d3}$. In the WCL case, we fix $\mathbf{w}_{1,p} = \mathbf{v}_{1,p}$. Note that U_1 receives the superposition $\mathbf{S}^{q-n_{d1}} \mathbf{x}_1 \oplus \mathbf{S}^{q-n_{d2}} \mathbf{x}_2$.

\mathbf{u}_c has to be decoded and canceled from the received signal vector $\mathbf{S}^{q-n_{d3}}\mathbf{x}_2$. Thus, U_2 can only decode \mathbf{v}_c , \mathbf{v}_{IN} and $\mathbf{w}_{1,p}$ if $w = v$ (cf. Figs. 5b and 6b), as long as

$$\begin{cases} R_c^u + R_c^v + R_{\text{IN}}^v \leq n_{d3} & \text{if } n_{d2} \geq n_{d3} \\ R_c^u + R_c^v + R_{\text{IN}}^v + R_{1,p}^w \leq n_{d3} & \text{if } n_{d2} \leq n_{d3} \end{cases}. \quad (38)$$

We now move to state the reliability conditions for U_1 . Recall that U_1 receives the superposition $\mathbf{S}^{q-n_{d1}}\mathbf{x}_1 \oplus \mathbf{S}^{q-n_{d2}}\mathbf{x}_2$ and aims at obtaining $\mathbf{u}_{2,p}$, \mathbf{u}_c and $\mathbf{w}_{1,p}$ if $w = u$ directly as well as \mathbf{u}_{IN} indirectly by superimposing \mathbf{v}_{IN} and $\mathbf{n}_{\text{IN}} = \mathbf{v}_{\text{IN}} \oplus \mathbf{u}_{\text{IN}}$. Similarly to U_2 's condition (38), we infer that the individual signals $\mathbf{S}^{q-n_{d1}}\mathbf{x}_1$ and $\mathbf{S}^{q-n_{d2}}\mathbf{x}_2$ have to be able to carry the set of signal components $\{\mathbf{n}_{\text{IN}}, \mathbf{u}_{2,p}\}$ and $\{\mathbf{w}_{1,p}, \mathbf{v}_{\text{IN}}, \mathbf{v}_c, \mathbf{u}_c\}$ if $w = u$ and only $\{\mathbf{v}_{\text{IN}}, \mathbf{v}_c, \mathbf{u}_c\}$ if $w = v$, respectively, i.e.,

$$l_3 + l_4 + R_{2,p}^u + R_{\text{IN}}^n \leq n_{d1}, \quad (39)$$

$$\begin{cases} R_{1,p}^w + R_{\text{IN}}^v + R_c^v + R_c^u \leq n_{d2} & \text{if } n_{d2} \geq n_{d3} \\ R_{\text{IN}}^v + R_c^v + R_c^u \leq n_{d2} & \text{if } n_{d2} \leq n_{d3} \end{cases}, \quad (40)$$

such that the desired signals $\mathbf{u}_{2,p}$, \mathbf{u}_c , \mathbf{u}_{IN} and $\mathbf{w}_{1,p}$ if $w = u$ are all received above noise level. The remaining conditions specify how overlaps between desired components are precluded. We avoid an overlap between $\mathbf{u}_{2,p}$ and \mathbf{u}_c if

$$l_4 + R_{2,p}^u \leq (n_{d1} - n_{d2})^+ \quad (41)$$

is satisfied. As shown in Figs. 5a and 6a, full interference neutralization by superposing \mathbf{v}_{IN} and \mathbf{n}_{IN} is ensured if on the one hand the lowest bit levels of \mathbf{v}_{IN} and \mathbf{n}_{IN} are aligned, i.e.,

$$R_c^u + R_c^v + R_{\text{IN}}^v + n_{d1} - n_{d2} = l_3 + l_4 + R_{\text{IN}}^n + R_{2,p}^u, \quad (42)$$

and, on the other hand, the allocated number of bits for \mathbf{v}_{IN} and \mathbf{n}_{IN} are identical, i.e.,

$$R_{\text{IN}}^v = R_{\text{IN}}^n. \quad (43)$$

We point out that through the alignment conditions (42) and (43), overlaps between $\mathbf{w}_{1,p}$ and \mathbf{n}_{IN} are prohibited. When all conditions (35)–(43) are satisfied, the achievable rates of U_1 and

U_2 become

$$R_{U_1} = \begin{cases} R_{2,p}^u + R_c^u + R_{\text{IN}}^n + R_{1,p}^w & \text{if } n_{d2} \geq n_{d3} \\ R_{2,p}^u + R_c^u + R_{\text{IN}}^n & \text{if } n_{d2} \leq n_{d3} \end{cases}, \quad (44a)$$

$$R_{U_2} = \begin{cases} R_c^v + R_{\text{IN}}^v & \text{if } n_{d2} \geq n_{d3} \\ R_c^v + R_{\text{IN}}^v + R_{1,p}^w & \text{if } n_{d2} \leq n_{d3} \end{cases}, \quad (44b)$$

respectively.

E. Maximizing \bar{L} ($n_F = 0$)

Through sections V-C–V-D, we were able to formulate conditions for feasible encoding and decoding at given fractional cache size μ for $n_F = 0$. We now formulate the underlying optimization problem to establish the achievability. Recall that our scheme maximizes \bar{L} by determining the optimal vector of design variables \mathbf{r}^* . The design parameters of our scheme are the rate allocation parameters and the respective null vectors. To this end, all design parameters are combined to the vector

$$\mathbf{r} = \left(R_{1,p}^w, R_{2,p}^u, R_c^u, R_{\text{IN}}^v, R_c^v, R_{\text{IN}}^n, l_1, l_2, l_3, l_4 \right)^T.$$

We then solve the following linear optimization problem:

$$\begin{aligned} \max_{\mathbf{r}} \quad & \bar{L} \triangleq \min\{R_{U_1}, R_{U_2}\} \\ \text{s.t.} \quad & (35)\text{--}(43) \text{ are satisfied,} \\ & \mathbf{r} \geq \mathbf{0}. \end{aligned} \quad (45)$$

In the sequel, we will solve the optimization problem for various SCL and WCL channel regimes and thus determine \bar{L}^* . Recall that this means that at most $\Delta_{\text{det}}(\mu, n_F = 0, \mathbf{n}) = 1/\bar{L}^*$ channel uses are required to provide each user with a single bit. Before we solve the problem (45) for SCL and WCL channel regimes, we will exemplify our scheme for a specific SCL and WCL channel setting.

Example 1 (Class I SCL channel regime). In this example, we consider the channel $\mathbf{n} = (2, 5, 4)^T$ for $n_F = 0$. This channel belongs to the Class I SCL channel regime. Theorem 1 gives us the broadcast corner point $A_1 = \left(\mu = 0, \Delta_{\text{det}}^*(\mu = 0, n_F = 0, \mathbf{n}) = 2/5 \right)$ and the wireless bottleneck corner point $B_2 = \left(\mu' = 1/3, \Delta_{\text{det}}^*(\mu = 1/3, n_F = 0, \mathbf{n}) = 1/3 \right)$.

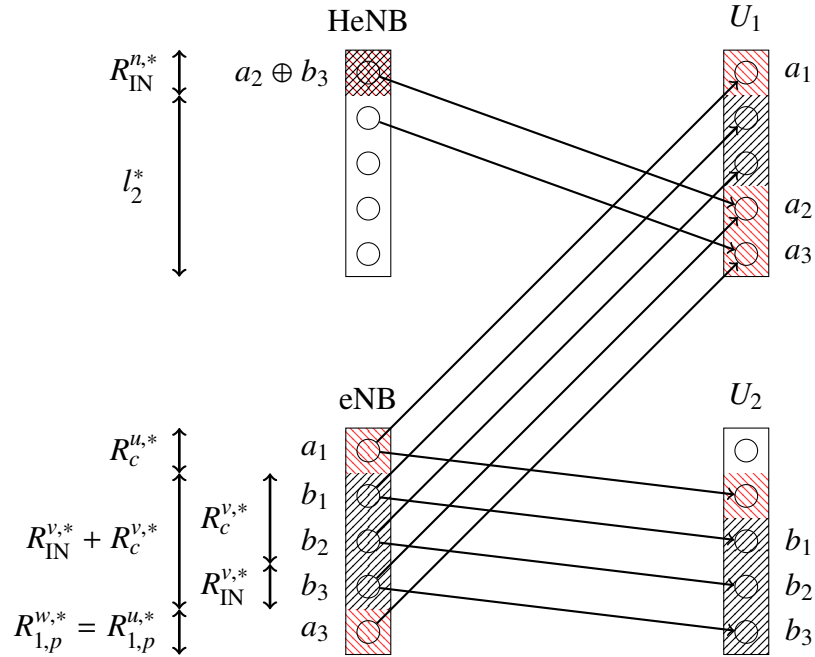


Fig. 7: Example of proposed scheme for $n_{d1} = 2$, $n_{d2} = 5$ and $n_{d3} = 4$. The cached content of the HeNB on the requested files W_{d1} and W_{d2} are $S_{d1} = (a_2)$ and $S_{d2} = (b_3)$. This corresponds to a fractional cache size of $\mu'(\mathbf{n}) = 1/3$.

At extreme point A_1 neither fronthauling nor edge caching involving the HeNB is performed. Thus, the F-RAN under study reduces to a broadcast channel in which the eNB is responsible for transmitting the requested files while the HeNB remains silent. Thus, the only relevant channel realizations are the eNB- U_1 and eNB- U_2 links with $n_{d2} = 5$ and $n_{d3} = 4$. We observe that the stronger of those two channels is the eNB- U_1 link with $n_{d2} = 5$ ($n_{d3} \leq n_{d2}$). The optimal scheme equally distributes the transmission load of $n_{d2} = 5$ bits to both users. That is, by sending $n_{d2}/2 = 5/2$ desired information bits in a single channel use; or, alternatively by sending one desired bit in $\Delta_{\det}^*(\mu = 0, n_F = 0, \mathbf{n}) = 2/5$ channel uses, to U_1 and U_2 , respectively. This scheme is feasible since the weaker channel n_{d3} supports the transmission of $n_{d2}/2$ bits ($n_{d2}/2 \leq n_{d3}$). These conditions are equivalent with the broadcast condition $\mathbf{n} \in \mathcal{I}_0$. We refer to the proof of Lemma 2 and Remark 3 for further details on this scheme.

The extreme point B_2 is achievable through a cache-only transmission scheme. It requires one channel use and achieves the wireless bottleneck DTB of $2/(n_{d1} + n_{d3}) = 1/3$ at fractional cache size $\mu'(\mathbf{n}) = (2n_{d1} + 2n_{d3} - 2n_{d2})/(n_{d1} + n_{d3}) = 1/3$. Fig. 7 illustrates the scheme for the case when U_1 and U_2 request $W_{d1} = (a_1, a_2, a_3)$ and $W_{d2} = (b_1, b_2, b_3)$, respectively. In this case where the channel of

the cross link n_{d2} is the strongest, it is advantageous that the eNB transmits not only common information to U_2 but also private and common information to U_1 . This implies that the rates $R_{1,w}^u$ and R_c^u are chosen to be non-zero whereas $l_1^* = 0$. When we fix $R_{\text{IN}}^{v,*} + R_c^{v,*} = (n_{d1} + n_{d3})/2 = 3$ all bits (b_1, b_2 and b_3) of W_{d2} are conveyed to U_2 . Note that the eNB- U_2 link is capable of reliably carrying $R_{\text{IN}}^{v,*} + R_c^{v,*} = 3$ bits to U_2 because $R_{\text{IN}}^{v,*} + R_c^{v,*} = 3 < n_{d3} = 4$ holds. The unused signal levels at the eNB of rate $R_c^{u,*} = (n_{d3} - n_{d1})/2 = 1$ and $R_{1,p}^{w,*} = n_{d2} - n_{d3} = 1$ are allocated to send common information a_1 and private information a_3 to U_1 , respectively. To retrieve the remaining desired bit of U_1 (a_2), the interfering bit b_3 of v_{IN} is neutralized by sending the single XOR combination ($R_{\text{IN}}^{n,*} = n_{d1} + n_{d3} - n_{d2} = 1$) $a_2 \oplus b_3$ at the *highest* signal level of the HeNB. This is feasible since the HeNB retains a_2 and b_3 separately in its cache during the placement phase. This constitutes a fractional cache size $\mu'(\mathbf{n}) = 1/3$. With this strategy, U_1 receives $R_{1,p}^{w,*} + R_c^{u,*} = (2n_{d2} - n_{d1} - n_{d3})/2 = 2$ bits (a_1 and a_3) of W_{d1} from the eNB while the remaining $R_{\text{IN}}^{n,*} = n_{d1} + n_{d3} - n_{d2} = 1$ bits (a_2) are received through network coding which involves both HeNB and eNB. Since the HeNB's fractional cache size is $1/3$, the HeNB cannot send any additional private information. For that reason, $R_{2,p}^{u,*} = l_3^* = l_4^* = 0$ and $l_2^* = 2n_{d2} - n_{d1} - n_{d3} = 4$. Interestingly, as shown in Fig. 7 increasing the fractional cache size by some $\epsilon > 0$ to $\mu'(\mathbf{n}) + \epsilon$ cannot decrease the DTB any further. This is due to the fact that additional ϵ information on the requested files at the HeNB cannot be constructively used for extra interference neutralization. E.g., using the second most significant bit level at the HeNB in Fig. 7 for transmission can only distort the desired bit a_3 which U_1 already receives. This observation justifies why the DTB remains constant for $\mu > \mu'(\mathbf{n})$ as illustrated in Fig. 4a.

Any point between the two corner points A_1 and B_2 is achieved through file splitting and time sharing between the policies at those two corner points. Such scheme is often termed *memory sharing*.

Example 2 (Class I WCL channel regime). In this example, we consider the channel $\mathbf{n} = (2, 5, 6)^T$ for $n_F = 0$. This channel belongs to the Class I WCL channel regime. Theorem 1 gives us the corner points $A_1 = \left(\mu = 0, \Delta_{\text{det}}^*(\mu = 0, n_F = 0, \mathbf{n}) = 1/3 \right)$ and $B_2 = \left(\mu' = 1/2, \Delta_{\text{det}}^*(\mu = 1/2, n_F = 0, \mathbf{n}) = 1/4 \right)$. At extreme point A_1 , we apply a similar broadcasting scheme as in example 1 for $\mu = 0$. Recall that for $\mu = 0, n_F = 0$, the F-RAN under study simplifies to a broadcast channel in which the eNB is solely responsible for transmitting the requested files. In comparison to example 1, however, the difference is that now out of the two channel links – eNB- U_1 and

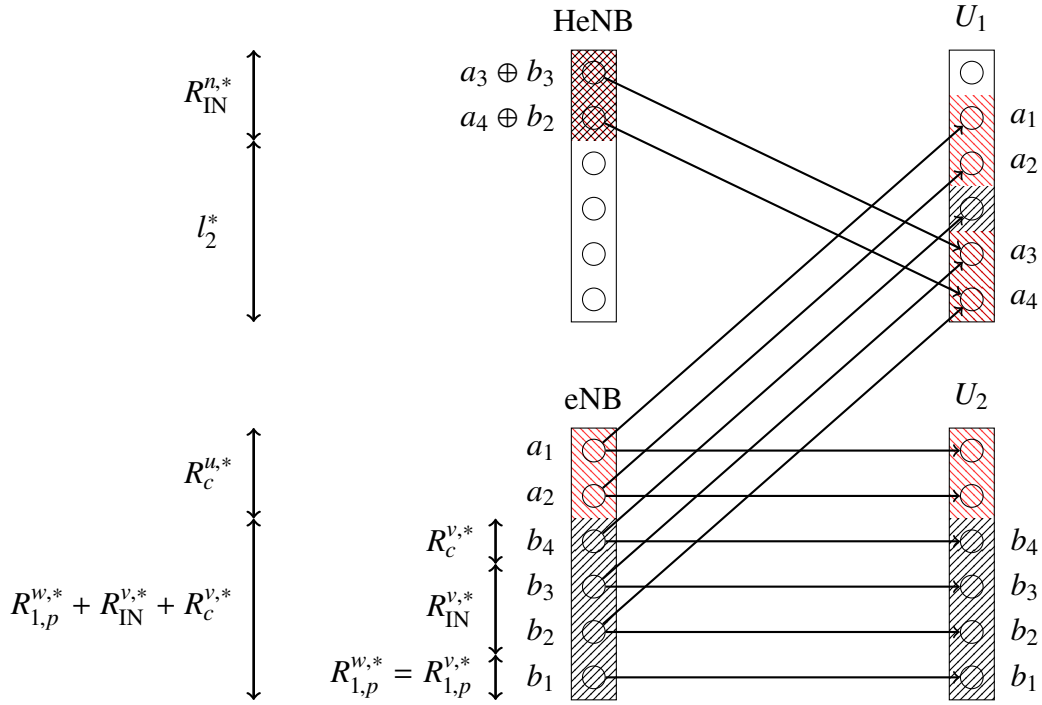


Fig. 8: Example of proposed scheme for $n_{d1} = 2$, $n_{d2} = 5$ and $n_{d3} = 6$. The cached content of the HeNB on the requested files W_{d1} and W_{d2} are $S_{d1} = (a_3, a_4)$ and $S_{d2} = (b_2, b_3)$. This constitutes a fractional cache size of $\mu'(\mathbf{n}) = 1/2$.

eNB- U_2 – the stronger channel is the eNB- U_2 link with $n_{d3} = 6$ ($n_{d3} \geq n_{d2}$). Again, we apply load balancing by equally distributing the transmission load of $n_{d3} = 6$ bits to both users. Thus, we send $n_{d3}/2 = 3$ desired bits in a single channel use to each user such that the DTB becomes $\Delta_{\text{det}}^*(\mu = 0, n_F = 0, \mathbf{n}) = 1/3$. This scheme is feasible since both the weaker and the stronger channel allow the reliable transmission of $n_{d3}/2 = 3$ bits since $n_{d3}/2 \leq n_{d2}$ and $n_{d3}/2 \leq n_{d3}$ holds true. Recall that these two conditions are equivalent to the broadcast condition $\mathbf{n} \in \mathcal{I}_1$.

At the other extreme point B_2 , a cache-only transmission scheme at $\mu'(\mathbf{n}) = 2n_{d1}/(n_{d1}+n_{d3}) = 1/2$ is required to attain the wireless bottleneck DTB of $2/(n_{d1}+n_{d3}) = 1/4$. Fig. 8 illustrates the scheme for the case when U_1 and U_2 request the files $W_{d1} = (a_1, a_2, a_3, a_4)$ and $W_{d2} = (b_1, b_2, b_3, b_4)$, respectively. In this example, the strongest link in the network is the eNB- U_2 link capable of conveying at most $n_{d3} = 6$ bits in total to the receivers reliably. Since the cross-link is weaker than the eNB- U_2 link ($n_{d2} \leq n_{d3}$) and the HeNB- U_1 link is significantly weaker than the cross-link ($n_{d1} \leq n_{d2}/2$), we allocate parts of the requested file W_{d1} of U_1 to the top-most bit levels of the eNB. As U_2 is only connected to the eNB, the remaining less significant bit levels of

the eNB have to be able to carry and convey *all* $R_{U_2}^* = R_{1,p}^{w,*} + R_{\text{IN}}^{v,*} + R_c^{v,*} = (n_{d1} + n_{d3})/2 = 4$ bits of the requested file W_{d2} . Thus, we are able to utilize $R_c^{u,*} = n_{d3} - (n_{d1} + n_{d3})/2 = (n_{d3} - n_{d1})/2 = 2$ most significant bit levels of the eNB for transmitting desired information a_1 and a_2 to U_1 . Note that this is feasible since $R_c^{u,*} = (n_{d3} - n_{d1})/2 = 2 \leq n_{d2} = 5$. At fractional cache size $\mu'(\mathbf{n}) = 1/2$, the HeNB is aware of half of each file content. For instance, with respect to W_{d1} and W_{d2} we assume in Fig. 8 that the cache content is $S_{d1} = (a_3, a_4)$ and $S_{d2} = (b_2, b_3)$, respectively. With S_{d1} and S_{d2} , the HeNB is capable of forming exactly $R_{\text{IN}}^{n,*} = n_{d1} = 2$ XOR-combinations $a_3 \oplus b_3$ and $a_4 \oplus b_2$ to neutralize the received interference of $R_{\text{IN}}^{v,*} = n_{d1} = 2$ bits b_2 and b_3 at U_1 . Thus, in this case U_1 receives $R_{U_1}^* = R_{\text{IN}}^{n,*} + R_c^{u,*} = n_{d1} + (n_{d3} - n_{d1})/2 = 4$ desired bits and $R_c^{v,*} = n_{d2} - R_{\text{IN}}^{n,*} - R_c^{u,*} = (2n_{d2} - n_{d1} - n_{d3})/2 = 1$ undesired bit b_4 . Note that U_1 does not receive $R_{1,p}^{w,*} = n_{d3} - n_{d2} = 1$ bit (b_1) at all. It is easy to see that the remaining parameters are set to $R_{2,p}^{u,*} = l_1^* = l_3^* = l_4^* = 0$ and $l_2^* = n_{d3} - n_{d1} = 4$. Interestingly, similarly to example 1, we can see in Fig. 8 that increasing the fractional cache size by some $\epsilon > 0$ to $\mu'(\mathbf{n}) + \epsilon$ cannot help the HeNB to decrease the DTB any further. This is due to the fact that additional ϵ information on the requested files at the HeNB cannot be constructively used at all since all bit levels at the HeNB are already occupied with XOR combinations $a_3 \oplus b_3$ and $a_4 \oplus b_2$. This explains why the DTB remains constant for $\mu > \mu'(\mathbf{n})$.

In the remainder of sub-section V-A, we will show the achievability of all relevant corner points that are based on cache-only transmission policies ($n_F = 0$). To this end, we specify the optimal rate allocation parameters introduced as part of the generalized block structure that optimizes the linear program (45). We start with Class I channel regimes and end with Class IV channel regimes.

Class I: Now, we present the DTB-optimal scheme for all Class I channel regimes. We distinguish between Class I SCL channel regimes for which $n_{d2} \geq n_{d3}$ holds and Class I WCL channel regimes where $n_{d2} \leq n_{d3}$ applies. The achievable DTB for both cases is given by the following proposition.

Proposition 3. The achievable DTB for Class I channel regimes of the network under study for

$n_F = 0$ and $\mu \in [0, 1]$ is given for $n_{d2} \geq n_{d3}$ by

$$\Delta_{\det}(\mu, n_F = 0, \mathbf{n}) = \begin{cases} \max \left\{ \frac{2-\mu}{n_{d2}}, \frac{2}{n_{d1}+n_{d3}} \right\} & \text{if } n_{d1} + n_{d3} \geq n_{d2} \geq n_{d3} \geq n_{d1} \\ \max \left\{ \frac{2-\mu}{n_{d2}}, \frac{1}{n_{d3}} \right\} & \text{if } 2n_{d3} \geq n_{d2} \geq n_{d1} \geq n_{d3} \\ \max \left\{ \frac{2-\mu}{n_{d2}}, \frac{1}{n_{d3}} \right\} & \text{if } n_{d1} \geq n_{d2} \geq n_{d3}, 2n_{d3} \geq n_{d2} \end{cases}, \quad (46)$$

and for $n_{d2} \leq n_{d3}$ by

$$\Delta_{\det}(\mu, n_F = 0, \mathbf{n}) = \begin{cases} \max \left\{ \frac{2-\mu}{n_{d3}}, \frac{1}{n_{d3}} \right\} & \text{if } n_{d1} \geq n_{d3} \geq n_{d2}, 2n_{d2} \geq n_{d3} \\ \max \left\{ \frac{2-\mu}{n_{d3}}, \frac{1}{n_{d2}} \right\} & \text{if } n_{d1} + n_{d3} \geq 2n_{d2} \geq n_{d3} \geq n_{d2} \geq n_{d1} \\ \max \left\{ \frac{2-\mu}{n_{d3}}, \frac{2}{n_{d1}+n_{d3}} \right\} & \text{if } 2n_{d2} \geq n_{d1} + n_{d3} \geq n_{d3} \geq n_{d2} \geq n_{d1} \\ \max \left\{ \frac{2-\mu}{n_{d3}}, \frac{1}{n_{d1}} \right\} & \text{if } 2n_{d2} \geq n_{d3} \geq n_{d1} \geq n_{d2} \end{cases}. \quad (47)$$

In what follows, we present the scheme for all Class I channel regimes specified in proposition 3 in detail. To this end, we establish the achievability at corner points A_1 and B_2 and apply arguments of convexity for achievability at intermediary points.

The achievability for corner point A_1 readily follows from Lemma 2 and Eq. (12) (cf. Example 1 and 2) for the SCL and WCL cases. At this point, the optimal DTB corresponds to

$$\Delta_0(\mathbf{n}) = \begin{cases} \frac{2}{n_{d2}} & \text{if } 2n_{d3} \geq n_{d2} \geq n_{d3} \\ \frac{2}{n_{d3}} & \text{if } 2n_{d2} \geq n_{d3} \geq n_{d2}. \end{cases} \quad (48a)$$

$$\quad (48b)$$

We observe that the achievable DTB is in accordance with proposition 3 for $\mu = 0$ for all Class I channel regimes. Next, we consider corner point B_2 . At this point the fractional cache size corresponds to:

$$\mu'(\mathbf{n}) = 2 - \max\{n_{d2}, n_{d3}\} \Delta'_{\text{LB}}(\mathbf{n}) = \begin{cases} 2 - n_{d2} \Delta'_{\text{LB}}(\mathbf{n}) & \text{if } n_{d2} \geq n_{d3} \\ 2 - n_{d3} \Delta'_{\text{LB}}(\mathbf{n}) & \text{if } n_{d2} \leq n_{d3} \end{cases}. \quad (49)$$

For given $\mu'(\mathbf{n})$ according to Eq. (49), we solve the linear optimization problem (45). The solution for the channel regimes to which the channel realizations of Example 1 and Example 2 belong to are specified in Table I. Concretely, using the rate allocation specified in columns two and three of Table I for $\mathbf{n} = (2, 5, 4)^T$ and $\mathbf{n} = (2, 5, 6)^T$, respectively, reduces the generalized scheme to the schemes described in Examples 1 and 2. The solution for all Class I SCL and WCL channel regimes are provided in Table II and Table III of Appendix C. Under this rate allocation the achievable DTB is given in Eqs. (46) and (47) for Class I channel regimes with

$n_{d2} \geq n_{d3}$ and $n_{d2} \leq n_{d3}$ at $\mu'(\mathbf{n})$, respectively. Achievable points between corner points A_1 and B_2 are attainable if memory sharing is applied. Recall that memory sharing schemes are typically composed of two schemes of neighboring corner points, e.g., A_1 and B_2 . Thus, for Class I, memory sharing is only feasible in intersecting channel regimes $\mathcal{R}_{A_1} \cap \mathcal{R}_{B_2}$, where *both* schemes, i.e., for A_1 and B_2 , are feasible.

Regimes \mathcal{R}_{B_2}	$n_{d1} + n_{d3} \geq n_{d2} \geq n_{d3} \geq n_{d1}$	$2n_{d2} \geq n_{d1} + n_{d3} \geq n_{d3} \geq n_{d2} \geq n_{d1}$
$R_{1,p}^{w,*} = R_{1,p}^{u,*}$	$n_{d2} - n_{d3}$	$n_{d3} - n_{d2}$
$R_c^{\mu,*}$	$\frac{n_{d3} - n_{d1}}{2}$	$\frac{n_{d3} - n_{d1}}{2}$
$R_{2,p}^{\mu,*}$	0	0
$R_{\text{IN}}^{\nu,*}$	$n_{d1} + n_{d3} - n_{d2}$	n_{d1}
$R_c^{\nu,*}$	$\frac{2n_{d2} - n_{d1} - n_{d3}}{2}$	$\frac{2n_{d2} - n_{d1} - n_{d3}}{2}$
$R_{\text{IN}}^n,*$	$n_{d1} + n_{d3} - n_{d2}$	n_{d1}
l_1^*	0	0
l_2^*	$2n_{d2} - n_{d1} - n_{d3}$	$n_{d3} - n_{d1}$
l_3^*	0	0
l_4^*	0	0
\bar{L}^*	$\frac{n_{d1} + n_{d3}}{2}$	$\frac{n_{d1} + n_{d3}}{2}$
$\Delta'_{\text{LB}}(\mathbf{n})$	$\frac{2}{n_{d1} + n_{d3}}$	$\frac{2}{n_{d1} + n_{d3}}$
$\mu'(\mathbf{n})$	$2 - \frac{2n_{d2}}{n_{d1} + n_{d3}}$	$2 - \frac{2n_{d3}}{n_{d1} + n_{d3}}$

TABLE I: Rate allocation parameters for corner point B_2 at fractional cache size $\mu'(\mathbf{n})$ for channel regimes of Example 1 (second column) and 2 (third column).

Class II: Now, we present the DTB-optimal scheme for all Class II channel regimes. Hereby, the achievable DTB for this class is given by the following proposition.

Proposition 4. The achievable DTB for Class II channel regimes of the network under study for $n_F = 0$ and $\mu \in [0, 1]$ equals

$$\Delta_{\text{det}}(\mu, n_F = 0, \mathbf{n}) = \begin{cases} \max \left\{ \frac{1-\mu}{n_{d2}}, \frac{2-\mu}{n_{d3}}, \frac{1}{n_{d3}} \right\} & \text{if } n_{d1} \geq n_{d3} \geq 2n_{d2} \\ \max \left\{ \frac{1-\mu}{n_{d2}}, \frac{2-\mu}{n_{d3}}, \frac{1}{n_{d1}} \right\} & \text{if } n_{d1} + n_{d2} \geq n_{d3} \geq n_{d1} \geq n_{d2}, n_{d3} \geq 2n_{d2} \end{cases}. \quad (50)$$

The achievability for corner point A_1 readily follows from Lemma 2 and Eq. (12). At this point, the optimal DTB for this extreme point corresponds to

$$\Delta_0(\mathbf{n}) = \frac{1}{n_{d2}} \text{ if } n_{d3} \geq 2n_{d3}. \quad (51)$$

The achievability of the neighboring extreme point B_1 is derived as the solution of the optimization problem (45) for

$$\mu''(\mathbf{n}) = \frac{n_{d3} - 2n_{d2}}{n_{d3} - n_{d2}}. \quad (52)$$

The optimal rate allocation parameters of this optimization problem are provided in Table IV of Appendix C. The achievability at the extreme point B_2 applicable for Class II channel regimes is listed in columns two and five of Table III included in Appendix C. All intermediary points are achievable through memory sharing in the channel regime $\mathcal{R}_{A_1} \cap \mathcal{R}_{B_1} \cap \mathcal{R}_{B_2}$. This establishes the results of proposition 4.

Class III: The DTB-optimal scheme for the Class III channel regime is presented. For Class III, the following proposition quantifies the achievable DTB.

Proposition 5. The achievable DTB for Class III channel regime of the network under study for $n_F = 0$ and $\mu \in [0, 1]$ corresponds to

$$\Delta_{\det}(\mu, n_F = 0, \mathbf{n}) = \max \left\{ \frac{1 - \mu}{n_{d2}}, \frac{1}{n_{d1}} \right\} \text{ if } n_{d3} \geq n_{d1} + n_{d2} \geq n_{d1} \geq n_{d2}. \quad (53)$$

Lemma 2 establishes the achievability of extreme point A_1 for Class III. At this point, the optimal DTB for this extreme point is given by

$$\Delta_0(\mathbf{n}) = \frac{1}{n_{d2}} \text{ if } n_{d3} \geq 2n_{d2}. \quad (54)$$

At corner point C_1 , we solve the optimization problem of (45) at given fractional cache size

$$\mu'''(\mathbf{n}) = \frac{n_{d1} - n_{d2}}{n_{d1}}. \quad (55)$$

to show the DTB achievability of $1/n_{d1}$ at $\mu'''(\mathbf{n})$. The resulting decision variables of this linear program are listed in Table V of Appendix C. For $\mu < \mu'''(\mathbf{n})$, memory sharing establishes the achievability for intermediary points as long as the operating channel regime is given by $\mathcal{R}_{A_1} \cap \mathcal{R}_{C_1}$.

Class IV: The DTB for Class IV channel regimes remains constant. The following proposition states its optimal value.

Proposition 6. The achievable DTB for Class IV channel regime of the network under study remains constant for any $\mu \in [0, 1]$ and corresponds to

$$\Delta_{\det}(\mu, n_F = 0, \mathbf{n}) = \begin{cases} \frac{1}{n_{d3}} & \text{if } n_{d1} + n_{d3} \geq n_{d2} \geq n_{d1} \geq n_{d3}, n_{d2} \geq 2n_{d3} \\ \frac{1}{n_{d3}} & \text{if } n_{d1} \geq n_{d2} \geq 2n_{d3} \\ \frac{1}{n_{d2}} & \text{if } n_{d3} \geq n_{d2} \geq n_{d1}, n_{d3} \geq 2n_{d2} \\ \max \left\{ \frac{1}{n_{d3}}, \frac{2}{n_{d2}} \right\} & \text{if } n_{d2} \geq n_{d1} + n_{d3} \end{cases}. \quad (56)$$

Proposition 6 readily follows from Lemma 2.

F. Upper Bound (Achievability) for $n_F \geq 0$

In this sub-section, we propose schemes to cover different operating channel regimes of the network under study for the cloud-only ($\mu = 0$) case. As previously explained, we will only focus on the achievability at corner points A_r , $r \in \{2, 3, 4\}$. Remaining intermediate points in the tradeoff curves on the DTB follow from the the convexity of the DTB (cf. Lemma 1). To show the achievability at extreme point

- (A) A_2 ,
- (B) A_3 ,
- (C) and A_4 ,

we borrow results on the achievability of the *cache-only case* of their respective, neighboring extreme point

- (A) B_2
- (B) B_1
- (C) and C_1

at cache sizes $\mu'(\mathbf{n})$, $\mu''(\mathbf{n})$ and $\mu'''(\mathbf{n})$, respectively. In the sequel, we use the notation of the building block structure of sub-section V-B. We denote the requested file of U_k , $k = \{1, 2\}$, by W_{dk} .

The general idea of our proposed scheme is to apply a fronthaul transmission policy in such a way that the optimal *wireless* DTB $\Delta_E^*(\mu_G(\mathbf{n}), n_F = 0, \mathbf{n})$ of the neighboring extreme points B_2 , B_1 and C_1 achieved at cache sizes $\mu_G(\mathbf{n}) \in \{\mu'(\mathbf{n}), \mu''(\mathbf{n}), \mu'''(\mathbf{n})\}$ become feasible at $\mu = 0$ at the cost of *additional* fronthaul latency. Recall that Δ_E^* is the DTB which incurs when at least \bar{L}^* bits are conveyed to each user through the wireless channel without invoking the fronthaul

link. Recall that the achievability of $\Delta_E^*(\mu_G(\mathbf{n}), n_F = 0, \mathbf{n})$ was discussed in sub-section V-A. The optimal rate allocation parameters \mathbf{r}^* are available in Tables II through V in Appendix C. To this end, the cloud server forms

- (a) $R_{2,p}^{u,*}$ bits of U_1 's requested file W_{d1}
- (b) and $R_{\text{IN}}^{n,*}$ XORed bits of both users requested files W_{d1} and W_{d2}

in the same manner as in the achievability scheme of B_2 , B_1 and C_1 , respectively. These bits are transmitted from the cloud server through the fronthaul link to the HeNB. Recall from Eq. (37) and Tables II through V that at the optimum solution $\mu_G(\mathbf{n})\bar{L}^* = R_{2,p}^{u,*} + R_{\text{IN}}^{n,*}$. Transmitting these $\mu_G(\mathbf{n})\bar{L}^*$ bits induces a fronthaul DTB of $\Delta_F = \mu_G(\mathbf{n})/n_F$. Thus, the overall DTB becomes $\Delta_E + \Delta_F$, that is, for extreme points

(A) A_2 :

$$\Delta'_{\text{LB}}(\mathbf{n}) + \frac{\mu'(\mathbf{n})}{n_F}, \quad (57)$$

(B) A_3 :

$$\Delta''_{\text{LB}}(\mathbf{n}) + \frac{\mu''(\mathbf{n})}{n_F}, \quad (58)$$

(C) and A_4 :

$$\Delta'_{\text{LB}}(\mathbf{n}) + \frac{\mu'''(\mathbf{n})}{n_F}, \quad (59)$$

which is identical to $\Delta_{\text{det}}^*(\mu = 0, n_F, \mathbf{n})$ of Theorem 1 for the underlying classes of channel regimes.

VI. PARALLEL TRANSMISSION – MAIN RESULT

In this section, we outline and discuss our main result on the minimum DTB for the F-RAN in Fig. 1 for a parallel fronthaul-edge transmission. Furthermore, we will contrast parallel transmission from serial transmission. The main result is stated in the following theorem.

Theorem 2. The DTB of the LDM-based cloud and cache-aided HetNet in Fig. 1 under parallel fronthaul-edge transmissions for any $n_F \geq 0$ and $\mu \in [0, 1]$ is given by

$$\Delta_{\text{det}}^*(\mu, n_F, \mathbf{n}) = \max \left\{ \frac{1 - \mu}{n_F + n_{d2}}, \frac{2 - \mu}{n_F + \max\{n_{d2}, n_{d3}\}}, \Delta'_{\text{LB}}(\mathbf{n}) \right\}. \quad (60)$$

Proof: (Theorem 2) Lower bounds on the DTB are provided in section VII while upper bounds can be found in section VIII. ■

Identically to Theorem 1, in the *same* four classes of channel regimes – Class I, II, III and IV – the DTB of Theorem 2 simplifies to:

- Class I:

$$\Delta_{\text{det}}^*(\mu, n_F, \mathbf{n}) = \begin{cases} \max \left\{ \frac{2-\mu}{n_F + \max\{n_{d2}, n_{d3}\}}, \Delta'_{\text{LB}}(\mathbf{n}) \right\} & \text{for } n_F \leq n_{F,\max}(\mathbf{n}) \\ \Delta'_{\text{LB}}(\mathbf{n}) & \text{for } n_F \geq n_{F,\max}(\mathbf{n}) \end{cases}, \quad (61)$$

- Class II:

$$\Delta_{\text{det}}^*(\mu, n_F, \mathbf{n}) = \begin{cases} \max \left\{ \frac{1-\mu}{n_F + n_{d2}}, \frac{2-\mu}{n_F + n_{d3}}, \Delta'_{\text{LB}}(\mathbf{n}) \right\} & \text{for } n_F \leq n_{F,\text{IM}}(\mathbf{n}) \\ \max \left\{ \frac{2-\mu}{n_F + n_{d3}}, \Delta'_{\text{LB}}(\mathbf{n}) \right\} & \text{for } n_{F,\text{IM}}(\mathbf{n}) \leq n_F \leq n_{F,\max}(\mathbf{n}) \\ \Delta'_{\text{LB}}(\mathbf{n}) & \text{for } n_F \geq n_{F,\max}(\mathbf{n}) \end{cases}, \quad (62)$$

- Class III:

$$\Delta_{\text{det}}^*(\mu, n_F, \mathbf{n}) = \begin{cases} \max \left\{ \frac{1-\mu}{n_F + n_{d2}}, \Delta'_{\text{LB}}(\mathbf{n}) \right\} & \text{for } n_F \leq n_{F,\max}(\mathbf{n}) \\ \Delta'_{\text{LB}}(\mathbf{n}) & \text{for } n_F \geq n_{F,\max}(\mathbf{n}) \end{cases}, \quad (63)$$

- Class IV:

$$\Delta_{\text{det}}^*(\mu, n_F, \mathbf{n}) = \Delta'_{\text{LB}}(\mathbf{n}) \quad \forall n_F. \quad (64)$$

Hereby, the intermediary and maximum fronthaul capacities $n_{F,\text{IM}}(\mathbf{n})$ and $n_{F,\max}(\mathbf{n})$ correspond to:

$$n_{F,\text{IM}}(\mathbf{n}) = n_{d3} - 2n_{d2} \quad (65a)$$

$$n_{F,\max}(\mathbf{n}) = \max \left\{ \frac{2}{\Delta'_{\text{LB}}(\mathbf{n})} - \max\{n_{d2}, n_{d3}\}, \frac{1}{\Delta'_{\text{LB}}(\mathbf{n})} - n_{d2} \right\} \quad (65b)$$

Remark 8 (Serial vs. Parallel Transmission Schemes). According to Theorem 2, we observe similar performance curves at channel regimes of classes I, II and III for both serial and parallel fronthaul-edge transmission policies (cf. Figs. 4 and 9). Two main differences are:

- 1) First, only for the latter, fractional cache sizes of corner points B_1 , B_2 and C_1 explicitly depend on the fronthaul capacity n_F . This dependency causes that increasing n_F by some positive δ will lead to a linear proportional decrease by δ in these points' fractional cache sizes. This behavior is shown by a left shift of B_1 , B_2 and C_1 in Figs. 9a–9c as we increase the fronthaul capacities from n_{F_1} to n_{F_2} (and n_{F_3} exclusively shown in Fig. 9b).
- 2) Second, only for the latter we require a finite fronthaul capacity $n_F = n_{F,\max}(\mathbf{n})$ to attain the lowest possible DTB $\Delta'_{\text{LB}}(\mathbf{n})$ (see Fig. 9d). In contrast, serial fronthaul-edge schemes

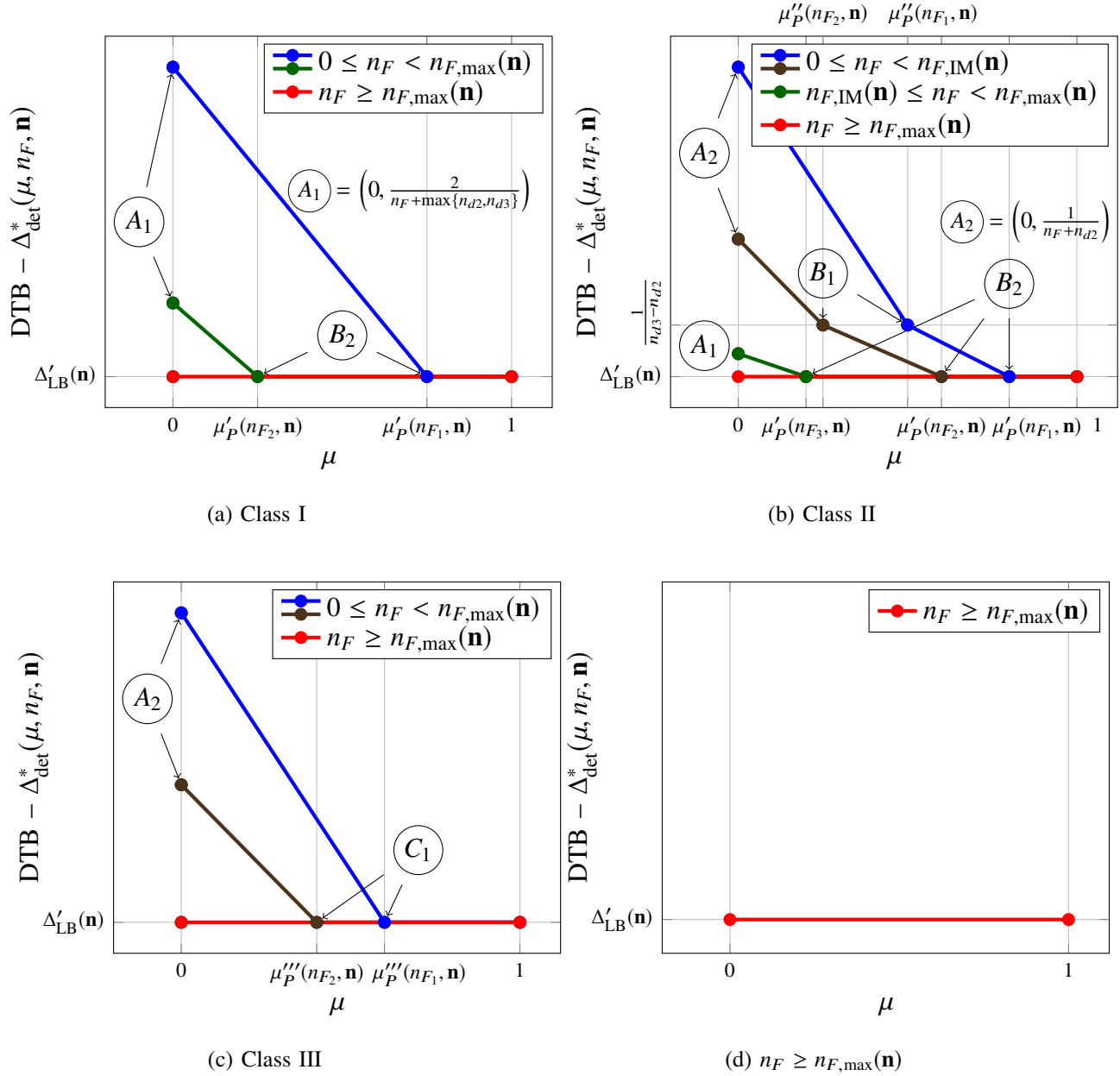


Fig. 9: DTB as a function of μ for three classes of channel regimes (Class I, II, III) at distinct fronthaul capacities n_{F_1} , n_{F_2} and n_{F_3} . Specifically, we assume that $0 \leq n_{F_1} \leq n_{F_2} \leq n_{F_3} \leq n_{F,\max}(\mathbf{n})$. As the fronthaul capacity increases, corner points B_1 , B_2 and B_3 shift to the left along the μ -axis until for $n_F \geq n_{F,\max}(\mathbf{n})$ the DTB does not change anymore as shown in Fig. 9d.

needed an *infinite* fronthaul capacity ($n_F = \infty$) to achieve the same DTB. In other words, fronthaul capacities in the range $n_F \in (n_{F,\max}(\mathbf{n}), \infty)$ have a DTB-reducing effect only under serial fronthaul-edge schemes. The intuition behind this result is that in parallel transmission policies cloud resources are effectively utilized to overcome partial caching while incurring less fronthaul latency than serial transmission schemes. As a consequence, a finite n_F suffices to obtain the DTB $\Delta'_{\text{LB}}(\mathbf{n})$.

Remark 9 (Maximum Fronthaul Capacity $n_{F,\max}(\mathbf{n})$). One can verify from Eq. (65b) that $n_{F,\max}(\mathbf{n}) \leq n_{d1}$. This suggests that the full-duplex HeNB is capable to forward a fronthaul message of a single time instant, say $t - 1$, through the wireless HeNB-to- U_1 link in the consecutive channel use t . Our achievability schemes (see section VIII) make implicit use of this observation.

VII. PARALLEL TRANSMISSION – LOWER BOUND

The lower bounds on the DTB for the case of parallel fronthaul transmission are presented in this section through the following proposition.

Proposition 7 (Lower Bound on the Minimum DTB for F-RAN with Parallel Fronthaul-Edge Transmission). For the LDM-based cloud and cache-aided HetNet in Fig. 1 under a parallel fronthaul-edge transmission setting, the optimal DTB $\Delta_{\text{det}}^*(\mu, n_F, \mathbf{n})$ is lower bounded as

$$\Delta_{\text{det}}^*(\mu, n_F, \mathbf{n}) \geq \Delta_{\text{LB},P}(\mu, \mathbf{n}), \quad (66)$$

where

$$\Delta_{\text{LB},P}(\mu, n_F, \mathbf{n}) = \max \left\{ \frac{1}{n_{d3}}, \frac{1}{\max\{n_{d1}, n_{d2}\}}, \frac{2}{\max\{n_{d1} + n_{d3}, n_{d2}\}}, \frac{1 - \mu}{n_F + n_{d2}}, \frac{2 - \mu}{n_F + \max\{n_{d2}, n_{d3}\}} \right\}. \quad (67)$$

Proof: The proof of Proposition 7 is presented in Appendix D. In comparison to the established bounds for the case of serial transmission with $n_F = 0$ (cf. Proposition 1), we ought to account for the received fronthaul message $\mathbf{S}^{q-n_F} \mathbf{x}_F^{TP}$ at the HeNB when establishing the DTB lower bounds. This fact becomes noticeable in the last two terms inside the outer max-expression of Eq. (67). ■

VIII. PARALLEL TRANSMISSION – UPPER BOUND

In this section, we will focus on establishing the achievability (upper bound) on the DTB for the case of parallel fronthaul-edge transmissions. To this end, first, we introduce the main ingredients of our transmission schemes, that includes the large block number assumption (see section VIII-A) and the generalized signal structure that all schemes, irrespective of the channel regime, have in common. Subsequently, we describe the transmission schemes for all channel regimes that achieve the optimal DTB provided in Theorem 2 (cf. Fig. 9). Due to the convexity of the DTB, we only establish the achievability of corner points in the latency-cache tradeoff curves. In Fig. 9, depending on the operating channel regime, the corner points are denoted by A_r , $r \in \{1, 2\}$, B_s , $s \in \{1, 2\}$, and C_1 . In this regard, we will show that corner points

- A_r , $r \in \{1, 2\}$, involve only fronthauling and do not require edge caching ($\mu = 0$); thus, representing cloud-only transmission policies, whereas
- B_1 , B_2 and C_1 involve both edge caching and fronthauling; thus, representing fronthaul-edge transmission policies.

In general, the DTB at fractional cache size μ which lies between two neighboring corner points (say D and E) cache sizes' is achieved through memory sharing between the policies at corner point D and E . For parallel fronthaul edge transmissions, corner points D and E are operational at channel regimes \mathcal{R}_D and \mathcal{R}_E for non-negative fronthaul capacities below $n_{F,\max}^D$ and $n_{F,\max}^E$, respectively. Thus, any intermediate point between D and E is achievable through memory sharing when we restrict the channel regime to be $\mathcal{R}_D \cap \mathcal{R}_E$ for fronthaul capacities less than $\min \left\{ n_{F,\max}^D, n_{F,\max}^E \right\}$.

A. Large Block Number

We recall that in the case of parallel fronthaul-edge transmission, the HeNB operates as a causal *full-duplex* relay endowed with additional cache capabilities. At any time instant t , $t = 1, 2, \dots, T_P$, the HeNB is thus able to *simultaneously* receive useful *uncached* information through fronthauling and to transmit local information as a function of its cached content and *past* fronthaul messages from time instants $1, 2, \dots, t-1$. Our transmission scheme operates over B blocks for which we use block-Markov coding [34], [35]. To this end, we split each file in the library into B blocks, so that each block is of finite size $\tilde{L} = L/B$ bits. We design our scheme in such a way that the wireless delivery time of each block is T_B channel uses; or in other words,

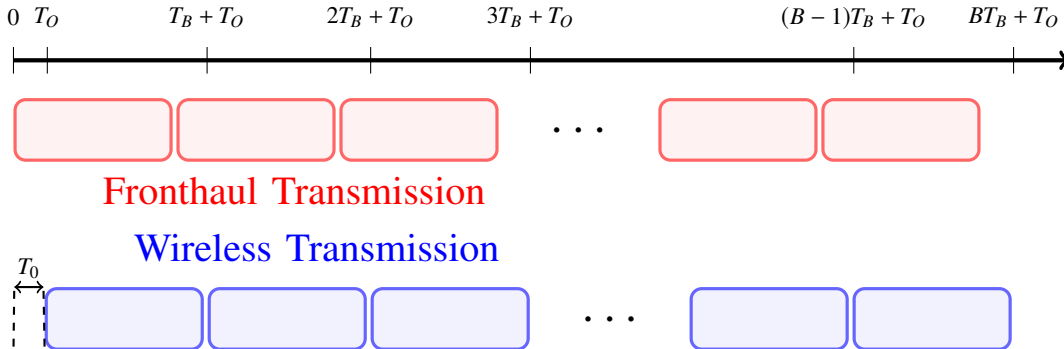


Fig. 10: The figure depicts the relationship between fronthaul and wireless transmission for a parallel fronthaul-edge transmission scheme. In this scheme, the fronthaul transmission starts and terminates prior to the wireless transmission by a finite time offset of T_O channel uses. This offset enables the HeNB to receive a-priori information which is used to initiate the wireless transmission of consecutive transmission blocks.

the achievable per-block DTB equals $\Delta_{\text{det},B}(\mu, n_F, \mathbf{n}) = T_B/\bar{L}$. This DTB becomes feasible if the fronthaul transmission initiates and terminates by an offset of T_O ($1 \leq T_O \leq T_B$) channel uses prior to the wireless transmission (see Fig. 10). Thus, prior to any per-block wireless transmission just enough a-priori information on each block is made available through fronthauling. The total delivery time to provide both users with their requested files adds up to $T_P = BT_B + T_O$. Hence, the total delivery time per bit for finite T_O that does not scale with B is given by

$$\Delta_{\text{det}}(\mu, n_F, \mathbf{n}) = \limsup_{L \rightarrow \infty} \frac{T_P}{L} = \Delta_{\text{det},B}(\mu, n_F, \mathbf{n}) + \lim_{B \rightarrow \infty} \frac{T_O}{B\bar{L}} = \Delta_{\text{det},B}(\mu, n_F, \mathbf{n}). \quad (68)$$

One can infer that for arbitrarily large number of blocks B , the offset duration T_O becomes negligible and thus the overall DTB converges to the per-block DTB. In the remainder of this sub-section, we will make use of the large block observation and therefore present optimal achievability schemes for a single block that require a finite offset $T_O = 1$. For that purpose, we now summarize the main transmit signal vector structure of eNB and HeNB that all block transmissions have in common.

B. Building Blocks

Similar to sub-section V-B, we propose a general signal vector structure that all schemes have in common. Due to the large block number assumption, we may restrict our focus to a single transmission block and *minimize* the per-block DTB $\Delta_{\text{det},B}$ or *maximize* the number of at least

\tilde{L} desired bits that are sent to both U_1 and U_2 in T_B channel uses, i.e., we solve one of the two *equivalent* optimization problems

$$\min_{\tilde{\mathbf{r}}} \Delta_{\text{det},B}(\tilde{\mathbf{r}}) \qquad \max_{\tilde{\mathbf{r}}} \tilde{L}(\tilde{\mathbf{r}}).$$

We denote the optimal solution and the optimal decision variables of above optimization problem on the right by \tilde{L}^* and $\tilde{\mathbf{r}}^*$, respectively. Specifically, in our proposed scheme, we will use $T_B = 2$ channel uses to transmit a single block of the requested file requiring an offset of $T_O = 1$ channel uses between fronthaul and wireless transmission. When $T_B = 2$, the optimal per-block DTB becomes $\Delta_{\text{det},B}^* = 2/\tilde{L}^*$. Recall that in the limiting case of large blocks, i.e., $B \rightarrow \infty$, the overall DTB Δ_{det}^* converges to the per-block DTB specified above. Thus, in what follows, we will outline the *per-block* signal vector structure of the b -th block, $b = 1, 2, \dots, B$ which encompasses consecutive channel uses $t_1 = 2b$ and $t_2 = 2b + 1$ if $T_O = 1$. For the b -th block the eNB reserves fronthaul

- (a) *capacity-dependent*
- (b) *and capacity-independent*

resources. All resources are transmitted in $T_B = 2$ channel instants $t \in [t_1 : t_2]$. First type of resource includes

- private information
 - $\mathbf{w}_{1,p}[t]$, $w \in \{u, v\}$ intended for either U_1 if $w = u$ or for U_2 if $w = v$,
- and common information
 - $\mathbf{u}_{2,c}[t]$ intended for U_1
 - $\mathbf{v}_{2,c}[t]$ intended for U_2 .

Latter resource type, which we will henceforth call fronthaul-edge block, comprises of

- common information
 - $\mathbf{u}_{1,c}[t]$ intended for U_1
 - $\mathbf{v}_{1,c}[t]$ intended for U_2
- and interference neutralizing information
 - $\mathbf{v}_{\text{IN}}[t]$ intended for U_2 .

The transmission structure of the HeNB, on the other hand, remains identical to the one presented in section V. The HeNB uses sub-signal $\mathbf{u}_{2,p}[t]$ to sent additional private information to U_1 and sub-signal $\mathbf{n}_{\text{IN}}[t] = \mathbf{v}_{\text{IN}}[t] \oplus \mathbf{u}_{\text{IN}}[t]$ for complete interference neutralization of $\mathbf{v}_{\text{IN}}[t]$ at U_1 . We

use the notation of sub-section V-B to denote the length of all signal vectors. As we shall see, at the eNB side only the rates $R_{\text{IN}}^v[t]$, $R_{1,c}^u[t]$ and $R_{1,c}^v[t]$ will be dependent on *both* the time t and fronthaul capacity n_F . The rate of transmission signal $\mathbf{w}_{1,p}[t]$, on the other hand, will be both time-independent and fronthaul capacity-independent ($R_{1,w}^p[t] = R_{1,w}^p$). All remaining rates of the eNB signals will only be independent of the fronthaul capacity n_F . As before, we will differentiate between SCL and WCL channel regimes. Next, we describe the encoding at the transmitters.

C. Encoding at the Transmitters

The transmission signals of the HeNB and eNB are chosen according to:

$$\mathbf{x}_1[t] = \begin{pmatrix} \mathbf{0}_{l_4[t]} \\ \mathbf{u}_{2,p}[t] \\ \mathbf{0}_{l_3[t]} \\ \mathbf{n}_{\text{IN}}[t] \\ \mathbf{0}_{l_2[t]} \end{pmatrix}, \quad (69a)$$

$$\mathbf{x}_2[t] = \begin{pmatrix} \mathbf{u}_{2,c}[t] \\ \mathbf{v}_{2,c}[t] \\ \mathbf{u}_{1,c}[t] \\ \mathbf{v}_{1,c}[t] \\ \mathbf{v}_{\text{IN}}[t] \\ \mathbf{w}_{1,p}[t] \\ \mathbf{0}_{l_1} \end{pmatrix} \text{ for } w \in \{u, v\}. \quad (69b)$$

Hereby, $\mathbf{w}_{\text{IN}}[t] = \mathbf{v}_{\text{IN}}[t] \oplus \mathbf{u}_{\text{IN}}[t]$ completely neutralizes the interfering signal $\mathbf{v}_{\text{IN}}[t]$ at U_1 . Furthermore, note that private information $\mathbf{w}_{1,p}[t]$ corresponds to $\mathbf{u}_{1,p}[t]$ in the SCL case ($n_{d2} \geq n_{d3}$) and to $\mathbf{v}_{1,p}[t]$ in the WCL case ($n_{d2} \leq n_{d3}$). For $q = \max\{n_{d1}, n_{d2}, n_{d3}\}$, it is obvious that the eNB, on the one hand, can generate its signal vector $\mathbf{x}_2[t]$ as long as

$$l_1 + R_{1,p}^w + R_{\text{IN}}^v[t] + R_{1,c}^v[t] + R_{1,c}^u[t] + R_{2,c}^v[t] + R_{2,c}^u[t] \leq q, \quad \forall t \in [t_1 : t_2], \quad (70)$$

while the HeNB, on the other hand, can construct its signal vector $\mathbf{x}_1[t]$ only if

$$l_2[t] + l_3[t] + l_4[t] + R_{2,p}^u[t] + R_{\text{IN}}^n[t] \leq q, \quad \forall t \in [t_1 : t_2], \quad (71)$$

$$R_{2,p}^u[t] + R_{\text{IN}}^n[t] \leq \mu \frac{\tilde{L}}{2} + \min\{n_F, n_{F,\max}(\mathbf{n})\}, \quad \forall t \in [t_1 : t_2]. \quad (72)$$

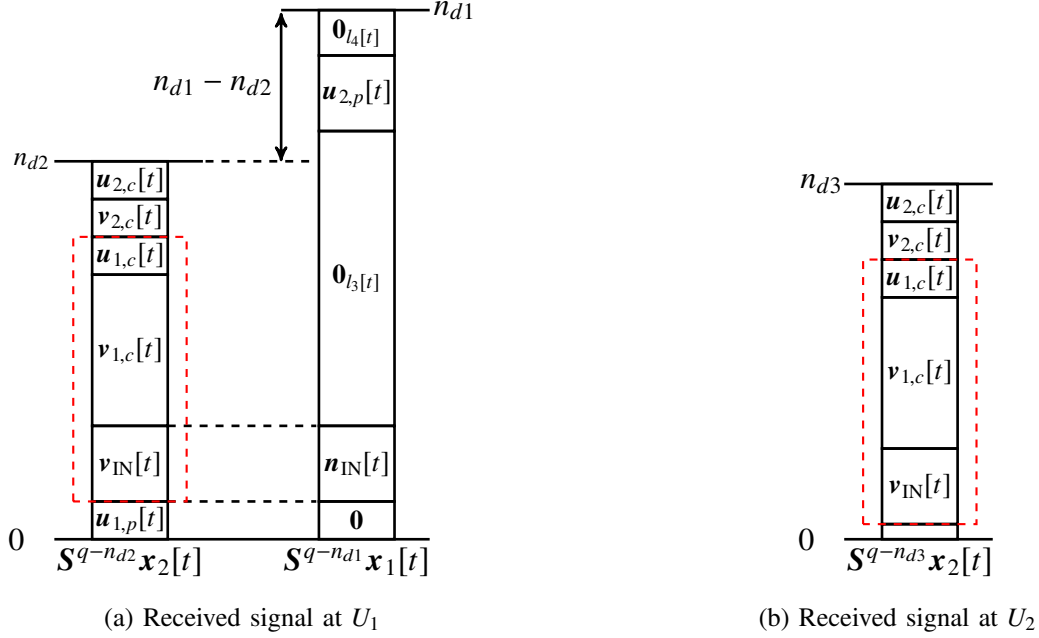


Fig. 11: The received signal vector of (a) U_1 and (b) U_2 are shown for the SCL case $n_{d2} \geq n_{d3}$. In the SCL case, we fix $w_{1,p}[t] = u_{1,p}[t]$. Note that at time instant t , U_1 receives the superposition $\mathbf{S}^{q-n_{d1}} \mathbf{x}_1[t] \oplus \mathbf{S}^{q-n_{d2}} \mathbf{x}_2[t]$. We highlight the fronthaul-edge block through a red dashed line.

The condition (72) holds since the HeNB is endowed with a finite-size cache of fractional size μ and a fronthaul link of finite capacity n_F bits per channel use. Specifically, in our scheme, at every time instant t , the HeNB uses its cache content and its received fronthaul signal $\mathbf{x}_F[t-1]$ at time instant $t-1$ to encode signals $\mathbf{u}_{2,p}[t]$ and $\mathbf{n}_{\text{IN}}[t]$. To this end, for $T_B = 2$ at most $\mu \tilde{L}/T_B = \mu \tilde{L}/2$ and $\min\{n_F, n_{F,\max}(\mathbf{n})$ bits emanate from the HeNB's local cache and the fronthaul signal $\mathbf{x}_F[t-1]$, respectively. Following, we will outline how the users decode their desired signals.

D. Decoding at the Receivers

The transmission according to the block structure of Eq. (69) forces that at the respective receivers successive decoding is applied. The received signal vector at U_1 and U_2 of the b -th block spanning consecutive time instants t_1 and t_2 are shown in Figs. 11 and 12 for the SCL ($n_{d2} \geq n_{d3}$) and WCL ($n_{d2} \leq n_{d3}$) case, respectively. On this basis, we will specify the conditions under which both U_1 and U_2 can decode their desired signal components *reliably*.

We first consider the per-block decoding operation of U_2 at time instants $t \in [t_1 : t_2]$. U_2

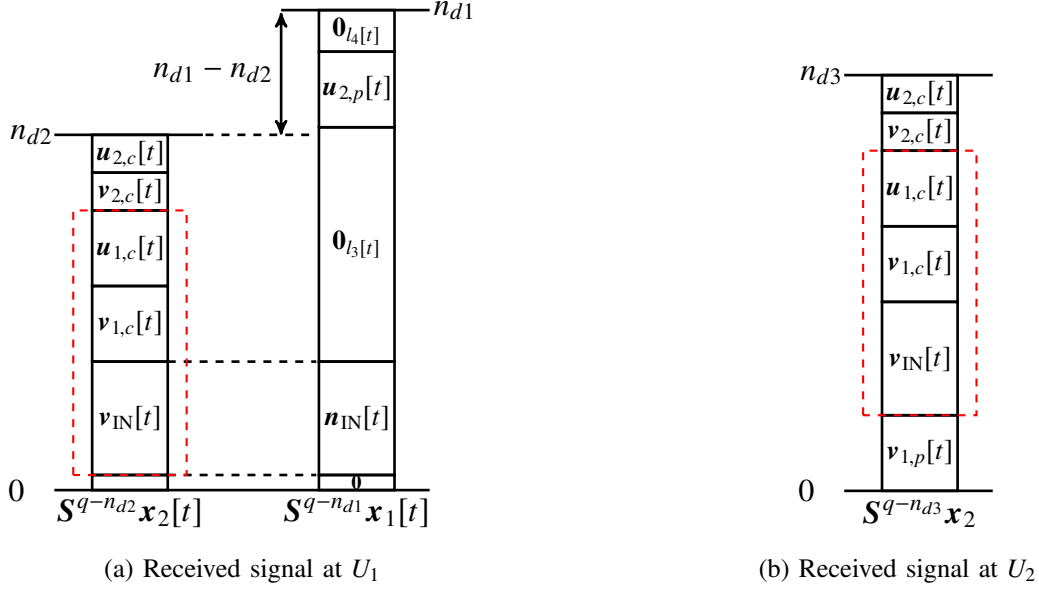


Fig. 12: The received signal vector of (a) U_1 and (b) U_2 are shown for the WCL case $n_{d2} \leq n_{d3}$. In the WCL case, we fix $w_{1,p}[t] = v_{1,p}[t]$. Note that at time instant t , U_1 receives the superposition $\mathbf{S}^{q-n_{d1}} \mathbf{x}_1[t] \oplus \mathbf{S}^{q-n_{d2}} \mathbf{x}_2[t]$.

is interested in retrieving $v_{1,c}[t]$, $v_{2,c}[t]$, $v_{\text{IN}}[t]$ and $w_{1,p}[t]$ if $w = v$ from its received signal $\mathbf{S}^{q-n_{d3}} \mathbf{x}_2[t]$. In successive decoding, a top-down decoding approach is necessary, i.e., U_2 starts decoding from the most significant bit levels and moves down to the least significant bits of $v_{\text{IN}}[t]$ if $w = u$ or $w_{1,p}[t]$ if $w = v$. Thus, U_2 can only decode all of its desired signals (cf. Figs. 11b and 12b), as long as

$$\begin{cases} R_{1,c}^u[t] + R_{2,c}^u[t] + R_{1,c}^v[t] + R_{2,c}^v[t] + R_{\text{IN}}^v[t] \leq n_{d3} & \text{if } n_{d2} \geq n_{d3} \\ R_{1,c}^u[t] + R_{2,c}^u[t] + R_{1,c}^v[t] + R_{2,c}^v[t] + R_{\text{IN}}^v[t] + R_{1,p}^w \leq n_{d3} & \text{if } n_{d2} \leq n_{d3} \end{cases} \quad (73)$$

Now let us move to state the reliability conditions for U_1 . Recall that at channel use $t \in [t_1 : t_2]$, U_1 receives the superposition $\mathbf{S}^{q-n_{d1}} \mathbf{x}_1[t] \oplus \mathbf{S}^{q-n_{d2}} \mathbf{x}_2[t]$ and aims at retrieving $u_{2,p}[t]$, $u_{2,c}[t]$, $u_{1,c}[t]$ and $w_{1,p}[t]$ if $w = u$ directly as well as $u_{\text{IN}}[t]$ through interference neutralization by overlaying $v_{\text{IN}}[t]$ and $n_{\text{IN}}[t] = v_{\text{IN}}[t] \oplus u_{\text{IN}}[t]$. Thus, we infer on the one hand that the individual received signals $\mathbf{S}^{q-n_{d1}} \mathbf{x}_1[t]$ and $\mathbf{S}^{q-n_{d2}} \mathbf{x}_2[t]$ have to contain the set of signal components $\{n_{\text{IN}}[t], u_{2,p}[t]\}$ and $\{w_{1,p}[t], v_{\text{IN}}[t], v_{1,c}[t], u_{1,c}[t], v_{2,c}[t], u_{2,c}[t]\}$ if $w = u$ and only $\{v_{\text{IN}}[t], v_{1,c}[t], u_{1,c}[t], v_{2,c}[t], u_{2,c}[t]\}$ if $w = v$, respectively, i.e.,

$$l_3[t] + l_4[t] + R_{2,p}^u[t] + R_{\text{IN}}^v[t] \leq n_{d1}, \quad (74)$$

$$\begin{cases} R_{1,p}^w + R_{\text{IN}}^v[t] + R_{1,c}^u[t] + R_{2,c}^u[t] + R_{1,c}^v[t] + R_{2,c}^v[t] \leq n_{d2} & \text{if } n_{d2} \geq n_{d3} \\ R_{\text{IN}}^v[t] + R_{1,c}^u[t] + R_{2,c}^u[t] + R_{1,c}^v[t] + R_{2,c}^v[t] \leq n_{d2} & \text{if } n_{d2} \leq n_{d3} \end{cases}. \quad (75)$$

On the other hand, at U_1 we avoid overlaps of desired signals if the conditions

$$l_4[t] + R_{2,p}^u[t] \leq (n_{d1} - n_{d2})^+, \quad (76)$$

$$R_{1,c}^u[t] + R_{2,c}^u[t] + R_{1,c}^v[t] + R_{2,c}^v[t] + R_{\text{IN}}^v[t] + n_{d1} - n_{d2} = l_3[t] + l_4[t] + R_{\text{IN}}^n[t] + R_{2,p}^u[t], \quad (77)$$

$$R_{\text{IN}}^v[t] = R_{\text{IN}}^n[t], \quad (78)$$

are satisfied. If all conditions (70)–(78) are met for $t \in [t_1 : t_2]$, the achievable *per-block* rates of U_1 and U_2 become

$$R_{U_1} = \begin{cases} 2R_{1,p}^w + \sum_{t \in [t_1:t_2]} R_{1,c}^u[t] + R_{2,c}^u[t] + R_{\text{IN}}^n[t] + R_{2,p}^u[t] & \text{if } n_{d2} \geq n_{d3} \\ \sum_{t \in [t_1:t_2]} R_{1,c}^u[t] + R_{2,c}^u[t] + R_{\text{IN}}^n[t] + R_{2,p}^u[t] & \text{if } n_{d2} \leq n_{d3} \end{cases}, \quad (79a)$$

$$R_{U_2} = \begin{cases} \sum_{t \in [t_1:t_2]} R_{\text{IN}}^v[t] + R_{1,c}^v[t] + R_{2,c}^v[t] & \text{if } n_{d2} \geq n_{d3} \\ 2R_{1,p}^w + \sum_{t \in [t_1:t_2]} R_{\text{IN}}^v[t] + R_{1,c}^v[t] + R_{2,c}^v[t] & \text{if } n_{d2} \leq n_{d3} \end{cases}, \quad (79b)$$

respectively.

E. Maximizing \tilde{L}

Recall that our scheme maximizes \tilde{L} by determining the optimal vector of design variables $\tilde{\mathbf{r}}^*$. The design parameters of our scheme are the rate allocation parameters and the respective null vectors for time instants t_1 and t_2 . We combine all design parameters to the vector

$$\tilde{\mathbf{r}} = \left(R_{1,p}^w, R_{1,c}^u[t_1 : t_2], R_{2,c}^u[t_1 : t_2], R_{2,p}^u[t_1 : t_2], R_{\text{IN}}^v[t_1 : t_2], R_{1,c}^v[t_1 : t_2], R_{2,c}^v[t_1 : t_2], R_{\text{IN}}^n[t_1 : t_2], l_1, l_2[t_1 : t_2], l_3[t_1 : t_2], l_4[t_1 : t_2] \right)^T.$$

The per-block user rate maximization problem can then be cast by the following linear optimization program:

$$\begin{aligned} \max_{\tilde{\mathbf{r}}} \quad & \tilde{L} \triangleq \min\{R_{U_1}, R_{U_2}\} \\ \text{s.t.} \quad & (70)\text{--}(78) \text{ are satisfied } \forall t \in [t_1 : t_2], \end{aligned} \quad (80)$$

$$\tilde{\mathbf{r}} \geq \mathbf{0}.$$

For various SCL and WCL channel regimes in all four classes of channel regimes, we will determine \tilde{L}^* and $\tilde{\mathbf{r}}^*$. Recall that this means under the large block number assumption that at

most $\Delta_{\det}(\mu, n_F = 0, \mathbf{n}) = 2/L^*$ channel uses are required to provide each user with a single bit. In the remainder of this sub-section, we will show the achievability of corner points A_1 , A_2 , B_1 , B_2 and C_1 . To this end, we specify the optimal rate allocation parameters $\tilde{\mathbf{r}}^*$.

Class I: Now, we present the DTB-optimal scheme for all Class I channel regimes. Again, we distinguish between Class I SCL channel regimes for which $n_{d2} \geq n_{d3}$ holds and Class I WCL channel regimes where $n_{d2} \leq n_{d3}$ applies. The achievable DTB for both cases is given by the following proposition.

Proposition 8. The achievable DTB for Class I channel regimes of the network under study for $n_F \geq 0$ and $\mu \in [0, 1]$ under a parallel-fronthaul edge transmission is given for $n_{d2} \geq n_{d3}$ by

$$\Delta_{\det}(\mu, n_F, \mathbf{n}) = \begin{cases} \max \left\{ \frac{2-\mu}{n_F+n_{d2}}, \frac{2}{n_{d1}+n_{d3}} \right\} & \text{if } n_{d1} + n_{d3} \geq n_{d2} \geq n_{d3} \geq n_{d1} \\ \max \left\{ \frac{2-\mu}{n_F+n_{d2}}, \frac{1}{n_{d3}} \right\} & \text{if } 2n_{d3} \geq n_{d2} \geq n_{d1} \geq n_{d3} \\ \max \left\{ \frac{2-\mu}{n_F+n_{d2}}, \frac{1}{n_{d3}} \right\} & \text{if } n_{d1} \geq n_{d2} \geq n_{d3}, 2n_{d3} \geq n_{d2} \end{cases}, \quad (81)$$

and for $n_{d2} \leq n_{d3}$ by

$$\Delta_{\det}(\mu, n_F, \mathbf{n}) = \begin{cases} \max \left\{ \frac{2-\mu}{n_F+n_{d3}}, \frac{1}{n_{d3}} \right\} & \text{if } n_{d1} \geq n_{d3} \geq n_{d2}, 2n_{d2} \geq n_{d3} \\ \max \left\{ \frac{2-\mu}{n_F+n_{d3}}, \frac{1}{n_{d2}} \right\} & \text{if } n_{d1} + n_{d3} \geq 2n_{d2} \geq n_{d3} \geq n_{d2} \geq n_{d1} \\ \max \left\{ \frac{2-\mu}{n_F+n_{d3}}, \frac{2}{n_{d1}+n_{d3}} \right\} & \text{if } 2n_{d2} \geq n_{d1} + n_{d3} \geq n_{d3} \geq n_{d2} \geq n_{d1} \\ \max \left\{ \frac{2-\mu}{n_F+n_{d3}}, \frac{1}{n_{d1}} \right\} & \text{if } 2n_{d2} \geq n_{d3} \geq n_{d1} \geq n_{d2} \end{cases}. \quad (82)$$

In what follows, we present the scheme for all Class I channel regimes specified in proposition 8 in detail. To this end, we establish the achievability at corner points A_1 and B_2 and apply arguments of convexity for achievability at intermediary points.

First, we consider corner point A_1 for which $\mu = 0$. At this fractional cache size, we solve the optimization problem (80). Table VI and Tables VII and VIII of Appendix E specify the optimal rate allocation parameters $\tilde{\mathbf{r}}^*$ for Class I SCL and WCL channel regimes, respectively, that attain a DTB of $2/(n_F + \max\{n_{d2}, n_{d3}\})$ at $\mu = 0$. We point out that Table VIII in general is applicable for $n_F \geq (n_{d3} - 2n_{d2})^+$. For Class I WCL channel regimes, however, $(n_{d3} - 2n_{d2})^+ = 0$.

Next, we show the achievability of corner point B_2 at fractional cache size $\mu'_p(n_F, \mathbf{n})$. We will show that the achievability at this corner point is directly deducible from the scheme for the corner point B_2 under serial fronthaul-edge transmission (see sub-section V-A). The same observation applies to corner points B_1 and C_1 as we shall see later. We use the indices (S)

and (P) to distinguish corner points of serial transmissions from those for parallel transmissions. Through careful comparison of Theorems 1 and 2, one can verify that

$$\mu'_S(\mathbf{n})\bar{L}^* = \mu'_P(n_F, \mathbf{n})\bar{L}^* + n_F. \quad (83)$$

Recall that in the delivery phase of serial transmission, $\mu'_S(\mathbf{n})\bar{L}^* = R_{2,p}^{u,S,*} + R_{\text{IN}}^{v,S,*}$ bits are required in total to attain the DTB of corner point B_2^S . Hereby, $R_{\text{IN}}^{v,S,*}$ bits originate as XOR combinations of the files W_{d_1} and W_{d_2} requested by U_1 and U_2 while $R_{2,p}^{u,S,*}$ bits are a raw data subset of file W_{d_1} . In this regard, Eq. (83) suggests that the HeNB's conveyed content (during the delivery phase) consisting of $\mu'_S(\mathbf{n})\bar{L}^*$ bits for corner point B_2^S is separable into two distinct components attributed to edge caching and fronthauling for the case of parallel transmission (similar observation for B_1^S and C_1^S). In the following, we explicitly account for the *separability in delivery content* suggested in Eq. (83) and propose how to map the achievability scheme of serial to parallel fronthaul-edge transmission. The mapping is done as follows:

We keep the signal structure for both parallel and serial transmissions identical by adjusting the rate allocation parameters of parallel transmissions according to

$$R_{1,p}^{w,P,*}[t] = R_{1,p}^{w,S,*}, \quad (84a)$$

$$R_{1,c}^{u,P,*}[t] = R_{1,c}^{v,P,*}[t] = 0, \quad (84b)$$

$$R_{2,c}^{u,P,*}[t] = R_c^{u,S,*}, \quad (84c)$$

$$R_{2,c}^{v,P,*}[t] = R_c^{v,S,*}, \quad (84d)$$

$$R_{2,p}^{u,P,*}[t] = R_{2,p}^{u,S,*}, \quad (84e)$$

$$R_{\text{IN}}^{n,P,*}[t] = R_{\text{IN}}^{v,P,*}[t] = R_{\text{IN}}^{n,S,*} = R_{\text{IN}}^{v,S,*}, \quad (84f)$$

$$l_i^{P,*}[t] = l_i^{S,*}, \quad i = 1, \dots, 4 \quad (84g)$$

for $t = [t_1 : t_2]$. As previously suggested, at the HeNB we account for the separability in delivery content. To this end, we decompose signals $\mathbf{u}_{2,p}[t]$ and $\mathbf{n}_{\text{IN}}[t]$ for the parallel transmission case into sub-signals attributed to edge caching and fronthauling (superscripts (C) and (F)) in agreement with

$$\mathbf{u}_{2,p}[t] = \left(\mathbf{u}_{2,p}^C[t], \mathbf{u}_{2,p}^F[t] \right)^T, \quad (85a)$$

$$\mathbf{n}_{\text{IN}}[t] = \left(\mathbf{n}_{\text{IN}}^C[t], \mathbf{n}_{\text{IN}}^F[t] \right)^T, \quad (85b)$$

with rate allocation

$$R_{2,p}^{F,*}[t] + R_{\text{IN}}^{n,F,*}[t] = n_F, \quad (86a)$$

$$R_{2,p}^{C,*}[t] + R_{\text{IN}}^{n,C,*}[t] = \mu'_S(\mathbf{n})\bar{L}^* - n_F \quad \text{at corner point } B_2, \quad (86b)$$

for $t = [t_1 : t_2]$. Recall that Tables II and III of Appendix C specify the optimal rate allocation parameters at corner point B_2^S (of serial transmissions) for Class I channel regimes. These tables can be readily utilized to construct the achievability scheme of parallel transmissions at corner point B_2^P in accordance with Eq. (84). This concludes the achievability at corner point B_2^P for the case of parallel transmission.

Class II: Now, we establish the achievability for all Class II channel regimes for the low ($n_F \leq n_{d3} - 2n_{d2}$) and high ($n_F \geq n_{d3} - 2n_{d2}$) fronthaul capacity regimes. The following proposition specifies the achievable DTB.

Proposition 9. The achievable DTB for Class II channel regimes of the network under study for $\mu \in [0, 1]$ under a parallel-fronthaul edge transmission is given for $n_F \leq n_{d3} - 2n_{d2}$ by

$$\Delta_{\text{det}}(\mu, n_F, \mathbf{n}) = \begin{cases} \max \left\{ \frac{1-\mu}{n_F+n_{d2}}, \frac{2-\mu}{n_F+n_{d3}}, \frac{1}{n_{d3}} \right\} & \text{if } n_{d1} \geq n_{d3} \geq 2n_{d2} \\ \max \left\{ \frac{1-\mu}{n_F+n_{d2}}, \frac{2-\mu}{n_F+n_{d3}}, \frac{1}{n_{d1}} \right\} & \text{if } n_{d1} + n_{d2} \geq n_{d3} \geq n_{d1} \geq n_{d2}, n_{d3} \geq 2n_{d2} \end{cases}, \quad (87)$$

and for $n_F \geq n_{d3} - 2n_{d2}$ by

$$\Delta_{\text{det}}(\mu, n_F, \mathbf{n}) = \begin{cases} \max \left\{ \frac{2-\mu}{n_F+n_{d3}}, \frac{1}{n_{d3}} \right\} & \text{if } n_{d1} \geq n_{d3} \geq 2n_{d2} \\ \max \left\{ \frac{2-\mu}{n_F+n_{d3}}, \frac{1}{n_{d1}} \right\} & \text{if } n_{d1} + n_{d2} \geq n_{d3} \geq n_{d1} \geq n_{d2}, n_{d3} \geq 2n_{d2} \end{cases}, \quad (88)$$

Next, we present the scheme for all Class II channel regimes specified in proposition 8 in detail. To this end, we establish the achievability at corner points A_2 , B_1 and B_2 for low fronthaul capacities $n_F \leq n_{d3} - 2n_{d2}$ as well as A_1 and B_2 for high fronthaul capacities $n_F \geq n_{d3} - 2n_{d2}$. Points between these corner points are achievable due to arguments of DTB-convexity.

To establish the achievability of A_1 and A_2 , we solve the linear optimization problem at $\mu = 0$. Hereby, by choosing the rate allocation parameters according to Table VIII included in Appendix E for $n_F \geq n_{d3} - 2n_{d2} \geq 0$ the DTB $2/(n_F+n_{d3})$ of corner point A_1 is attainable. On the other hand, fixing $\tilde{\mathbf{r}}$ in accordance with Table IX of Appendix E for $n_F \leq n_{d3} - 2n_{d2}$ accomplishes the achievable DTB $1/(n_F+n_{d2})$ of corner point A_2 .

We now move to corner points B_1 and B_2 for Class II channel regimes. For both corner points, the mapping of achievability schemes from serial to parallel transmission as given in Eq. (84)

applies. In fact, as far as B_2 for Class II channel regimes are concerned, the separability in the HeNB's delivery content as stated in Eq. (83) is identical. Thus, columns two and five of Table III of Appendix C allow for the direct mapping of serial and parallel transmission of Class II channel regimes. In terms of B_1 , however, the HeNB's delivery content separability in Eq. (83) changes to

$$\mu_S''(\mathbf{n})\bar{L}^* = \mu_P''(n_F, \mathbf{n})\bar{L}^* + n_F. \quad (89)$$

such that the RHS of Eq. (86b) is replaced by (89). Hereby with Table IV, the mapping can be readily established. This completes the achievability of corner points A_1, A_2, B_1 and B_2 for Class II channel regimes.

Class III: Now, we present the DTB-optimal scheme for the Class III channel regime under a parallel fronthaul-edge transmission for any $n_F \geq 0$. The following proposition quantifies the achievable DTB.

Proposition 10. The achievable DTB for Class III channel regime of the network under study for $\mu \in [0, 1]$ and $n_F \geq 0$ under a parallel-fronthaul edge transmission corresponds to

$$\Delta_{\text{det}}(\mu, n_F, \mathbf{n}) = \max \left\{ \frac{1 - \mu}{n_F + n_{d2}}, \frac{1}{n_{d1}} \right\} \text{ if } n_{d3} \geq n_{d1} + n_{d2} \geq n_{d1} \geq n_{d2}. \quad (90)$$

For corner point A_1 , we solve the optimization problem (80) at Class III channel regime for $\mu = 0$. This results in Table X of Appendix E.

The mapping of achievability schemes from serial to parallel fronthaul transmissions given in Eq. 84 also applies to corner point C_1 . The only difference is that the HeNB's delivery content is separable in consonance with

$$\mu_S'''(\mathbf{n})\bar{L}^* = \mu_P'''(n_F, \mathbf{n})\bar{L}^* + n_F. \quad (91)$$

For this particular corner point, Table V ought to be used to construct the mapping. This concludes the achievability of the Class III channel regime.

IX. CONCLUSION

In this paper, we have studied the fundamental limit on the delivery time of a cloud and cache-aided HetNet in the downlink. We utilize the delivery time per bit (DTB) as the performance metric that captures the worst-case per-bit delivery latency of requested files. This metric inherently captures aspects of achievable per-user rate fairness. The linear deterministic model

is used to completely characterize the optimal tradeoff between storage and delivery time for a HetNet with two transmitters and two receivers operating under parallel or serial fronthaul-edge transmissions at various channel regimes. A combination of private, common and interference-neutralizing information subject to optimized rate allocation is shown to be DTB-optimal. We identify channel regimes, where edge caching and fronthauling provide synergistic and non-synergistic benefits. Interestingly, for the case of serial transmission we determine three distinct classes of channel regimes, Class I, II and III, for which operating below a threshold fronthaul capacity is as if the fronthaul link is absent. On the contrary, in case of parallel transmission where the HeNB operates in full-duplex mode such threshold fronthaul capacity does not exist. Instead any positive fronthaul capacity below a maximum fronthaul capacity has a DTB-reducing effect. This is due to the fact that fronthaul and wireless transmission can occur simultaneously enabling the exploitation of cloud and caching resources in the most efficient manner.

APPENDIX A

LOWER BOUND FOR SERIAL TRANSMISSION FOR $n_F = 0$

In this section, we develop lower bounds on the DTB $\Delta_{\text{det}}^*(\mu, n_F, \mathbf{n})$ for the cache-only F-RAN ($n_F = 0$) to settle the optimality of our proposed achievability scheme for various regimes of channel parameters n_{d1}, n_{d2} and n_{d3} . Based on the definition of the DTB in (8) for serial transmission, we need to first consider the worst-case demand pattern $\mathbf{d} = (d_1, d_2)^T$; that is U_1 and U_2 request *distinct* files W_{d_1} and W_{d_2} ($d_1 \neq d_2$). Without loss of generality, we assume that $\mathbf{d} = (1, 2)^T$, i.e., $W_{d_1} = W_1$ and $W_{d_2} = W_2$. Given channel realization $\mathbf{n} = (n_{d1}, n_{d2}, n_{d3})^T$, we establish lower bounds on the delivery time T_E as the converse on $\Delta_{\text{det}}^*(\mu, n_F = 0, \mathbf{n})$. This suffices because in the cache-only setting, the cloud-to-HeNB is inactive during the delivery phase such that $T_F = 0$. The first lower bound is based on the idea that for any feasible scheme, reliable decoding of W_1 and W_2 is possible, when any arbitrary decoder is provided with side information containing $\mathbf{S}^{q-\max\{n_{d2}, n_{d3}\}} \mathbf{x}_2^{T_E}$, as well as cached contents S_1 and S_2 . This is due to the fact that through this side information, the decoder can recover $\mathbf{y}_1^{T_E}$ and hence W_1 as well as $\mathbf{y}_2^{T_E}$ and thus W_2 . We obtain the lower bound as follows:

$$\begin{aligned}
2L &= H(W_1, W_2) \\
&= I\left(W_1, W_2; \mathbf{S}^{q-\max\{n_{d2}, n_{d3}\}} \mathbf{x}_2^{T_E}, S_1, S_2\right) + H(W_1, W_2 | \mathbf{S}^{q-\max\{n_{d2}, n_{d3}\}} \mathbf{x}_2^{T_E}, S_1, S_2) \\
&= I\left(W_1, W_2; \mathbf{S}^{q-\max\{n_{d2}, n_{d3}\}} \mathbf{x}_2^{T_E}, S_1, S_2\right) + H(W_1 | \mathbf{S}^{q-\max\{n_{d2}, n_{d3}\}} \mathbf{x}_2^{T_E}, S_1, S_2)
\end{aligned}$$

$$\begin{aligned}
& + H(W_2 | \mathbf{S}^{q-\max\{n_{d2}, n_{d3}\}} \mathbf{x}_2^{TE}, S_1, S_2, W_1) \\
\stackrel{(a)}{\leq} & I(W_1, W_2; \mathbf{S}^{q-\max\{n_{d2}, n_{d3}\}} \mathbf{x}_2^{TE}, S_1, S_2) + H(W_1 | \mathbf{S}^{q-\max\{n_{d2}, n_{d3}\}} \mathbf{x}_2^{TE}, S_1, S_2, \mathbf{y}_1^{TE}) \\
& + H(W_2 | \mathbf{y}_2^{TE}, S_1, S_2, W_1, \mathbf{y}_1^{TE}) \\
\stackrel{(b)}{\leq} & I(W_1, W_2; \mathbf{S}^{q-\max\{n_{d2}, n_{d3}\}} \mathbf{x}_2^{TE}, S_1, S_2) + L\epsilon_L \\
= & H(\mathbf{S}^{q-\max\{n_{d2}, n_{d3}\}} \mathbf{x}_2^{TE}, S_1, S_2) + L\epsilon_L \\
\leq & H(\mathbf{y}_2^{TE}, \mathbf{S}^{q-\max\{n_{d2}, n_{d3}\}} \mathbf{x}_2^{TE}, S_1, S_2) + L\epsilon_L \\
\stackrel{(c)}{\leq} & H(\mathbf{S}^{q-\max\{n_{d2}, n_{d3}\}} \mathbf{x}_2^{TE}) + H(S_1) + H(\mathbf{y}_2^{TE} | \mathbf{S}^{q-\max\{n_{d2}, n_{d3}\}} \mathbf{x}_2^{TE}, S_1) \\
& + H(S_2 | \mathbf{S}^{q-\max\{n_{d2}, n_{d3}\}} \mathbf{x}_2^{TE}, S_1, \mathbf{y}_2^{TE}) + L\epsilon_L \\
\stackrel{(d)}{\leq} & H(\mathbf{S}^{q-\max\{n_{d2}, n_{d3}\}} \mathbf{x}_2^{TE}) + H(S_1) + H(W_2, S_2 | \mathbf{S}^{q-\max\{n_{d2}, n_{d3}\}} \mathbf{x}_2^{TE}, S_1, \mathbf{y}_2^{TE}) + L\epsilon_L \\
\stackrel{(e)}{\leq} & H(\mathbf{S}^{q-\max\{n_{d2}, n_{d3}\}} \mathbf{x}_2^{TE}) + H(S_1) + L\epsilon_L \\
\leq & T_E \max\{n_{d2}, n_{d3}\} + \mu L + L\epsilon_L, \tag{92}
\end{aligned}$$

where (a) is because \mathbf{y}_1^{TE} is a function of $\mathbf{S}^{q-\max\{n_{d2}, n_{d3}\}} \mathbf{x}_2^{TE}, S_1, S_2$ and it is because $\mathbf{S}^{q-\max\{n_{d2}, n_{d3}\}} \mathbf{x}_2^{TE}$ contains all information on \mathbf{y}_2^{TE} , (b) follows from Fano's inequality with ϵ_L being a term that vanishes as $L \rightarrow \infty$, (c) follows since conditioning does not increase entropy, (d) is since $H(\mathbf{y}_2^{TE} | \mathbf{S}^{q-\max\{n_{d2}, n_{d3}\}} \mathbf{x}_2^{TE}) = 0$ and the non-negativity of the discrete entropy and (e) is due to Fano's inequality $H(W_2 | \mathbf{y}_2^{TE}) \leq L\epsilon_L$ and $H(S_2 | W_2) = 0$.

Since the requested files W_1 and W_2 can also be retrieved from the received signals \mathbf{y}_1^{TE} and \mathbf{y}_2^{TE} , another lower bound is obtained as follows:

$$\begin{aligned}
2L & = H(W_1, W_2) \\
& = I(W_1, W_2; \mathbf{y}_1^{TE}, \mathbf{y}_2^{TE}) + H(W_1, W_2 | \mathbf{y}_1^{TE}, \mathbf{y}_2^{TE}) \\
\stackrel{(a)}{\leq} & I(W_1, W_2; \mathbf{y}_1^{TE}, \mathbf{y}_2^{TE}) + L\epsilon_L \\
& = H(\mathbf{y}_2^{TE}) + H(\mathbf{y}_1^{TE} | \mathbf{y}_2^{TE}) + L\epsilon_L \\
& = \sum_{t=1}^{T_E} \left[H(\mathbf{y}_2[t] | \mathbf{y}_2^{t-1}) + H(\mathbf{y}_1[t] | \mathbf{y}_1^{t-1}, \mathbf{y}_2^{TE}) \right] + L\epsilon_L \\
\stackrel{(b)}{\leq} & \sum_{t=1}^{T_E} \left[H(\mathbf{y}_2[t]) + H(\mathbf{y}_1[t] | \mathbf{y}_2[t]) \right] + L\epsilon_L
\end{aligned}$$

$$\begin{aligned}
& \stackrel{(c)}{\leq} T_E n_{d3} + \sum_{t=1}^{T_E} \left[H(\mathbf{S}^{q-n_{d1}} \mathbf{x}_1[t] \oplus \mathbf{S}^{q-n_{d2}} \mathbf{x}_2[t] | \mathbf{S}^{q-n_{d3}} \mathbf{x}_2[t]) \right] + L\epsilon_L \\
& \stackrel{(d)}{\leq} L\epsilon_L + T_E \cdot \begin{cases} n_{d1} + n_{d3} & \text{for } n_{d3} \geq n_{d2} \\ \max\{n_{d1} + n_{d3}, n_{d2}\} & \text{for } n_{d3} \leq n_{d2} \end{cases} \\
& = T_E \max\{n_{d1} + n_{d3}, n_{d2}\} + L\epsilon_L, \tag{93}
\end{aligned}$$

where (a) follows from Fano's inequality, (b) follows since conditioning does not increase the entropy and the independence of $\mathbf{y}_2[t]$ from \mathbf{y}_2^{t-1} , (c) is because the Bern(1/2) distribution maximizes the binary entropy of each component of all n_{d3} random elements of $\mathbf{y}_2[t]$, (d) follows from the fact that conditioning does not increase entropy and that the randomness in $\mathbf{S}^{q-n_{d2}} \mathbf{x}_2[t]$ is fully or partially contained in $\mathbf{S}^{q-n_{d3}} \mathbf{x}_2[t]$ depending on whether $n_{d3} \geq n_{d2}$ or $n_{d3} \leq n_{d2}$.

Also, file W_k , $k \in \{1, 2\}$, must be decodable if U_k is aware of $\mathbf{y}_k^{T_E}$, yielding the lower bound on T_E

$$\begin{aligned}
L & = H(W_k) \\
& = I(W_k; \mathbf{y}_k^{T_E}) + H(W_k | \mathbf{y}_k^{T_E}) \\
& \stackrel{(a)}{\leq} I(W_k; \mathbf{y}_k^{T_E}) + L\epsilon_L \\
& \leq H(\mathbf{y}_k^{T_E}) + L\epsilon_L \\
& \leq L\epsilon_L + T_E \cdot \begin{cases} \max\{n_{d1}, n_{d2}\} & \text{for } k = 1 \\ n_{d3} & \text{for } k = 2 \end{cases}, \tag{94}
\end{aligned}$$

where (a) is due to Fano's inequality.

Finally, file W_1 , is also decodable if U_1 is aware of the information subset $\{S_1, S_2, \mathbf{S}^{q-n_{d2}} \mathbf{x}_2^{T_E}\}$.

Thus, we find the lower on T_E as follows:

$$\begin{aligned}
L & = H(W_1) \stackrel{(a)}{=} H(W_1 | W_2) \\
& = I(W_1; S_1, S_2, \mathbf{S}^{q-n_{d2}} \mathbf{x}_2^{T_E} | W_2) + H(W_1 | S_1, S_2, \mathbf{S}^{q-n_{d2}} \mathbf{x}_2^{T_E}, W_2) \\
& \stackrel{(b)}{\leq} I(W_1; S_1, S_2, \mathbf{S}^{q-n_{d2}} \mathbf{x}_2^{T_E} | W_2) + L\epsilon_L \\
& = H(S_1, S_2, \mathbf{S}^{q-n_{d2}} \mathbf{x}_2^{T_E} | W_2) + L\epsilon_L \\
& \stackrel{(c)}{\leq} H(\mathbf{S}^{q-n_{d2}} \mathbf{x}_2^{T_E}) + H(S_1) + L\epsilon_L \\
& \leq T_E n_{d2} + \mu L + L\epsilon_L. \tag{95}
\end{aligned}$$

Step (a) follows from the independence of files W_1 and W_2 , (b) follows by applying Fano's inequality to the conditional entropy and (c) is due to $H(S_2|W_2) = 0$ and conditioning does not increase entropy.

Rearranging the expressions (92), (93), (94) and (95) and letting $L \rightarrow \infty$ such that $\epsilon_L \rightarrow 0$, yields the desired lower bound on the DTB.

APPENDIX B

LOWER BOUND FOR SERIAL TRANSMISSION FOR $n_F \geq 0$

In this section, we develop lower bounds on the DTB $\Delta_{\text{det}}^*(\mu, n_F, \mathbf{n})$ for the F-RAN with non-negative fronthauling capacity ($n_F \geq 0$). Through this setting, we change the definition of q in the LDM to $q = \max\{n_F, n_{d1}, n_{d2}, n_{d3}\}$. We use the same request pattern as in Appendix A and develop two lower bounds on weighted linear combinations of wireless and fronthaul delivery time T_E and T_F . For this purpose, we extend the bounds (92) and (95) by incorporating the fronthaul transmission through the message $\mathbf{S}^{q-n_F} \mathbf{x}_F^{T_F}$. The bounds (93) and (94) on the wireless delivery time T_E remain valid.

We modify bound (95) as follows:

$$\begin{aligned}
2L &= H(W_1, W_2) \\
&= I\left(W_1, W_2; \mathbf{S}^{q-n_F} \mathbf{x}_F^{T_F}, \mathbf{S}^{q-\max\{n_{d2}, n_{d3}\}} \mathbf{x}_2^{T_E}, S_1, S_2\right) \\
&\quad + H\left(W_1, W_2 | \mathbf{S}^{q-n_F} \mathbf{x}_F^{T_F}, \mathbf{S}^{q-\max\{n_{d2}, n_{d3}\}} \mathbf{x}_2^{T_E}, S_1, S_2\right) \\
&\stackrel{(a)}{\leq} T_E \max\{n_{d2}, n_{d3}\} + T_F n_F + \mu L + L \epsilon_L.
\end{aligned} \tag{96}$$

Similarly to (95), we obtain the bound

$$\begin{aligned}
L &= H(W_1) = H(W_1 | W_2) \\
&= I\left(W_1; S_1, S_2, \mathbf{S}^{q-n_F} \mathbf{x}_F^{T_F}, \mathbf{S}^{q-n_{d2}} \mathbf{x}_2^{T_E} | W_2\right) + H\left(W_1 | S_1, S_2, \mathbf{S}^{q-n_F} \mathbf{x}_F^{T_F}, \mathbf{S}^{q-n_{d2}} \mathbf{x}_2^{T_E}, W_2\right) \\
&\stackrel{(a)}{\leq} T_E n_{d2} + T_F n_F + \mu L + L \epsilon_L,
\end{aligned} \tag{97}$$

where (a) follows by applying the exact same bounding technique as in (92) and (95). Rearranging the expressions (96) and (97) and letting $L \rightarrow \infty$ such that $\epsilon_L \rightarrow 0$, yields the following two

lower bounds on linear combinations of T_E and T_F .

$$\frac{T_E}{L} + \frac{T_F}{L} \frac{n_F}{\max\{n_{d2}, n_{d3}\}} \geq \frac{2 - \mu}{\max\{n_{d2}, n_{d3}\}}, \quad (98a)$$

$$\frac{T_E}{L} + \frac{T_F}{L} \frac{n_F}{n_{d2}} \geq \frac{1 - \mu}{n_{d2}}. \quad (98b)$$

We can easily see from (98a) and (98b) that for $n_F \leq \max\{n_{d2}, n_{d3}\}$ and $n_F \leq n_{d2}$, the RHS of both inequalities function as lower bounds for $(T_E+T_F)/L$. These RHSs are in agreement with two lower bounds on the DTB for cache-only schemes (see (22)).

APPENDIX C

OPTIMAL RATE ALLOCATION FOR ACHIEVABILITY IN SERIAL TRANSMISSION

In this section, we state the optimal rate allocation parameters at corner points B_1, B_2 and C_1 when solving the rate maximization problem (45) under serial transmission.

Regimes \mathcal{R}_{B_2}	$n_{d1} + n_{d3} \geq n_{d2} \geq n_{d3} \geq n_{d1}$	$2n_{d3} \geq n_{d2} \geq n_{d1} \geq n_{d3}$	$n_{d1} \geq n_{d2} \geq n_{d3}, 2n_{d3} \geq n_{d2}$
$R_{1,p}^{w,*} = R_{1,p}^{u,*}$	$n_{d2} - n_{d3}$	$n_{d2} - n_{d3}$	$n_{d2} - n_{d3}$
$R_c^{u,*}$	$\frac{n_{d3} - n_{d1}}{2}$	0	0
$R_{2,p}^{u,*}$	0	0	0
$R_{IN}^{v,*}$	$n_{d1} + n_{d3} - n_{d2}$	$2n_{d3} - n_{d2}$	$2n_{d3} - n_{d2}$
$R_c^{v,*}$	$\frac{2n_{d2} - n_{d1} - n_{d3}}{2}$	$n_{d2} - n_{d3}$	$n_{d2} - n_{d3}$
$R_{IN}^{n,*}$	$n_{d1} + n_{d3} - n_{d2}$	$2n_{d3} - n_{d2}$	$2n_{d3} - n_{d2}$
l_1^*	0	0	$n_{d1} - n_{d2}$
l_2^*	$2n_{d2} - n_{d1} - n_{d3}$	$2n_{d2} - n_{d1} - n_{d3}$	$n_{d2} - n_{d3}$
l_3^*	0	$n_{d1} - n_{d3}$	$n_{d2} - n_{d3}$
l_4^*	0	0	$n_{d1} - n_{d2}$
\bar{L}^*	$\frac{n_{d1} + n_{d3}}{2}$	n_{d3}	n_{d3}
$\Delta'_{LB}(\mathbf{n})$	$\frac{2}{n_{d1} + n_{d3}}$	$\frac{1}{n_{d3}}$	$\frac{1}{n_{d3}}$
$\mu'(\mathbf{n})$	$2 - \frac{2n_{d2}}{n_{d1} + n_{d3}}$	$2 - \frac{n_{d2}}{n_{d3}}$	$2 - \frac{n_{d2}}{n_{d3}}$

TABLE II: Rate allocation parameters for corner point B_2 at fractional cache size $\mu'(\mathbf{n})$ in all Class I SCL channel regimes.

APPENDIX D

LOWER BOUND FOR PARALLEL TRANSMISSION

In this section, we develop lower bounds on the DTB $\Delta_{\det}^*(\mu, n_F, \mathbf{n})$ for the F-RAN with non-negative fronthauling capacity ($n_F \geq 0$) under a parallel fronthaul-edge transmission setting. We

Regimes \mathcal{R}_{B_2}	$n_{d1} \geq n_{d3} \geq n_{d2}$	$n_{d3} \geq n_{d2} \geq n_{d1}$		$n_{d1} + n_{d2} \geq n_{d3} \geq n_{d1} \geq n_{d2}$
		$n_{d1} + n_{d3} \geq 2n_{d2} \geq n_{d3}$	$2n_{d2} \geq n_{d1} + n_{d3} \geq n_{d3}$	
$R_{1,p}^{w,*} = R_{1,p}^{v,*}$	$n_{d3} - n_{d2}$	$n_{d3} - n_{d2}$	$n_{d3} - n_{d2}$	$n_{d3} - n_{d2}$
$R_c^{\mu,*}$	0	$n_{d3} - n_{d2}$	$\frac{n_{d3} - n_{d1}}{2}$	$n_{d3} - n_{d1}$
$R_{2,p}^{\mu,*}$	$n_{d3} - n_{d2}$	0	0	$n_{d1} - n_{d2}$
$R_{IN}^{v,*}$	n_{d2}	$2n_{d2} - n_{d3}$	n_{d1}	$n_{d1} + n_{d2} - n_{d3}$
$R_c^{v,*}$	0	0	$\frac{2n_{d2} - n_{d1} - n_{d3}}{2}$	0
$R_{IN}^{n,*}$	0	$2n_{d2} - n_{d3}$	n_{d1}	$n_{d1} + n_{d2} - n_{d3}$
l_1^*	$n_{d1} - n_{d3}$	0	0	0
l_2^*	0	$n_{d3} - n_{d1}$	$n_{d3} - n_{d1}$	$n_{d3} - n_{d1}$
l_3^*	0	$n_{d1} + n_{d3} - 2n_{d2}$	0	$n_{d3} - n_{d1}$
l_4^*	$n_{d1} - n_{d3}$	0	0	0
\bar{L}^*	n_{d3}	n_{d2}	$\frac{n_{d1} + n_{d3}}{2}$	n_{d1}
$\Delta'_{LB}(\mathbf{n})$	$\frac{1}{n_{d3}}$	$\frac{1}{n_{d2}}$	$\frac{2}{n_{d1} + n_{d3}}$	$\frac{1}{n_{d1}}$
$\mu'(\mathbf{n})$	1	$2 - \frac{n_{d3}}{n_{d2}}$	$2 - \frac{2n_{d3}}{n_{d1} + n_{d3}}$	$2 - \frac{n_{d3}}{n_{d1}}$

TABLE III: Rate allocation parameters for corner point B_2 at fractional cache size $\mu'(\mathbf{n})$ in all Class I WCL channel regimes.

Regimes \mathcal{R}_{B_1}	$n_{d1} \geq n_{d3} \geq 2n_{d2}$	$n_{d1} + n_{d2} \geq n_{d3} \geq n_{d1} \geq n_{d2},$ $n_{d3} \geq 2n_{d2}$	
		$R_{1,p}^{w,*} = R_{1,p}^{v,*}$	$n_{d3} - n_{d2}$
$R_c^{\mu,*}$	n_{d2}	n_{d2}	n_{d2}
$R_{2,p}^{\mu,*}$	$n_{d3} - 2n_{d2}$	$n_{d3} - 2n_{d2}$	$n_{d3} - 2n_{d2}$
$R_{IN}^{v,*}$	0	0	0
$R_c^{v,*}$	0	0	0
$R_{IN}^{n,*}$	0	0	0
l_1^*	$n_{d1} - n_{d3}$	0	0
l_2^*	0	$n_{d3} - n_{d1}$	$n_{d3} - n_{d1}$
l_3^*	n_{d2}	n_{d2}	n_{d2}
l_4^*	$n_{d1} + n_{d2} - n_{d3}$	$n_{d1} + n_{d2} - n_{d3}$	$n_{d1} + n_{d2} - n_{d3}$
\bar{L}^*	$n_{d3} - n_{d2}$	$n_{d3} - n_{d2}$	$n_{d3} - n_{d2}$
$\Delta'_{LB}(\mathbf{n})$	$\frac{1}{n_{d3} - n_{d2}}$	$\frac{1}{n_{d3} - n_{d2}}$	$\frac{1}{n_{d3} - n_{d2}}$
$\mu''(\mathbf{n})$	$\frac{n_{d3} - 2n_{d2}}{n_{d3} - n_{d2}}$	$\frac{n_{d3} - 2n_{d2}}{n_{d3} - n_{d2}}$	$\frac{n_{d3} - 2n_{d2}}{n_{d3} - n_{d2}}$

TABLE IV: Rate allocation parameters for corner point B_1 at fractional cache size $\mu''(\mathbf{n})$

Regime \mathcal{R}_{C_1}	$n_{d3} \geq n_{d1} + n_{d2} \geq n_{d1} \geq n_{d2}$
$R_{1,p}^{w,*} = R_{1,p}^{v,*}$	$n_{d3} - n_{d2}$
$R_c^{\mu,*}$	n_{d2}
$R_{2,p}^{\mu,*}$	$n_{d1} - n_{d2}$
$R_{IN}^{v,*}$	0
$R_c^{v,*}$	0
$R_{IN}^{n,*}$	0
l_1^*	0
l_2^*	$n_{d3} - n_{d1}$
l_3^*	n_{d2}
l_4^*	0
\bar{L}^*	n_{d1}
$\Delta'_{LB}(\mathbf{n})$	$\frac{1}{n_{d1}}$
$\mu'''(\mathbf{n})$	$\frac{n_{d1} - n_{d2}}{n_{d1}}$

TABLE V: Rate allocation parameters for corner point C_1 at fractional cache size $\mu'''(\mathbf{n})$

change the definition of q in the LDM to $q = \max\{n_F, n_{d1}, n_{d2}, n_{d3}\}$. We use the same request pattern as in Appendix A and develop two lower bounds on the delivery time T_P . For this purpose, we modify the bounds (96) and (97) by replacing T_E with T_P ($T_E \leftrightarrow T_P$). The bounds (93) and (94) on the delivery time T_P remain valid.

We modify bound (96) as follows:

$$\begin{aligned}
2L &= H(W_1, W_2) \\
&= I(W_1, W_2; \mathbf{S}^{q-n_F} \mathbf{x}_F^{T_P}, \mathbf{S}^{q-\max\{n_{d2}, n_{d3}\}} \mathbf{x}_2^{T_P}, S_1, S_2) \\
&\quad + H(W_1, W_2 | \mathbf{S}^{q-n_F} \mathbf{x}_F^{T_P}, \mathbf{S}^{q-\max\{n_{d2}, n_{d3}\}} \mathbf{x}_2^{T_P}, S_1, S_2) \\
&\stackrel{(a)}{\leq} T_P(n_F + \max\{n_{d2}, n_{d3}\}) + \mu L + L\epsilon_L.
\end{aligned} \tag{99}$$

Similarly to (97), we obtain the bound

$$\begin{aligned}
L &= H(W_1) = H(W_1 | W_2) \\
&= I(W_1; S_1, S_2, \mathbf{S}^{q-n_F} \mathbf{x}_F^{T_P}, \mathbf{S}^{q-n_{d2}} \mathbf{x}_2^{T_P} | W_2) + H(W_1 | S_1, S_2, \mathbf{S}^{q-n_F} \mathbf{x}_F^{T_P}, \mathbf{S}^{q-n_{d2}} \mathbf{x}_2^{T_P}, W_2) \\
&\stackrel{(a)}{\leq} T_P(n_F + n_{d2}) + \mu L + L\epsilon_L,
\end{aligned} \tag{100}$$

where (a) follows by applying the exact same bounding technique as in (92) and (95). Rearranging the expressions (99) and (100) and letting $L \rightarrow \infty$ such that $\epsilon_L \rightarrow 0$, yields the following two lower bounds on the DTB for the parallel fronthaul-edge transmission setting.

$$\frac{T_P}{L} \geq \frac{2 - \mu}{n_F + \max\{n_{d2}, n_{d3}\}}, \tag{101a}$$

$$\frac{T_P}{L} \geq \frac{1 - \mu}{n_F + n_{d2}}. \tag{101b}$$

Combining bounds (93), (94), (101a) and (101b) on the DTB for the parallel fronthaul-edge transmission case finalizes the proof.

APPENDIX E

OPTIMAL RATE ALLOCATION FOR ACHIEVABILITY IN PARALLEL TRANSMISSION

In this section, we state the optimal rate allocation parameters at corner points A_1 and A_2 when solving the rate maximization problem (80) under parallel transmission.

Regimes \mathcal{R}_{A_1}	$n_{d1} + n_{d3} \geq n_{d2} \geq n_{d3} \geq n_{d1}$		$2n_{d3} \geq n_{d2} \geq n_{d1} \geq n_{d3}$		$n_{d1} \geq n_{d2} \geq n_{d3}, 2n_{d3} \geq n_{d2}$	
Time t	t_1	t_2	t_1	t_2	t_1	t_2
$R_{1,p}^{w,*} = R_{1,p}^{u,*}$	$n_{d2} - n_{d3}$	$n_{d2} - n_{d3}$	$n_{d2} - n_{d3}$	$n_{d2} - n_{d3}$	$n_{d2} - n_{d3}$	$n_{d2} - n_{d3}$
$R_{1,c}^{u,*}$	$(n_{F,\max}(\mathbf{n}) - n_F)^+$	0	$(n_{F,\max}(\mathbf{n}) - n_F)^+$	0	$(n_{F,\max}(\mathbf{n}) - n_F)^+$	0
$R_{2,c}^{u,*}$	$n_{d3} - n_{d1}$	0	0		0	
$R_{2,p}^{u,*}$	0					
$R_{IN}^{v,*}$	$\min \{n_F, n_{F,\max}(\mathbf{n})\}$					
$R_{1,c}^{v,*}$	0	$(n_{F,\max}(\mathbf{n}) - n_F)^+$	0	$(n_{F,\max}(\mathbf{n}) - n_F)^+$	0	$(n_{F,\max}(\mathbf{n}) - n_F)^+$
$R_{2,c}^{v,*}$	$n_{d2} - n_{d3}$	$n_{d2} - n_{d1}$	$n_{d2} - n_{d3}$		$n_{d2} - n_{d3}$	
$R_{IN}^{n,*}$	$\min \{n_F, n_{F,\max}(\mathbf{n})\}$					
l_1^*	0		0		$n_{d1} - n_{d2}$	
l_2^*	$2n_{d2} - n_{d1} - n_{d3}$		$2n_{d2} - n_{d1} - n_{d3}$		$n_{d2} - n_{d3}$	
l_3^*	$(n_{F,\max}(\mathbf{n}) - n_F)^+$		$n_{d1} - n_{d3} + (n_{F,\max}(\mathbf{n}) - n_F)^+$		$n_{d2} - n_{d3} + (n_{F,\max}(\mathbf{n}) - n_F)^+$	
l_4^*	0		0		$n_{d1} - n_{d2}$	
$n_{F,\max}(\mathbf{n})$	$n_{d1} + n_{d3} - n_{d2}$		$2n_{d3} - n_{d2}$		$2n_{d3} - n_{d2}$	
\tilde{L}^*	$\min \{n_{d2} + n_F, n_{d2} + n_{F,\max}(\mathbf{n})\}$		$\min \{n_{d2} + n_F, n_{d2} + n_{F,\max}(\mathbf{n})\}$		$\min \{n_{d2} + n_F, n_{d2} + n_{F,\max}(\mathbf{n})\}$	
$\Delta_{\det}^*(0, n_F, \mathbf{n})$	$\frac{2}{\min \{n_{d2} + n_F, n_{d2} + n_{F,\max}(\mathbf{n})\}}$		$\frac{2}{\min \{n_{d2} + n_F, n_{d2} + n_{F,\max}(\mathbf{n})\}}$		$\frac{2}{\min \{n_{d2} + n_F, n_{d2} + n_{F,\max}(\mathbf{n})\}}$	

TABLE VI: Rate allocation parameters for corner point A_1 at fractional cache size $\mu = 0$ in all Class I SCL channel regimes.

Regimes \mathcal{R}_{A_1}	$n_{d3} \geq n_{d2} \geq n_{d1}$			
	$n_{d1} + n_{d3} \geq 2n_{d2} \geq n_{d3}$		$2n_{d2} \geq n_{d1} + n_{d3} \geq n_{d3}$	
Time t	t_1	t_2	t_1	t_2
$R_{1,p}^{w,*} = R_{1,p}^{v,*}$	$n_{d3} - n_{d2}$			
$R_{1,c}^{u,*}$	$(n_{F,\max}(\mathbf{n}) - n_F)^+$	0	$(n_{F,\max}(\mathbf{n}) - n_F)^+$	0
$R_{2,c}^{u,*}$	$n_{d3} - n_{d2}$		$n_{d3} - n_{d2}$	$n_{d2} - n_{d1}$
$R_{2,p}^{u,*}$	0			
$R_{IN}^{v,*}$	$\min \{n_F, n_{F,\max}(\mathbf{n})\}$			
$R_{1,c}^{v,*}$	0	$(n_{F,\max}(\mathbf{n}) - n_F)^+$	0	$(n_{F,\max}(\mathbf{n}) - n_F)^+$
$R_{2,c}^{v,*}$	0		$2n_{d2} - n_{d1} - n_{d3}$	0
$R_{IN}^{n,*}$	$\min \{n_F, n_{F,\max}(\mathbf{n})\}$			
l_1^*	0			
l_2^*	$n_{d3} - n_{d1}$			
l_3^*	$n_{d1} + n_{d3} - 2n_{d2} + (n_{F,\max}(\mathbf{n}) - n_F)^+$		$(n_{F,\max}(\mathbf{n}) - n_F)^+$	
l_4^*	0			
$n_{F,\max}(\mathbf{n})$	$2n_{d2} - n_{d3}$		n_{d1}	
\tilde{L}^*	$\min \{n_{d3} + n_F, n_{d3} + n_{F,\max}(\mathbf{n})\}$		$\min \{n_{d3} + n_F, n_{d3} + n_{F,\max}(\mathbf{n})\}$	
$\Delta_{\det}^*(0, n_F, \mathbf{n})$	$\frac{2}{\min \{n_{d3} + n_F, n_{d3} + n_{F,\max}(\mathbf{n})\}}$		$\frac{2}{\min \{n_{d3} + n_F, n_{d3} + n_{F,\max}(\mathbf{n})\}}$	

TABLE VII: Rate allocation parameters for corner point A_1 at fractional cache size $\mu' = 0$ in Class I WCL channel regimes for $n_F \geq 0$

Regimes \mathcal{R}_{A_1}	$n_{d1} \geq n_{d3} \geq n_{d2}$		$n_{d1} + n_{d2} \geq n_{d3} \geq n_{d1} \geq n_{d2}$	
Time t	t_1	t_2	t_1	t_2
$R_{1,p}^{w,*} = R_{1,p}^{v,*}$	$n_{d3} - n_{d2}$		$n_{d3} - n_{d2}$	
$R_{1,c}^{u,*}$	$\min\{n_{d2}, (n_{d3} - n_F)^+\}$	$(n_{d3} - n_{d2} - n_F)^+$	$\min\{n_{d2}, \max\{n_{d1} - n_F, n_{d3} - n_{d1}\}\}$	$\max\{n_{d3} - n_{d2} - n_F, n_{d3} - n_{d1}\}$
$R_{2,c}^{u,*}$	0		0	
$R_{2,p}^{u,*}$	$\min\{n_{d3} - n_{d2}, n_F\}$	$\min\{\max\{n_{d3} - 2n_{d2}, n_F - n_{d2}\}^+, n_{d3} - n_{d2}\}$	$\min\{n_F, n_{d1} - n_{d2}\}$	$\min\{\max\{n_{d3} - 2n_{d2}, n_F - n_{d1} - n_{d2} + n_{d3}\}^+, n_{d1} - n_{d2}\}$
$R_{IN}^{v,*}$	$(\min\{n_{d2} + n_F - n_{d3}, n_{d2}\})^+$	$\min\{2n_{d2} - n_{d3} + n_F, n_{d2}, n_F\}$	$(\min\{n_{d2} + n_F - n_{d1}, n_{d1} + n_{d2} - n_{d3}\})^+$	$\min\{2n_{d2} - n_{d3} + n_F, n_{d1} + n_{d2} - n_{d3}, n_F\}$
$R_{1,c}^{v,*}$	0	$(\min\{2n_{d2} - n_{d3}, n_{d2} - n_F\})^+$	0	$(\min\{2n_{d2} - n_{d3}, n_{d1} + n_{d2} - n_{d3} - n_F\})^+$
$R_{2,c}^{v,*}$	0		0	
$R_{IN}^{n,*}$	$(\min\{n_{d2} + n_F - n_{d3}, n_{d2}\})^+$	$\min\{2n_{d2} - n_{d3} + n_F, n_{d2}, n_F\}$	$(\min\{n_{d2} + n_F - n_{d1}, n_{d1} + n_{d2} - n_{d3}\})^+$	$\min\{2n_{d2} - n_{d3} + n_F, n_{d1} + n_{d2} - n_{d3}, n_F\}$
l_1^*	$n_{d1} - n_{d3}$		0	
l_2^*	0		$n_{d3} - n_{d1}$	
l_3^*	$\min\{n_{d2}, (n_{d3} - n_F)^+\}$	$(\max\{n_{d3} - n_{d2} - n_F, n_{d2} - n_F\})^+$	$\min\{n_{d2}, \max\{n_{d1} - n_F, n_{d3} - n_{d1}\}\}$	$\max\{n_{d3} - n_{d2} - n_F, n_{d3} - n_{d1}, n_{d2} - n_F\}$
l_4^*	$n_{d1} - n_{d3} + (n_{d3} - n_{d2} - n_F)^+$	$\max\{\min\{n_{d1} + n_{d2} - n_{d3}, n_{d1} - n_F, n_{d1} - n_{d2}\}, n_{d1} - n_{d3}\}$	$(n_{d1} - n_{d2} - n_F)^+$	$(\min\{n_{d1} + n_{d2} - n_{d3}, n_F, \max(\mathbf{n}) - n_F, n_{d1} - n_{d2}\})^+$
$n_{F, \max(\mathbf{n})}$	n_{d3}		$2n_{d1} - n_{d3}$	
\tilde{L}^*	$\min\{n_{d3} + n_F, n_{d3} + n_{F, \max(\mathbf{n})}\}$		$\min\{n_{d3} + n_F, n_{d3} + n_{F, \max(\mathbf{n})}\}$	
$\Delta_{\det}^*(0, n_F, \mathbf{n})$	$\frac{2}{\min\{n_{d3} + n_F, n_{d3} + n_{F, \max(\mathbf{n})}\}}$		$\frac{2}{\min\{n_{d3} + n_F, n_{d3} + n_{F, \max(\mathbf{n})}\}}$	

TABLE VIII: Rate allocation parameters for corner point A_1 at fractional cache size $\mu = 0$ for $n_F \geq (n_{d3} - 2n_{d2})^+$. If $(n_{d3} - 2n_{d2})^+ = 0$, we describe the remaining Class I WCL channel regimes. Otherwise, if $(n_{d3} - 2n_{d2})^+ \geq 0$, the rate allocation parameters represent Class II channel regimes.

REFERENCES

- [1] J. Kakar, S. Gherekhloo, Z. H. Awan, and A. Sezgin, "Fundamental Limits on Latency in Cloud- and Cache-Aided HetNets," *IEEE International Conference on Communications*, May 2017.
- [2] Cisco, "The Zettabyte Era: Trends and Analysis," Tech. Rep., 2014.
- [3] E. Bastug, M. Bennis, and M. Debbah, "Living on the edge: The role of proactive caching in 5G wireless networks," *IEEE Communications Magazine*, vol. 52, no. 8, pp. 82–89, Aug 2014.
- [4] X. Wang, A. V. Vasilakos, M. Chen, Y. Liu, and T. T. Kwon, "A survey of green mobile networks: Opportunities and challenges," *Mob. Netw. Appl.*, vol. 17, no. 1, pp. 4–20, Feb. 2012.
- [5] X. Wang, M. Chen, T. Taleb, A. Ksentini, and V. C. M. Leung, "Cache in the air: exploiting content caching and delivery techniques for 5G systems," *IEEE Communications Magazine*, vol. 52, no. 2, pp. 131–139, February 2014.
- [6] J. G. Andrews, "Seven ways that hetnets are a cellular paradigm shift," *IEEE Communications Magazine*, vol. 51, no. 3, pp. 136–144, March 2013.

Regimes \mathcal{R}_{A_2}	$n_{d1} \geq n_{d3} \geq 2n_{d2}$	$n_{d1} + n_{d2} \geq n_{d3} \geq n_{d1} \geq n_{d2}, n_{d3} \geq 2n_{d2}$
Time t	$[t_1 : t_2]$	$[t_1 : t_2]$
$R_{1,p}^{w,*} = R_{1,p}^{v,*}$	$n_{d3} - n_{d2}$	$n_{d3} - n_{d2}$
$R_{1,c}^{u,*}$	0	0
$R_{2,c}^{u,*}$	n_{d2}	n_{d2}
$R_{2,p}^{u,*}$	$\min \{n_F, n_{F, \text{IM}}(\mathbf{n})\}$	$\min \{n_F, n_{F, \text{IM}}(\mathbf{n})\}$
$R_{\text{IN}}^{v,*}$	0	0
$R_{1,c}^{v,*}$	0	0
$R_{2,c}^{v,*}$	0	0
$R_{\text{IN}}^{n,*}$	0	0
l_1^*	$n_{d1} - n_{d3}$	0
l_2^*	0	$n_{d3} - n_{d1}$
l_3^*	n_{d2}	n_{d2}
l_4^*	$\max \{n_{d1} - n_{d2} - n_F, n_{d1} + n_{d2} - n_{d3}\}$	$\max \{n_{d1} - n_{d2} - n_F, n_{d1} + n_{d2} - n_{d3}\}$
$n_{F, \text{IM}}(\mathbf{n})$	$n_{d3} - 2n_{d2}$	$n_{d3} - 2n_{d2}$
\tilde{L}^*	$2 \min \{n_{d2} + n_F, n_{d2} + n_{F, \text{IM}}(\mathbf{n})\}$	$2 \min \{n_{d2} + n_F, n_{d2} + n_{F, \text{IM}}(\mathbf{n})\}$
$\Delta_{\text{det}}^*(0, n_F, \mathbf{n})$	$\frac{1}{\min \{n_{d2} + n_F, n_{d2} + n_{F, \text{IM}}(\mathbf{n})\}}$	$\frac{1}{\min \{n_{d2} + n_F, n_{d2} + n_{F, \text{IM}}(\mathbf{n})\}}$

TABLE IX: Rate allocation parameters for corner point A_2 at fractional cache size $\mu' = 0$ in all Class II channel regimes for $n_F \leq n_{d3} - 2n_{d2}$.

Regimes \mathcal{R}_{A_2}	$n_{d3} \geq n_{d1} + n_{d2} \geq n_{d1} \geq n_{d2}$
Time t	$[t_1 : t_2]$
$R_{1,p}^{w,*} = R_{1,p}^{v,*}$	$n_{d3} - n_{d2}$
$R_{1,c}^{u,*}$	0
$R_{2,c}^{u,*}$	n_{d2}
$R_{2,p}^{u,*}$	$\min \{n_F, n_{F, \text{max}}(\mathbf{n})\}$
$R_{\text{IN}}^{v,*}$	0
$R_{1,c}^{v,*}$	0
$R_{2,c}^{v,*}$	0
$R_{\text{IN}}^{n,*}$	0
l_1^*	0
l_2^*	$n_{d3} - n_{d1}$
l_3^*	n_{d2}
l_4^*	$(n_{F, \text{max}}(\mathbf{n}) - n_F)^+$
$n_{F, \text{max}}(\mathbf{n})$	$n_{d1} - n_{d2}$
\tilde{L}^*	$2 \min \{n_{d2} + n_F, n_{d2} + n_{F, \text{max}}(\mathbf{n})\}$
$\Delta_{\text{det}}^*(0, n_F, \mathbf{n})$	$\frac{1}{\min \{n_{d2} + n_F, n_{d2} + n_{F, \text{max}}(\mathbf{n})\}}$

TABLE X: Rate allocation parameters for corner point A_2 at fractional cache size $\mu' = 0$ in all Class III channel regimes for $n_F \geq 0$.

- [7] K. Shanmugam, N. Golrezaei, A. G. Dimakis, A. F. Molisch, and G. Caire, "Femtocaching: Wireless content delivery through distributed caching helpers," *IEEE Transactions on Information Theory*, vol. 59, no. 12, pp. 8402–8413, Dec 2013.
- [8] D. P. Malladi, "Heterogeneous networks in 3G and 4G," *IEEE Communications Theory Workshop*, May 2012.
- [9] A. Lozano, R. W. Heath, and J. G. Andrews, "Fundamental limits of cooperation," *IEEE Transactions on Information Theory*, vol. 59, no. 9, pp. 5213–5226, Sept 2013.
- [10] S. Gharekhloo, A. Chaaban, and A. Sezgin, "Cooperation for Interference Management: A GDoF Perspective," *IEEE Transactions on Information Theory*, vol. 62, no. 12, pp. 6986–7029, Dec 2016.
- [11] A. Checko, H. L. Christiansen, Y. Yan, L. Scolari, G. Kardaras, M. S. Berger, and L. Dittmann, "Cloud RAN for mobile networks – a technology overview," *IEEE Communications Surveys Tutorials*, vol. 17, no. 1, pp. 405–426, 2015.
- [12] M. Peng, S. Yan, K. Zhang, and C. Wang, "Fog-computing-based radio access networks: issues and challenges," *IEEE Network*, vol. 30, no. 4, pp. 46–53, July 2016.
- [13] S. M. Azimi, O. Simeone, and R. Tandon, "Fundamental limits on latency in small-cell caching systems: An information-theoretic analysis," in *2016 IEEE Global Communications Conference (GLOBECOM)*, Dec 2016, pp. 1–6.
- [14] Y. Liu and E. Erkip, "Completion time in broadcast channel and interference channel," in *Annual Allerton Conference on Communication, Control, and Computing (Allerton)*, Sept 2011, pp. 1694–1701.
- [15] M. A. Maddah-Ali and U. Niesen, "Fundamental limits of caching," *Trans. on Info. Theory*, vol. 60, no. 5, pp. 2856–2867, May 2014.
- [16] —, "Cache-aided interference channels," in *IEEE ISIT*, June 2015, pp. 809–813.
- [17] A. Sengupta, R. Tandon, and O. Simeone, "Cache aided wireless networks: Tradeoffs between storage and latency," in *CISS*, March 2016, pp. 320–325.
- [18] F. Xu, M. Tao, and K. Liu, "Fundamental tradeoff between storage and latency in cache-aided wireless interference networks," *CoRR*, vol. abs/1605.00203, 2016.
- [19] J. Hachem, U. Niesen, and S. N. Diggavi, "Degrees of freedom of cache-aided wireless interference networks," *CoRR*, vol. abs/1606.03175, 2016. [Online]. Available: <http://arxiv.org/abs/1606.03175>
- [20] M. M. Amiri, Q. Yang, and D. Gündüz, "Coded caching for a large number of users," in *2016 IEEE Information Theory Workshop (ITW)*, Sept 2016, pp. 171–175.
- [21] K. Wan, D. Tuninetti, and P. Piantanida, "On caching with more users than files," in *IEEE International Symposium on Information Theory*, July 2016, pp. 135–139.
- [22] A. Liu and V. K. N. Lau, "Exploiting base station caching in mimo cellular networks: Opportunistic cooperation for video streaming," *IEEE Transactions on Signal Processing*, vol. 63, no. 1, pp. 57–69, Jan 2015.
- [23] N. Naderializadeh, M. A. Maddah-Ali, and A. S. Avestimehr, "Fundamental limits of cache-aided interference management," *IEEE Transactions on Information Theory*, vol. PP, no. 99, pp. 1–1, 2017.
- [24] R. Tandon and O. Simeone, "Cloud-aided wireless networks with edge caching: Fundamental latency trade-offs in fog radio access networks," in *IEEE ISIT*, July 2016, pp. 2029–2033.
- [25] S. Gharekhloo and A. Sezgin, "Latency-limited broadcast channel with cache-equipped helpers," *IEEE Transactions on Wireless Communications*, no. 99, 2017.
- [26] A. Vahid, M. A. Maddah-Ali, S. Avestimehr, and Y. Zhu, "Binary fading interference channel with no CSIT," *IEEE Transactions on Information Theory*, vol. PP, no. 99, pp. 1–1, 2017.
- [27] Y. Ugur, Z. H. Awan, and A. Sezgin, "Cloud radio access networks with coded caching," in *WSA 2016*, March 2016, pp. 1–5.

- [28] S. H. Park, O. Simeone, and S. Shamai, “Joint optimization of cloud and edge processing for fog radio access networks,” in *IEEE ISIT*, July 2016.
- [29] M. Tao, E. Chen, H. Zhou, and W. Yu, “Content-centric sparse multicast beamforming for cache-enabled cloud ran,” *IEEE Transactions on Wireless Communications*, vol. 15, no. 9, pp. 6118–6131, Sept 2016.
- [30] D. Chen, S. Schedler, and V. Kuehn, “Backhaul traffic balancing and dynamic content-centric clustering for the downlink of fog radio access network,” in *2016 IEEE 17th International Workshop on Signal Processing Advances in Wireless Communications (SPAWC)*, July 2016, pp. 1–5.
- [31] A. S. Avestimehr, S. N. Diggavi, and D. N. C. Tse, “Wireless network information flow: A deterministic approach,” *IEEE Transactions on Information Theory*, vol. 57, no. 4, pp. 1872–1905, April 2011.
- [32] A. Chaaban and A. Sezgin, “On the Generalized Degrees of Freedom of the Gaussian Interference Relay Channel,” *IEEE Transactions on Information Theory*, vol. 58, no. 7, pp. 4432–4461, July 2012.
- [33] T. M. Cover and J. A. Thomas, *Elements of Information Theory*. Wiley, 2006.
- [34] T. Cover and A. E. Gamal, “Capacity theorems for the relay channel,” *IEEE Transactions on Information Theory*, vol. 25, no. 5, pp. 572–584, Sep 1979.
- [35] F. M. Willems, “Informationtheoretical results for the discrete memoryless multiple access channel,” Ph.D. dissertation, Ph.D. dissertation, Katholieke Universiteit Leuven, Belgium, 1982.